Configurations of a piled row breakwater for a protected shallow water marina

By
Werner Gous

Thesis presented in fulfilment of the requirements for the degree of Master of Science in Engineering in the Faculty of Engineering at Stellenbosch University

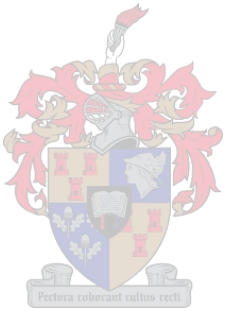

Supervisor: Mr Geoff Toms
Department of Civil Engineering

April 2014

Declaration

By submitting this thesis electronically, I declare that the entirety of the work contained therein is my own, original work, that I am the sole author thereof (save to the extent explicitly otherwise stated), that reproduction and publication thereof by Stellenbosch University will not infringe any third party rights and that I have not previously in its entirety or in part submitted it for obtaining any qualification.

Date:

Verklaring

Deur hierdie tesis elektronies in te lewer, verklaar ek dat die geheel van die werk hierin vervat, my eie, oorspronklike werk is, dat ek die alleenouteur daarvan is (behalwe in die mate uitdruklik anders aangedui) dat reproduksie en publikasie daarvan deur die Universiteit Stellenbosch nie derdepartyregte sal skend nie en dat ek dit nie vantevore, in die geheel of gedeeltelik, ter verkryging van enige kwalifikasie aangebied het nie.

Datum:

Abstract

For the safekeeping or harbouring of small craft, whether for leisure or commercial use, a tranquil basin is the principle requirement in designing a functional harbour facility. Waves transmitted through the perimeter structures of a marina result in agitation of the basin and thereby a reduction in tranquillity. Similarly, waves reflected off the perimeter structures that line entrance channels could result in difficulty when manoeuvring through the entrance channel water areas.

An alternative to the conventional breakwater becomes a necessity when the conventional mass-filled or caisson breakwaters are not feasible in technical or financial terms. One of the alternative options could be to consider a piled row breakwater. In broad terms, this consists of closely spaced piles that attenuate wave energy whilst not forming an impermeable barrier, allowing for currents and sediment to pass through. When comparing the different options for creating a piled row breakwater the quantity of material used to achieve a desired level of wave dissipation could be the most important aspect in considering possible alternatives, as this would relate directly to construction costs and time when considering implementation.

A literature review revealed multiple references to theories that predicted the transmitted and reflected waves for various breakwater porosities and wave conditions. However, there is limited coverage in literature enabling prospective designers. For example, literature describing the applicable ranges of shape configurations that one should start off with when developing concepts is not readily available.

This thesis study used physical modelling to compare the wave transmission properties of breakwaters comprised of three different piled element shapes, namely round, square and diagonal square piles. The pile element shapes are compared for varying porosity values over a range of input wave parameters. A comparison of the transmission incurred by these configurations with previous work is presented and it was found that the physical model experiment closely simulated the predicted values. The tests were scaled from actual conditions in possible marina locations and therefore the performance criteria measured could be applied in reverse to potential site locations.

From analysis of the physical model results, it was clear that the highest energy loss was found, in general, to occur with low porosities (below 10%), as could be expected. For a fixed screen configuration in terms of pile element shape and porosity, the performance is heavily dependent on wave steepness, the steeper waves incurring a lower transmission coefficient than the less steep waves. For a given porosity, circular piles performed the best (transmit the least) followed by square piles and then diagonal square. When comparing the material used, diagonal square piles yielded better performing breakwaters due to the expanded cross section gained in elevation.

The work has provided useful insight into the performance of piled row breakwaters in restricting transmission of wave energy. Design guidance has been provided when considering the parameters for deriving conceptual layouts for piled row breakwater structures.

Recommendations were put forward for further work in this field, including potential study areas, data gathering, and study methods, as well as more applied uses of piles, for example in combination with other elements in a marina.

Opsomming

Vir die veilige bewaring van klein vaartuie, hetsy vir ontspanning of kommersiële gebruik, is die hoofvereiste in die ontwerp van 'n funksionele hawe fasiliteit dat die beskermde hawegebied ‘n rustende water oppervlak sal moet handhaaf. Golwe wat oorgedra word deur die omtrek golfbrekers van ‘n hawe deur middel van transmissie veroorsaak oppervlak versteurings in die hawe bak en dus ook ongewensde versteurings in die vasmeer kondisies. Op ‘n soortgelyke wyse, veroorsaak golwe wat gereflekteer word vanaf die toegangs kanaal golfbrekers problematiese kondisies vir die navigeer van bote deur die kanaal.

Die behoefte aan 'n golfbreker alternatief vir die konvensionele oplossing word genoodsaak wanneer die konvensionele stortrots of caisson golfbrekers nie haalbaar is nie as gevolg van tegniese of finansiële aspekte (Park *et al*. 2000). Een van die opsies wat oorweeg kan word as 'n alternatief is ‘n heipaal-ry tipe breekwater. In breë terme, bestaan dit uit naby gespasieërde heipale om golf energie te breek, sonder om ‘n ondeurdringbare versperring te vorm. Wanneer die verskillende opsies vir die skep van 'n heipaal-ry tipe breekwater vergelyk word, kan die hoeveelheid konstruksie materiaal benodig per opsie die belangrikste vergelykende parameter word. Die rede hiervoor is die direkte verwantskap aan konstruksie kostes sowel as tyd aspekte wat gepaardgaan met die konstruksie materiaal hoeveelhede.

Vanuit die literatuurstudie is verskeie verwysings geïdentifiseer waarin vorige teorieë oor oordrag en refleksie van golwe evalueer word vir wisselende porositeit waardes en intree golf waardes. Daar is egter 'n beperkte dekking in die literatuur wat ontwerps-riglyne betref. Byvoorbeeld, die toepaslike omvang van die vorm konfigurasies wat oorweeg moet word wanneer konsep ontwerp gedoen word, is nie geredelik beskikbaar nie.

Hierdie tesis vergelyk, deur middel van fisiese skaal model toetse, drie heipaal-ry element vorms, naamlik ronde, vierkantige en diagonal geroteerde vierkante vir verskillende porositeit waardes oor 'n verskeidenheid van golf inset parameters. 'n Vergelyking is getref tussen die toetsdata en vorige werk en daar is bevind dat die fisiese model eksperiment die voorspelde waades uit die literatuur redelik akkuraat kon naboots. Die toets kondisies is geskaal vanaf werklike moontlike marina terreine en dus kon die toets resultate toegepas word in die ontwerp van potensiële terreine.

Vanuit die data-analise, is waargeneem dat die hoogste energie verliese oor die algemeen plaasvind by laer porosititeit waardes (onder 10%) soos wat verwag kon word. Vir 'n gegewe golfbreker opset, in terme van die heipaal element vorm en porositeit, is die verrigting hoogs afhanklik van die golf steilheid, met hoër verrigting by steiler golwe. Vir 'n gegewe porositeit, sal ronde heipaal elemente die beste verrigting gee, gevolg deur vierkante heipale en laastens diagonal geroteerde vierkante. Vir soortgelyke hoeveelheid heipale, sal diagonal geroteerde vierkante beter verrigting lewer moontlik as gevolg van die verlengde deursnit dimensie in vooraansig.

Hierdie navorsing het goeie insig verskaf oor golfdeurlaatbaarheid en weerkaatsing van heipaal-ry breekwaters. Ontwerp riglyne word ook verskaf wat betref die parameters wat gebruik kan word vir die konsep ontwikkelings fase vir heipaal-ry breekwaters.

Aanbevelings word gemaak vir verdere navorsingswerk in hierdie veld, insluitend moontlike studie-areas, data insameling, studie metodes, sowel as vir meer toegepasde situasies, byvoorbeeld waar die heipaal elemente in kombinasie met ander marina komponente ontwerp moet word.

Acknowledgements

The completion of this thesis would not have been possible without the special contributions and support by certain people. My deepest gratitude is extended to each of you.

Firstly, I would like to mention my supervisor at Stellenbosch University, Mr Geoff Toms, for his technical guidance and seemingly never ending patience with me as a part time student. A warm thank you is due to Mr Toms for his mentorship and oversight.

Also, I would like to thank my current and recent line managers at my employer, Aurecon. The financial support through a post graduate bursary as well as the personal support offered as leaders, even during busy times is highly appreciated.

For his time in introducing the laboratory equipment, I wish to thank Mr Chris Baret from PRDW for taking his personal time to walk through the setup of the large wave flume, a.k.a. “The Old Lady” and sharing his experiences.

At the Civil Engineering hydraulics laboratory, the assistance from Mr Christiaan Visser and Noel has been most valuable to assist with arrangements and setting up of the model test.

The assistance from fellow student, Mr Isak Wüst, is much appreciated for his willingness to assist when required with lending an extra hand with the equipment.

A special word of thanks is offered to the Coastal Engineering and Port Infrastructure Research Group at the Council for Scientific and Industrial Research’s Built Environment Department. In particular, I would like to thank Mr Kishan Tulsi for his advice and time on the setup of the wave probe arrays. To Mr Luther Terblanche for his time in setting up and availing the software for the post processing of the data. Also to the late Mr Dave Phelp who always showed interest in others’ work and sharing of ideas. Mr Phelp will be sorely missed by the international coastal community after his sudden passing this year.

To my parents for all their words of encouragement and support in this journey.

Most importantly, to my dear wife, Winell, for her endless patience and support that made it possible for me to complete the studies. Thank you for unselfishly looking after our two blessings, Madelein and Samuel, when I could not, for packing the lunchboxes for the long days and your unbounded love. I hope to contribute to your career in a reciprocating way (even if it’s just in our late night discussions over a coffee on the Theory of Knowledge).

Table of Contents

List of Figures

List of Tables

1 Introduction

1.1 Background

For the safekeeping or harbouring of small craft, whether for leisure or commercial use, a tranquil basin is the principle requirement in designing a functional harbour facility (Allsop & Hettiarachchi, 1988). The creation of a harbour basin is achieved through either digging out on-land or flooding the basin, or through building breakwaters to create an enclosed water area, or through a combination of these methods. It is also quite common for large commercial ports that have been constructed in exposed conditions, to have a smaller inner harbour for small craft, such as yacht clubs in basins that are mostly protected from open ocean swell. In addition to wave penetration through entrance channels (i.e. water areas that essentially have to remain open for vessels to navigate through) wave transmission through or over the breakwaters of a harbour basin contributes to the wave disturbance and, accordingly, to the state of tranquillity of the basin. The use of a mass-filled rubble mound breakwater from dumped material core with armouring layers is a trusted and proven option, although it could become a very expensive one depending on the water depth and the availability of rock within a reasonable distance. Caisson-type structures are also well proven in exposed conditions, as well as in combination with mass-filled foundations.

The need for an alternative to the conventional breakwater becomes essential when conventional breakwaters are not feasible in technical or financial terms (Park *et al.* (2000)). One of the options that could be considered as an alternative is a piled row breakwater. In broad terms, it consists of closely spaced piles to attenuate wave energy whilst not forming an impermeable barrier. It would therefore allow for currents and sediment to pass through, although this could have both positive and negative implications for marina design.

The configuration for the piled row breakwater considered in the current study consists of closely installed piles, driven or socketed into the seabed, and potentially held together by means of interconnecting structural ties if required, above or below the water line. See Figure 1-1 for a definition sketch of the piled row breakwater as taken from Suh *et al.*, 2011. The plan geometry of piles does not necessarily have to be linear and previous research into the use of semi-curved or semi-enclosed configurations has been documented (Nilsen *et al.*, 2000). By definition, piles are closely spaced, i.e. there is relatively little space between them, and this setup is intended to provide shelter on the lee side of the structure, while not providing a solid barrier, so that water circulation is still possible through the screen. The functional requirement of the piled row breakwater being that dissipation of wave energy is achieved while current flow through an

installation is permitted. This could be of importance for several marina locations where water circulation and sediment movement should be treated as sensitive. It is, however, not necessarily a benefit to have the permeable barriers in that water currents and induced siltation could have negative impacts on the design and operations of the marina. Further alternatives for piled row breakwaters include single curtain contiguous piles, multiple parallel row piles, as well as piles in combination with solid structures, as used in some caissons that act as wave dissipaters (Kakuno & Liu, 1993).

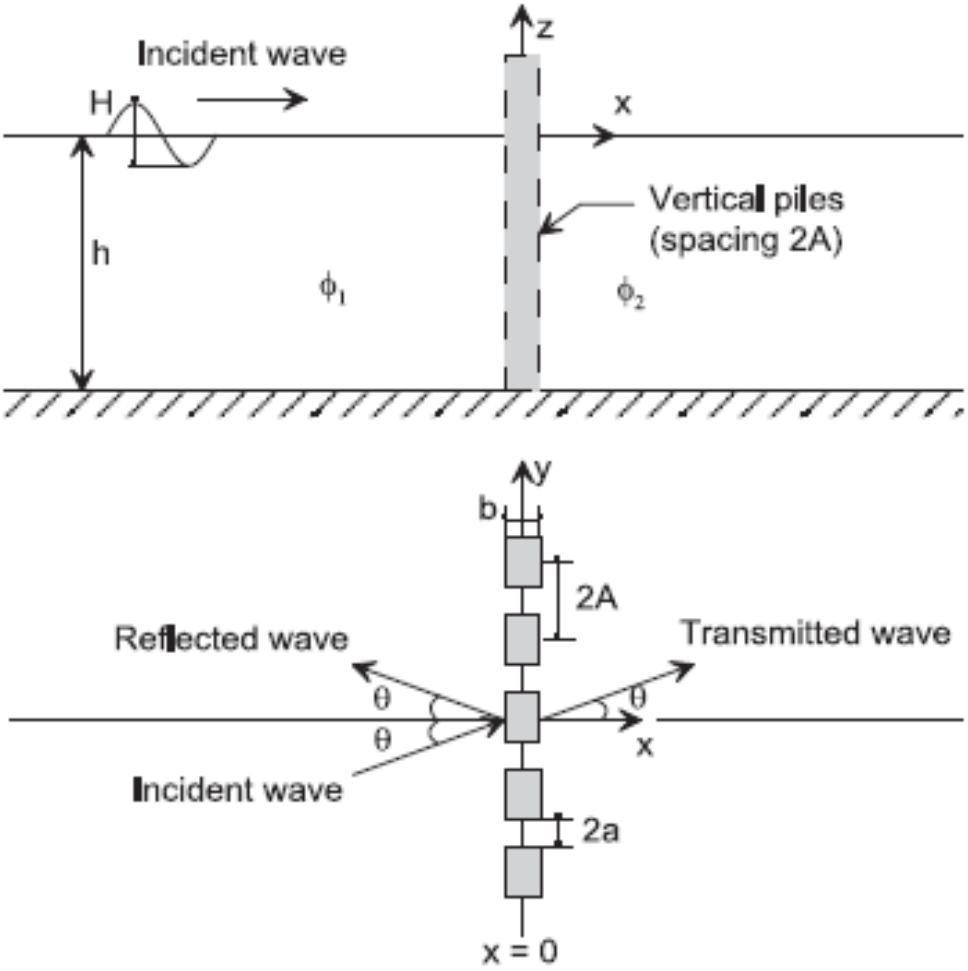

Figure 1-1: Definition sketch of piled breakwater (from Suh, Ji & Kim, 2011)

The alternative of considering piled row breakwaters as opposed to conventional structures is also driven by practical and constructability constraints, for example the material availability of rock and/or sand fill could be scarce or of prohibitive cost to place in location. The construction of a piled row breakwater versus a conventional breakwater has significant advantages in terms of mobilisation of construction plant, construction duration, as well as procurement of the material. There are known benefits from using a piled row breakwater over a conventional rubble mound type from an environmental perspective as well, such as a smaller construction and permanently invasive footprint, less restriction of water and sediment flows. The creation of a

temporary basin for construction of smaller craft or leisure craft by piled rows, could also be an added benefit seeing that it is considerably more practical to remove a piled row breakwater, compared to removing a rubble mound fill or vertical seawall breakwater.

Research thrusts have focussed on various technical aspects, such as design considerations, theoretical hydrodynamic interactions and the refinement of related theories of hydrodynamics of wave and pile interaction. Recent research has attempted to advance the numerical modelling of the water particle movement (Schlenkhoff *et al.*, 2012). For engineering applications, for example for use as a marina breakwater, design aspects of the piled row breakwater would include forces on individual pile or pile groups, wave run-up, drag, wave reflection, wave transmission and also induced scour around the foundations. As shown in the literature study section of the report, various empirical formulae regarding this aspect have been published.

From experience, a small craft harbour or shallow water marina within a protected water body is often a crucial consideration in terms of a larger development's viability and feasibility. The reason for this is the relatively high input costs required for the formation of a protected basin. Internal dug out basins, as well as conventional rubble mound breakwaters, have the potential to sway the decision on whether a new development will be viable or not. This investment must be offset by the expected value that is added to a development by the provision of a boating facility with harbour and mooring functions for recreational and commercial boating communities. It is, therefore, often required to look in detail at alternative methods to create the required facilities for a functional marina. Piled row breakwaters have the potential to be considered as an alternative to conventional breakwaters, although to date there has been no design guideline supported by literature or design codes. To reference efficient configurations that would assist in early selection of workable concepts would be ideal from a designer perspective. Available literature does provide limited insight into the performance of piled row breakwaters; however, more understanding of the sensitivities of the configurations of the screens and the expected performance for varying input wave parameters is required before a concept can be selected for consideration in early engineering phases.

Further alternatives to conventional breakwater types in milder wave climates, such as in protected water bodies, include the use of submerged breakwaters, floating breakwaters and impermeable screens or wave fences, although these are not discussed in this thesis.

1.2 Motivation

Not many case studies regarding the efficiency and performance of existing piled row breakwater solutions have been monitored and reported. Although literature has provided insights into wave pile interaction and hydrodynamic aspects, often the empirical equations are not solved easily and could contain a complex number of terms that are not user friendly. The wave pile interactions and the associated wave dynamics through the screen become complex over a range of varying porosities and input wave parameters. Therefore, there is a need to gain more insights into the available empirical methods and also the variables related to the performance of and wave interactions of piled row breakwaters.

1.3 Objective

The primary objective of this study is to investigate the performance of various piled row breakwater configurations and to validate this with literature and available performance criteria.

1.4 Methodology

1.4.1 Study Area Boundaries

Initially, a broad range of topics was sourced to gain an understanding of the research work done to date and an appreciation of the theories involved and their complexity. It is evident, from the literature sourced and viewed, that several aspects could be researched in more detail, pertaining particularly to the broader field of wave dissipation by piled elements.

There are certain aspects related to the research area of piled row breakwaters that will not be dealt with in this study, although these could be refined and studied further, possibly under a separate topic or as an advancement of this topic as a separate research effort. These include:

- Geotechnical conditions and their influences on the selection of a piled row breakwater;
- Wave runup, drag and slam forces due to wave-pile interaction;
- Wave induced scour around piles;
- Pile material options (i.e. structural steel vs. reinforced concrete vs. timber);
- Perforation of the pile casing or volume to increase attenuation by slowing down wave flow through the inner diameter of the pile;
- Horizontal structural members intended to act as barriers in the piled system;
- Design of the cylindrical elements as well as the global stability of the structure ;

- Dynamic response of the pile and related conditions resulting in liquefaction of the foundation;
- Effect on the environment of wave reflection seaward of the incident wave;
- Currents and their effects, e.g. due to ambient and induced hydrodynamics;
- Cost-benefit and financial feasibility comparison;
- Environmental impacts for the alternative sub-options;

This research topic is aimed at exploring the technical performance of piled breakwaters for the purpose of constructing a protected mooring facility (such as a marina or small craft harbour) for recreational navigation facilities for vessels that are generally not classified as commercial liners. To keep this study focussed, the piled breakwater elements (piled wave screen) are in general assumed to be founded in a constant depth of water and protruding above the mean water level for all design conditions, i.e. the piles are not considered at any stage to be completely submerged, nor is any horizontal face extending beyond the width of the piles under consideration.

1.4.2 Proposed Methodology

The selection of performance parameters for piled breakwaters that were to be studied was refined, based on further interrogation of wave propagation theory and available literature. The main parameter to be studied was identified as basin tranquillity. This implied an investigation into the efficiency of a piled breakwater in acting as a wave attenuation structure, through reducing the wave energy transmitted through the structure. Basin tranquillity was therefore studied in a physical model environment, by means of measuring wave heights on the leeward side of the piled breakwater compared to those on the seaward side, and recorded as the transmission characteristics of the piled breakwater configuration.

The wave environment selection for the testing was also studied prior to laboratory work commencing. Although no known guideline for wave energy versus piled breakwater type and configuration has been sourced, it has been assumed that the study would focus on the incident wave for a typical sea state for a local fetch limited or depth limited wave climate in an enclosed water body. The study of swell waves is therefore excluded from this study, apart from a desktop overview of the expected performance of piled wave screens within the limitations of the test equipment.

The following goals of the study act as the building blocks in achieving the objective:

- To investigate the performance of various piled row breakwater configurations for varying input waves through physical testing. Performance of the test models to be studied in terms of the wave reflection coefficient (K_R) and the wave transmission coefficient (K_T).
- To validate the test results with literature by comparing results with previous test and predicted results.
- To set up first order empirical equations for the different configurations through curve fitting in spreadsheet-type software for the test ranges as per the current study.
- Lastly, the application of findings to a possible marina site as a trial of testing the findings of the study.

The methodology that was defined for the study was set out as in Table 1-1 in stages, with the tasks per stage summarised in the right hand column: The chapter numbers in brackets below the stage description refers to the report section where these stages have been captured in more detail.

Study Stage	Main Tasks per Stage	Outcomes per Stage
Stage 1: Literature review (*Chapter 1 & 2*)	➢ Literature sourcing around topic (broad search) ➢ Review and filtering ➢ Summary of relevant work ➢ Definition of topic (more focussed)	➢ Literature study ➢ Topic Definition ➢ Motivation for Topic ➢ Setting of Objectives
Stage 2: Physical modelling (*Chapter 3*)	➢ Planning of laboratory work ➢ Surveying and set-up ➢ Building of model breakwaters ➢ Testing	➢ Survey of equipment ➢ Model scale decision ➢ Familiarisation with laboratory equipment capabilities ➢ Setup of model for varied configurations ➢ Data acquisition
Stage 3: Data processing & Analysis (*Chapter 4*)	➢ Sorting and post processing of test data ➢ Preparation of data sets for analysis	➢ Computation of reflection and transmission coefficients for respective configurations. ➢ First order comparison between configurations
Stage 4: Data Analysis (*Chapter 5*)	➢ Validation of recorded data with available sources (graphs and equations) ➢ Analysis of recorded data	➢ Comparison with test data from literature and calculated predicted results ➢ Comparison between test configurations.
Stage 5: Curve-fitting for test data (*Chapter 6*)	➢ Trendline development for various data sets	➢ Additional equations for future use
Stage 6: Application of test results to a possible marina site (*Chapter 7*)	➢ Interpretation of results for a possible site	➢ Applied case of research
Stage 7: Conclusion & Recommendations (*Chapter 8*)	➢ Summary of key aspects ➢ Identification of future research work in the wave screen field	➢ Concluded research findings ➢ Recommendations for future research

Table 1-1 Methodology in study Stages and Tasks per Stage

1.5 Structure of Report

The report has been laid out to follow the flow of the methodology as shown in the foregoing section. The first chapter and introduction was aimed at setting the background for the study and serves as an introduction to the field in general and the topic selected for research. Chapter Two outlines the literature review that was conducted. Chapter Three summarises the physical modelling stage, while Chapter Four summarises the data processing and initial analysis. Chapter Five contains the data analysis, including validation and dissemination of the data sourced through the laboratory testing. Chapter Six aims to present additional fitted curves with their associated equations. Chapter Seven addresses a practical application of the piled wave screen in a possible location, while Chapter 8 presents the close of the report with conclusions and recommendations.

2 Literature Review

2.1 Terminology

Various academic papers and technical references were screened for inputs on wave transmission, reflection and energy dissipation by piled row and slotted screen breakwaters. During the current study, preference was given to material that could present a data set, derived graphs, and theoretical or empirical equations in order to develop a comparative baseline between empirical equations, previously published test data, and data from the current research paper. For the purpose of gaining a better understanding of wave interactions around piled rows in the coastal environment, selected papers relating to piled groins were also studied. The application of piled groins perpendicular to the shoreline is somewhat different to that of breakwaters, although the wave interactions with groin structures are still of interest.

The core theme in many of the academic papers researched was built around the various wave interactions with cylindrical piled elements and the hydrodynamic effects of the wave-pile interactions. Methods used to derive relationships for predicting the reflection and transmission of waves are given a brief overview. Theoretical approaches have also been reviewed and are outlined in the sections that follow.

Nomenclature in use for piled row breakwaters and related structures, include the following:

- Pervious or Piled Wave screens (Allsop & Hettiarachchi, 1988), (Thomson, 2000)
- Pile supported Breakwater (Papini, 2003),
- Piled cylinder breakwaters, (Wiegel, 1961 as per Zhu, 2011)
- Slotted wavescreens, (Thomson, 2000)

and there might be others as well. In this paper the term piled row breakwater will be used mostly.

For the purpose of referring to porosity (*e*) for this thesis, the diagram in Figure 2-1 indicates the potential set-ups for a generic porosity.

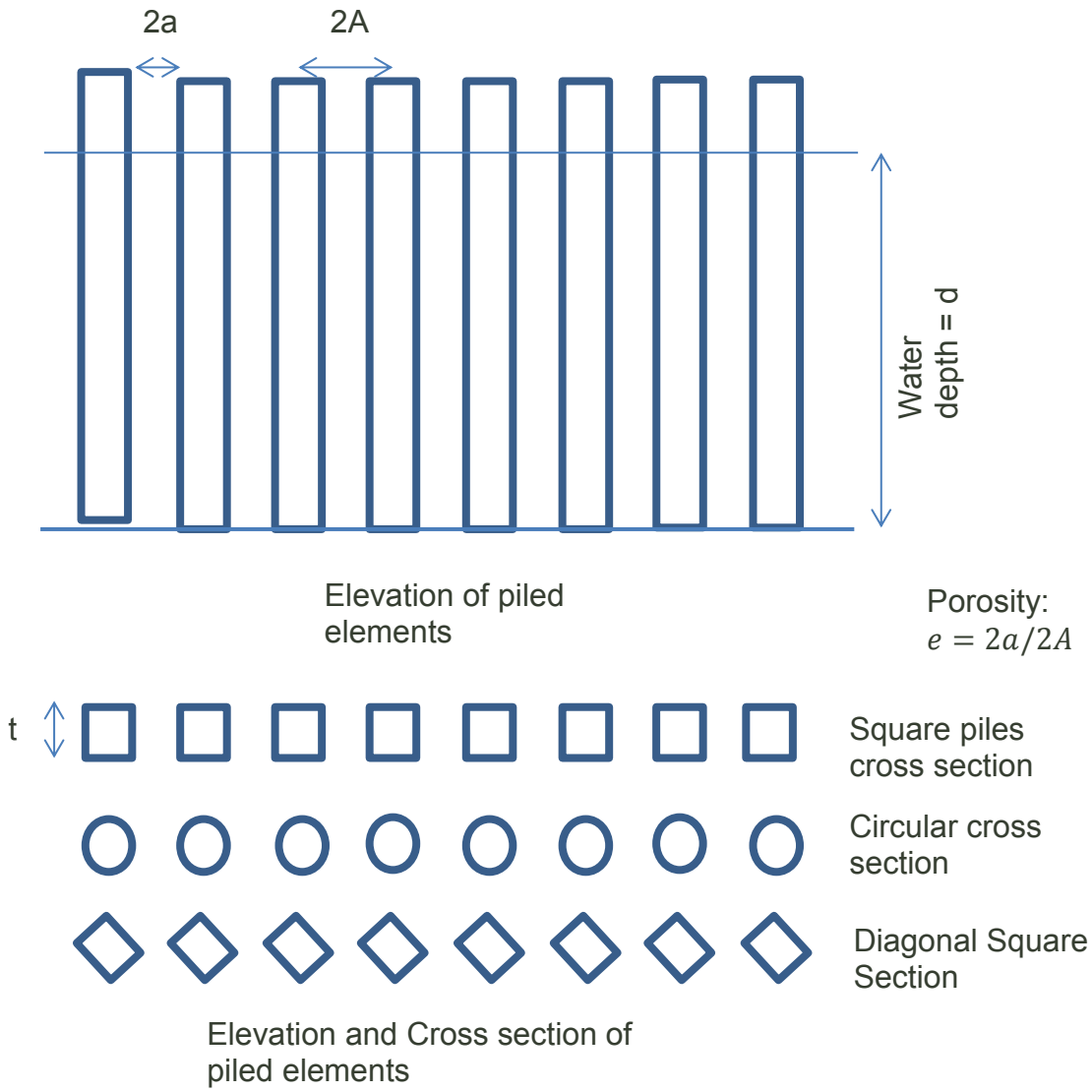

Figure 2-1: Definition schematic for the purposes of this study

2.2 Applications

The main purpose identified for the use of piled breakwaters in practice and research was to provide a transmitted wave height that had been reduced from the incident wave height, while also minimising the piled elements. Groins or breakwaters created by piled rows have been used in various types of applications. The most common applications sourced included:

- Permeable pile groins (Raudkivi, 1996), for coastal protection. The groins were constructed as elements normal to the shoreline orientation and intended to introduce increased hydraulic roughness on the longshore current. (see section 2.5.1)

- Shore parallel breakwaters (Reedijk, 2003), for use in erosion protection. The solution studied entailed creating shore parallel installations with piled rows. Due to the lower energy wave transmitted by the shore parallel structure, the reduced wave climate on the leeward side of these parallel breakwaters resulted in less shoreline erosion compared to the unprotected sections.
- Breakwater caissons (Kakuno, 1993[i]), in harbour applications in Japan. The example discussed in literature involves caisson structures that have permeable fronts facing the incident waves, with single or multiple wavescreens installed over the width of the caisson, and a solid rear panel.
- Tug harbour breakwaters (Nilsen, 2003), where offshore tug harbours created by piled rows were studied to serve as possible alternatives to the conventional breakwaters. The Main driver was the lack of availability of affordable rock for more conventional breakwaters.
- Small craft harbour breakwaters, such as installations in Knysna in South Africa, although the concept employed a wave fence on piles.

Some of the regularly researched variations of piled row breakwaters include the following:

- Horizontal Panels (for example Thomson, 2000),
- Pile supported breakwater (for example Isaacson, 1998 and Atkins & Mocke, 2009),

2.3 Theory Review for single row of piles

Values resulting from tests performed and published in literature were sourced, in addition to papers that reviewed and developed theories. The *Coastal Engineering Manual* (2008) sites references Allsop & Hettiarachchi (1988) who produced a set of transmission and reflection coefficients (see Figure 2-2) for corresponding relative depths ($\frac{d}{L}$) over porosity (*e*) of perforated screen walls. Although the data is not compared in any detail with predicted results from theories or empirical equations, it presents the high level trend that can be expected in performance in respect of the reflection and transmission coefficient trends for the change in porosity. The paper also suggests that the optimum porosity could lie in the range of 0.15 to 0.25, but cautions that this method is put forward as a simplified one. More analytical papers were therefore required to gain more in depth understanding of wave screens and wave interactions.

Early numerical models that predicted transmission coefficients based on slotted thin vertical barriers did not account for energy loss within barrier due to viscous effects according to Isaacson *et al.*(1998). Advances have been made in the theoretical approach by Wiegel (1961) (as summarised by (Isaacson, 1998).

Although initially intended for analysing pile supported breakwaters, i.e. see Figure 2-3, Isaacson *et al.* (1998) adjusted previously derived eigenfunction expansion method equations and found good correlation with laboratory tests when compared with the predicted data.

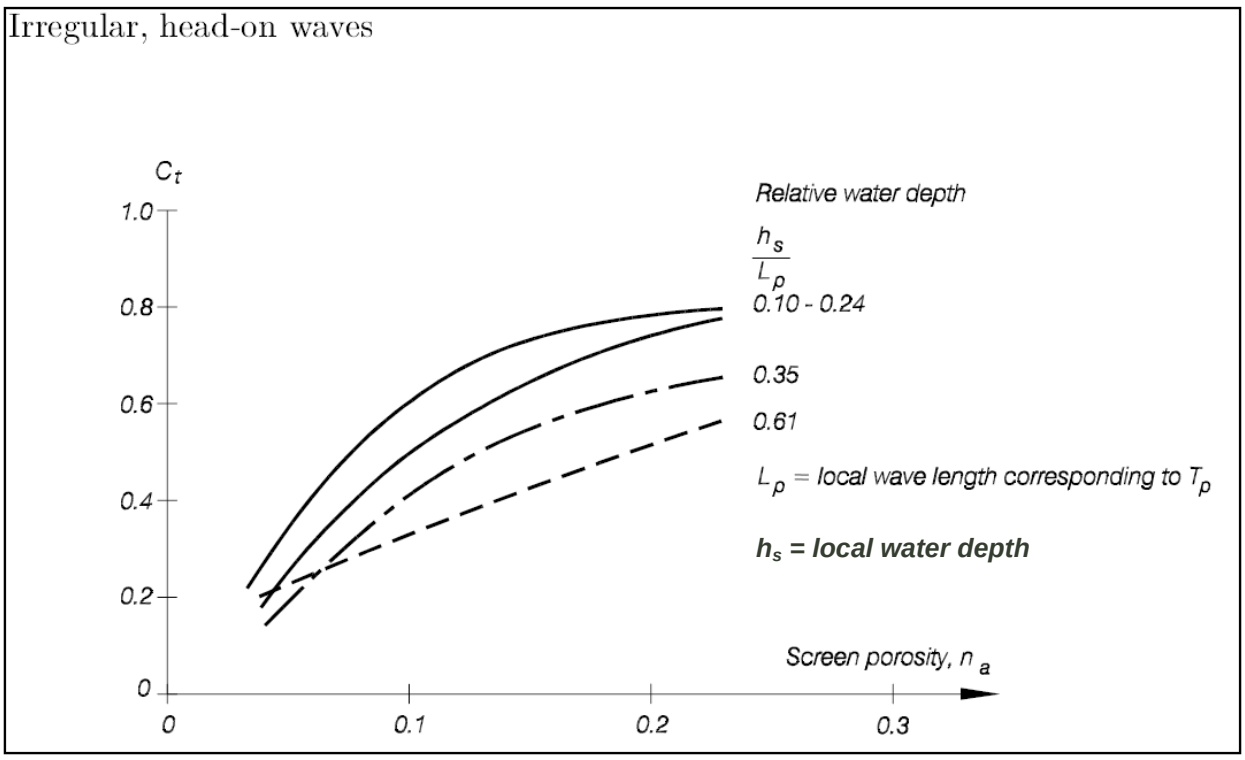

Figure 2-2: Transmission coefficient for single wave screens, Allsop & Hettiarachchi (1988)

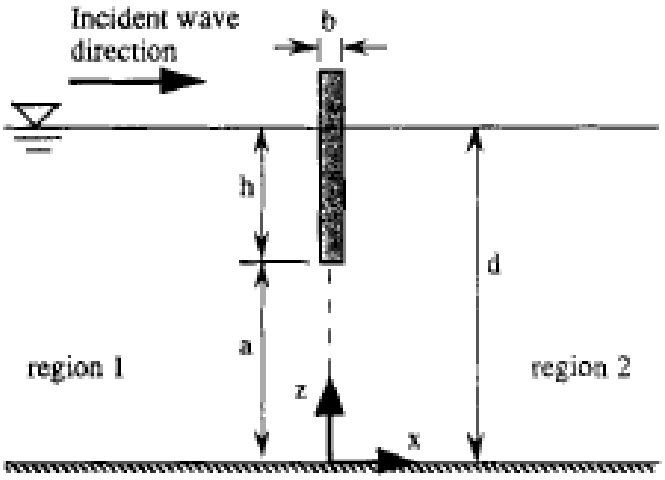

Figure 2-3: Pile supported breakwater (Isaacson, 1998)

For fluids that are incompressible and inviscid in theory and flow being assumed as irrotational, the fluid motion has been approximated in terms of a velocity potential (Φ), which satisfies the Laplace equation within the fluid region. Linear wave theory is assumed to be relevant, so the wave height amplitude is small enough to satisfy this requirement. The boundaries that apply to the approximation of Φ are the seabed, free surface and far field conditions. Isaacson's approach and theorem used included provision for the following parameters:

- Velocity potential in front and on the leeward side of the breakwater, being proportional to the pressure difference across the barrier;
- A permeability parameter that is generally complex, and not solvable by normal numerical approaches;
- The thickness of the breakwater;

Isaacson states that various other authors attempted in defining the permeability through the physics of flow within the breakwater gaps. The resulting resistance experienced by flow through the breakwater, was also expressed in terms of a friction parameter and a drag coefficient, while inertial effects would be expressed in terms of added mass, in order to balance the velocity potential equation. The introduction of a friction coefficient resulted in the breakwater thickness that could be isolated to a constant value, if known from physical testing.

The manipulation of Isaacson's derived empirical formulae is only done through a complex matrix system. This did not form part of the study, although the above summarised approach on the theory by Isaacson captures the essence of the velocity potential approach. For the overall

performance of the barrier, the energy dissipation coefficient is defined within the following equation:

$$1 = K_R^2 + K_T^2 + K_{EL}$$

Equation 2-1: K_{EL} as defined by Isaacson (1998)

where K_{EL} represents the energy loss coefficient, K_R the reflection coefficient and K_T the transmission coefficient. The energy loss coefficient is defined as the proportion of incident waves energy flux dissipated by the breakwater (Isaacson *et al.*, 1998).

Formulae for wave runup on the piles and wave force on the breakwater elements were also derived and should form part of the design considerations, but did not form part of this thesis.

Validation of the formulae derived by Isaacson was undertaken by comparison with results from previously developed theories (reference in Isaacson made to Hagirawa, 1984 and Yuh, 1995). Although acceptable similar trends were identified, the differences between the data sets were ascribed to differing approaches in dealing with the derivation of the resistance component. In accounting for the apparent energy losses through the breakwater, Isaacson derived a friction coefficient whereas Hagirawa related it to a drag coefficient.

Correlation of the Isaacson formulae was done through physical model testing for varying parameters. Porosity ranges from 5% to 50% were tested in a wave flume of 20 m length and 0.62 m width. Constant water depth was used throughout with incident wave inputs varied in terms of periods and various wave steepness values. The expected trends of decreasing transmission coefficients with lowering porosities were observed, with the reflection coefficient showing opposite trends. The energy loss at the wave screen was non-zero, also as expected. From the experimental results Isaacson noted the decrease in K_T and increase in K_R for an increase in wave steepness.

In summary, the work by Isaacson *et al.* is of engineering interest in that it examined transmission and reflection, wave runup and well as wave forces, and it presents data for comparison with future tests in research.

Further conclusions were that energy dissipation within the slotted barrier is related to friction and added mass coefficients that were estimated. The theoretical method put forward in general would be seen to have overestimated the wave transmission through the screen at high wave steepness values.

Kim (1993) developed a theory for offshore structures and the interaction of waves with variable number of vertical Circular Cylinders. This was derived from a diffraction theory originally developed for *N* bottom mounted vertical cylinders and is more applicable to offshore structures and specific reference given to tension leg platforms in deep water conditions. This paper also considered the theory of velocity potential (incident, diffraction & radiation) to develop equations. Surge and sway forces on the piles were calculated and compared to test data from offshore installations. The value of this study is that actual field data is continuously recorded for offshore oil installations and this probably represents the best site data available, although it is not included in a usable format in the paper. The underlying basis of developing equations from the velocity potential is also of importance. The work of Kim would be more applicable to the concept design stage for deep draft multi column structures, and not to shallow water marinas, although it is valuable in the area of hydrodynamic interaction with groups of piles and would be very difficult to relate to shallow water wave environments.

Kakuno & Liu (1993) developed theories for scattering of water waves by vertical cylinders by considering a slit-type breakwater, where a caisson type structure with front slotted screen and solid vertical rear section is used in lieu of a conventional breakwater. The study, however, focussed on the performance of the front screen.

Similar to other studies, a theorem based on velocity potential was developed by Kakuno and Liu (1993). They stated that "*when flow separation is ignored, water wave-scattering is analogue to waveguide problem in acoustics and electromagnetics*" , although for this paper it is only worth taking note of the aforementioned and no further discussion on these related theories are discussed. It was further determined that a single empirical coefficient, *f*, was required for calibrating theory with experimental data. To support this, laboratory experiments were carried out in wave flume with circular and square cylinders where it was found that the empirical coefficient differed for these two shapes (for circular f = 0.75 and rectangular f = 1.5).

From comparisons of theoretical and experimental data, Kakuno & Liu developed a modified method of matched asymptotic expansions for studying the scattering of water waves by an array of vertical cylinders. It was suggested that this work could also be applied to the scattering of shallow-water waves by horizontal cylinders.

Further key aspects of the work by Kakuno & Liu was that flow separation and energy dissipation was modelled empirically and no methods were derived from first principles for these aspects. The empirical coefficient *f* was found to be dependent on Reynolds (*Re*) and Keulegan-Carpenter (*KC*) numbers, although it was further proven by laboratory tests that the slotted screen had low dependency on *R* and *KC* respectively.

A paper by Raudkivi (1996) that focussed more on the use of piled groins contains theoretical views on the working of the piled row breakwater. Raudkivi hypothesised the wave interaction at a piled row as follows:

"*Each slot acts as a point source of wave energy for the lee side. The superposition of these elementary waves radiating from the slots (Huygen-principle) leads to wave fronts parallel to the groin.*"

Furthermore it stated that orbital velocities that act more or less parallel to the pile groin reduce the effective permeability of a pile groins, but otherwise the individual effects remain as for diffraction through gaps.

Park *et al.* (2000) presents an analytical model developed (also through eigenfunction expansion methods) and compared with laboratory experiments. They stated that concrete and timber slotted units gained popularity as alternative to be investigated in cases where conventional breakwaters would not be feasible. (Benefits of these type of slotted breakwaters have been mentioned in section 1.1). Equations for the wave screens are also derived from velocity potential, but differentiated between rectangular cylinders (by means of a plate orifice formula) and circular cylinders (the latter being more complex). The equations presented were also not easy to solve and presented a similar stumbling blocks for being solved simplistically.

Laboratory work was conducted for the various porosities and shapes with the results being published as per Figure 2-5. From the data measured, the frequency averaged reflection and transmission coefficients (K_R and K_T respectively), overall agreement between measurement and calculation was good. However, the model tends to over-predict K_R and under-predict K_T while under-predicting energy loss coefficients for small gap widths compared to measured data. This could be ascribed to the model that neglects the effect of evanescent waves near cylinders (Park *et al.*, 2000).

Both measurement and calculation show wave reflection and transmission become larger and smaller, respectively, as wave steepness increased. From the latter findings Park et al. concluded that a piled row breakwater should be more effective for steeper waves in protecting a harbour area.

Thomson (2000) studied previous literature and set up tests to derive comparative values from previous work, as well as some equations. No theory or numerical work was undertaken to form new equations from ground principles; however, of high value was an overview of previous literature on the topic. A very high level overview of papers by Wiegel (1961), Hayashi (1966,

1968) were quoted with simplistic empirical equations. For example, the transmission coefficient component solely depended on the porosity of the breakwater, and not to incoming wave parameters.

The author of this thesis found the derived empirical equations put forward by Thomson highly valuable. The equations below contain variables for porosity (*e*), wave height (*H*), wave length (*L*), water depth (d) and wave period (*T*) as well as a relationship to gravitational acceleration (*g*). The equations were derived from measured data and are therefore useful to compare to data from testing in this study.

Equation 2-2: Empirical formula for transmission coefficient (Thomson, 2000)

$$K_T = 0.804 + 0.267 \ln(e) - 0.089\left(\frac{H}{L}\right) + 0.037 \ln \frac{d}{gT^2}$$

Equation 2-3: Alternative empirical formula for transmission coefficient (Thomson, 2000)

$$K_T = 0.834(e)^{0.399}\left(\frac{H}{4}\right)^{-0.136}\left(\frac{d}{gT^2}\right)$$

Thomson also included comparative work for single versus double and triple screens. Although this paper was sourced while the current study was already well advanced, the equations put forward by Thomson were of particular interest for use as predicting expected performance for various pile configurations. Useful references are presented amongst others to Mei (1983), Gardner (1986), Isaacson (1988) as well as Grune and Kohlhase (1974). Thomson summarised that the screen depth, i.e. the pile element thickness in the direction of wave propagation, was not found to be that critical, and therefore omitted from previous studies.

As for wave steepness, Kriebel (1992) is referenced in that he also stated the relationship between increasing wave steepness and related reduction in K_T.

Papini (2003) also studied the wave interactions with a pile-supported breakwater by comparing tests with theory. Papini continued work derived by Isaacson (1998).

Suh *et al*. (2011) worked on the determination of a friction coefficient in the permeability parameter of a perforated wall developed based on best fit between measured and predicted values of hydrodynamic parameters such as reflection and transmission coefficients. Empirical

formulae were proposed in terms of known variables, for example porosity (e) and the thickness of perforated wall and water depth. From this the friction coefficient was derived. A mathematical model was developed to calculate the hydrodynamic characteristics of a perforated wall and to calculate the permeability parameter. Thereafter, methods from Kim & Vu were compared to show the importance of the permeability parameter.

Hydraulic experiments were carried out to find an empirical formula for the friction coefficient, (*γ*), and subsequently a new friction formula was derived. Suh *et al.* summarised previous calculation methods which is useful that some of these equations can be solved with relative ease. Suh revisited empirical equations from Mei (1989) and Kriebel's (1992) work which are solvable without unknowns and continues to derive a hybrid method for which no formulae are presented. The equations of Mei and Kriebel are shown below with parameters that require further solving by substitution.

Equation 2-4: Reflection Coefficient equations from Mei (1989) as summarised by Suh (2011)

$$K_R = 1 - \frac{wU_0}{\frac{gkH}{2}}$$

Where:

$\omega = \sqrt{gk\ tanh\ (kd)}$

$$U_0 = \frac{H_i/2}{h}\sqrt{gh}\frac{\sqrt{1+2\alpha}-1}{\alpha}$$

$$\alpha = \frac{4}{3\pi}\frac{fH_i/2}{h}$$

k = wave number

Equation 2-5: Transmission Coefficient equations from Mei (1989) as summarised by Suh (2011)

$$K_T = \frac{U\circ}{\left(\left(\frac{H}{2}\right)/d\right)\sqrt{9.81d}}$$

Substitution equations for parameters w and U_0 are presented in the text by Suh *et al.* (2011).

Equation 2-6: Transmission coefficient equations by Kriebel (1992) as summarised by Suh (2011)

$$K_T = \frac{\sqrt{1+4T_T} - 1}{2T_T}$$

Equation 2-7: Reflection coefficient equations by Kriebel (1992) as summarised by Suh (2011)

$$K_R = 1 - K_T$$

T_T is the transmission function which is defined in the text by Suh and solvable. The only criticism on Kriebel's formulae is that it is derived with no energy losses being accounted for. It is therefore proposed to use the energy loss equation as per Equation 2-1 (Isaacson, 1998).

Further summaries from the Suh paper include the following review of previous equations:

- For Yu (1995), friction and added mass coefficients are unknown. Therefore, this was not used further in this thesis.
- Various authors (Sollitt & Cross, Losada, Yu, Isaacson, Zhu et al) proposed to use added mass coefficient $C_m = 0$ or $s = 1$ between predicted and experimental values of reflection and transmissions coefficients of perforated structures.
- Li (2006) proposed empirical formulae for the friction coefficient as a function of wall thickness and water depth
- Kim (1998) yielded incorrect results for long waves. It is noted that long waves penetrate much more easily through a permeable barrier than shorter crested waves. This also correlates with the findings so far on wave steepness.

Zhu (2011) followed an impedance analytical method to study interaction of regular plane waves with a row of rectangular piles by postulating further derivations of the velocity potential and flow resistance of fluid passing through, with an added mass coefficient to account for losses. No explicit equation is offered for further calculation of predicted values.

Li *et al*. (2013) has developed testing methods and theoretical approaches to study wave run-up and forces on piles in more detail than had been available in previous work. This work was not taken into account in the current study although it is useful to note the advancements of this work and that there are still many fields in and surrounding the piled row breakwater environment that requires further research, as mentioned in section 1.4.1.

2.4 Theory Review for Multiple screens

A further application of piled row breakwaters is by utilising multiple parallel rows, at uniform spacing over the length of the breakwaters. This would be intended to duplicate the attenuating effect of the piled row over a defined distance.

Twu and Lin (1991) studied the multiple piled screen in a navigation infrastructure application. The study pointed out that the absorption effect is heavily reliant on the spacing between the screens, with a strong dependency on relative depth and wave steepness.

Thompson (2000) also studied results from multiple wave screens for comparison with single screens. He found that the porosity of the first screen is the determining factor for the overall performance of the wave absorber.

For the purpose of this study it is only worth mentioning that multiple screens have been researched to some extent through physical modelling and statistical analysis. Thomson did, however, attempt to derive empirical equations with the following variables, i.e. screen porosity, wave steepness, $d/(g \times T^2)$, and the second screen's porosity.

2.5 Applications & Case Studies

2.5.1 Piled cylinders as screens in Coastal Protection

Permeable pile groins (i.e. orientated normal to a coastline) by Raudkivi (1996) were studied in a broad effort to capture some historical performance of these structures from shoreline profiles. The study indicated over 150 years of installation records, although with little technical data on performance and efficiency of the installations.

Compared to piled row breakwaters, the installations for stabilisation of coastlines would generally require to be higher porosity installations, with the result that the effect of piled row groins on waves being little to negligible. For coastal stabilisation to be affected, the pile groins must function by affecting the velocity, velocity-distribution, and turbulence. Raudkivi stated the scarcity on these aspects in literature. Raudkivi states that the effectiveness of the piled row groins in the shoreline lies with the added hydraulic roughness on the longshore current with negligible effect on waves. Various benefits of this type of stabilisation structure are offered and include the following (See Figure 2-4):

- Reducing but not blocking longshore current
- Not saw-toothed result on the shoreline, i.e. less accentuated eroded sections in the leeward side of groins.

For the purpose of this thesis, this application discussion is useful, but will not be discussed in further detail.

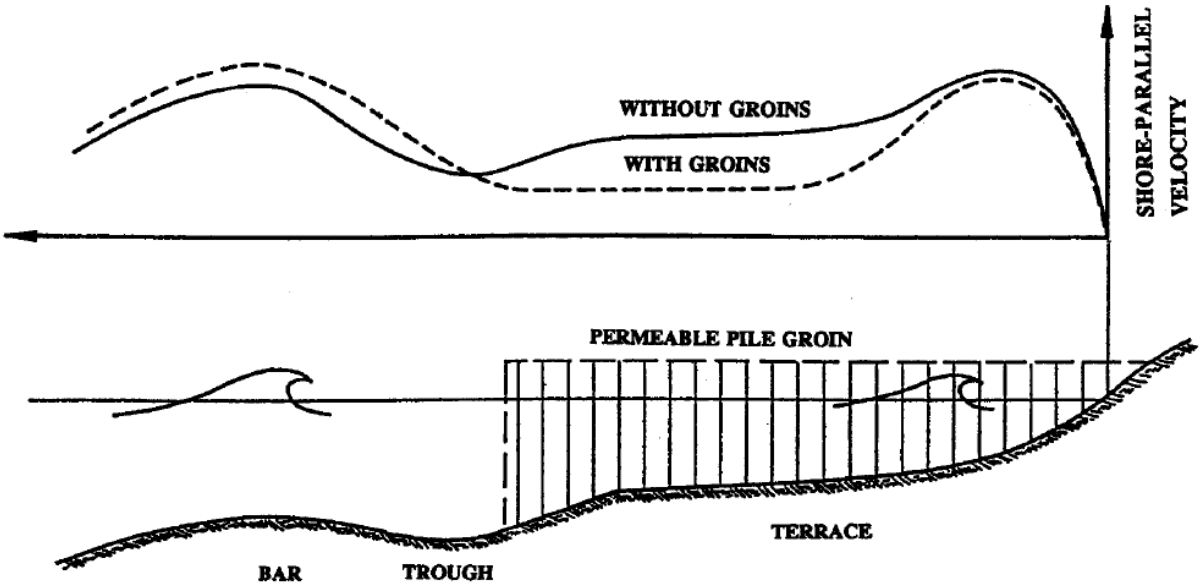

Figure 2-4: Schematic beach profile on southern coast of baltic sea (from Raudkivi, 1996)

Another case study by Reedijk & Allsop (2003) was reviewed that considered a series of parallel pile row breakwaters (i.e. orientated parallel to a coastline) for Pelangi Beach, Malaysia. The design was done for a site where serious coastal erosion threatened a popular recreational beach and resort area. The motivations cited for the use of piled rows for the structure as opposed to conventional dumped rock breakwater was the relative mild wave climate, the desire to have minimal lasting visual impacts and the permitted movement of sediment through the breakwaters (See Figure 2-5).

The wave transmission coefficient was designed to 60% at high water. From Figure 2-6 and Figure 2-7 the growth of the shoreline leeward of the piled row demonstrates the effectiveness of the installation. However, no mention is made on whether the long term intention was to develop beaches up to the breakwaters, effectively resulting in transmission coefficients of 0%.

It is interesting to note that the installation of the piles was done by land based rigs that could access the breakwater location on low tide. Pile elements were from concrete spun piles.

No theoretical or numerical explanations are offered in this paper, but it is valuable to refer to as a working case study.

Figure 2-5: Elevation of the piles at low tide, showing relative close spacing (Reedijk & Allsop, 2003)

Figure 2-6: Overview of growing beach behind parallel pile row, by Reedijk (2003)

Figure 2-7: Surveyed shoreline (yellow line) overlain on shoreline prior to installation; Parallel pile row breakwaters shown by red line, by Reedijk (2003)

In another case study (Atkins & Mocke *et al*., 2009) the use of a parallel pile supported wavescreen was discussed. The primary purpose of the design was to provide protected mooring for a marina in Blairgowrie, Australia. The breakwater consisted of an impermeable vertical panel, which only extended from above the water level downwards to the seafloor, supported on a row of piles (See Figure 2-9). The paper focussed on the construction of the harbour as well as the salient formation in the lee of the parallel breakwater (See Figure 2-10).

The growth of the salient was compared to prediction methods by Black as well as USACE and it was found that neither of these methods correctly predicted the growth rate behind this type of breakwater. It would be prudent to take note of the likelihood that salient growth could occur in a marina environment, especially as sediment transport is not cut off by permeable pile rows. No current methods for predicting this type of shoreline response was sourced during this thesis.

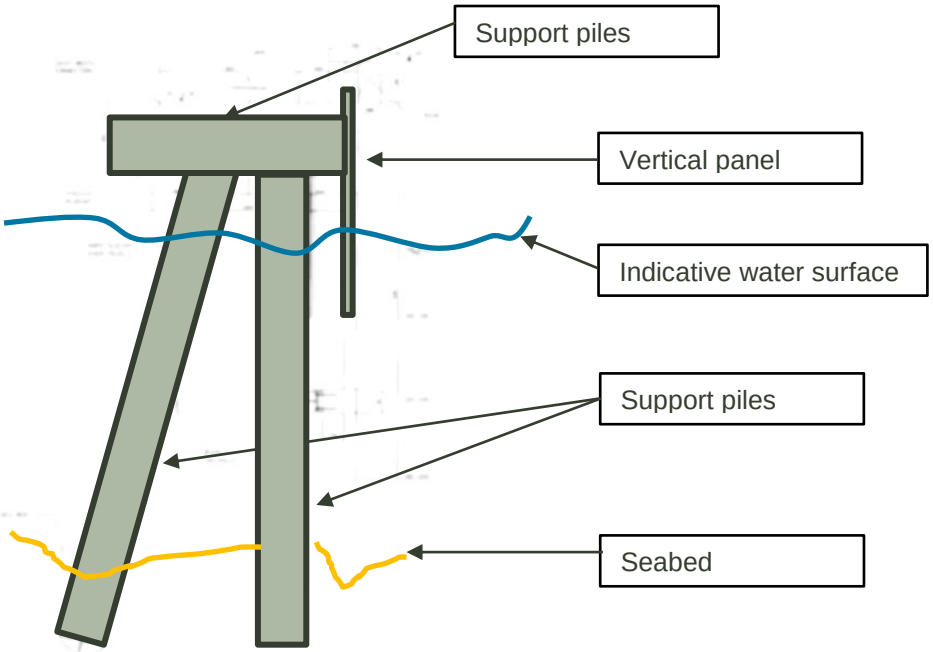

Figure 2-8: Schematic cross section through the wave screen indicating vertical impermeable panel (adapted from Atkins & Mocke 2009)

Figure 2-9: Image during construction of Blairgowrie wave screen, showing piles and impermeable panel to the right of the image (Atkins & Mocke, 2009)

Figure 2-10 - Salient growth (Y_{off} dimension) behind offshore piled parallel wave screen at Blairgowrie by Atkins & Mocke (2009). Salient line shown in red.

Important to note is that this application was an impermeable screen supported on piles, but there were certain aspects of importance to the wave screen study field. Some of the key observations include the following:

i) Construction was done over water with marine based equipment. This could be assumed to be similar to installation of a piled row breakwater.

ii) Salient growth slowed over time behind the installed parallel breakwater, indicating some equilibrium achieved on the shoreline some time after the installation.

iii) Salient growth did not correspond too well with the Reef formulae of Black et al (2003). The rate of salient growth over longer term, compared to that derived by Black could point out that this wave screen had a lower effectiveness than an artificially constructed reef.

iv) Bed scour around the piles seemed accentuated in comparison to what was anticipated.

v) The author of the Blairgowrie paper hypothesised that the observed slowdown in the salient growth rate could be attributed to the increased wave energy that penetrated the harbour as scour increased and stabilised and that this could be due to longer period waves.

2.5.2 Creation of a tug harbour in open sea as an alternative to more conventional methods

Nilsen *et al.* (2000) conducted a study and preliminary design phase for a piled arch tug harbour concept on behalf of Robe River Iron Associates. The intent was to study the viability of a harbour for port service vessels, including tugs and the line service boat, to be formed from a piled structure in an arch shape, because of the non-availability of rock for a more conventional breakwater.

Physical modelling was undertaken to determine the reflection and transmission coefficients after which the coefficients were used in a numerical model setup to run a range of configuration options. This was an effective way of overcoming the problem of the theoretical approach to determine the coefficients, which have been shown in the theoretical overview section, could be a daunting task, based on the complexity of certain theories and postulated equations.

Various configurations in terms of the arch size and shapes, as well as the pile spacing were explored to build up a database of transmission and reflection coefficients. One such a configuration is shown in Figure 2-11.

Key outcomes of this exercise were:

- A study that was developed with both numerical and physical modelling to leverage the advantages of both aspects.
- Preliminary designs of the tug harbour structure was performed as a reality check on the type of prototypes recommended. The value of this is that the eventual preliminary designs have been compared to conventional construction methods and found to be a very suitable alternative
- Wave testing done for swell and cyclone climates, i.e. not only protected environments
- Operational conditions were taken from actual port authority requirements and therefore this case study was quite realistic although the implementation had not yet been undertaken.
- Little difference noted between 120 degree and 180 degree arch breakwaters for wave attack normal to the symmetrical axis of the harbour.
- 7% porosity yielded transmission coefficients in the order of 50%
- The raking of piles, with pile heads collinear, raking every second pile in the same direction, provided poor performance of the breakwater.

- Further closing of gaps between piles, by additional angles and attached smaller elements, did yield lower transmission coefficients, i.e. better performance.
- For double row piles, the spacing between the parallel pile rows were approximately equal to one quarter of the wave length yielded the best results.

The technical feasibility of this piled arch breakwater concept was proven through the investigations, although it has not yet been constructed.

Figure 2-11: Example of physical model scale breakwater for laboratory testing (Nilsen *et al.* 2000)

2.6 Theory in Practice

For the literature reviewed to be applied when selecting options for concept development as part of engineering practice, a broad approach would be required to ensure all the variables have been understood. The literature provided insights on expected piled row breakwater performance, however the author had not obtained a document that provided guidance to designers, that could therefore be of assistance when evaluating and developing options for implementation. It would be advisable to consult a range of papers and case studies to understand all aspects that it was necessary to consider before a concept could be evaluated, which would include at least the following aspects and interrelationships:

- Application of porosity range – literature suggests porosities lower than 50% to be considered from the offset (Allsop & Hettiarachchi (1988), Isaacson (1998))
- Selected single or multiple screens for the piled row breakwater – their expected performance (Twu & Lin (1991), Thomson (2000) & Nilsen (2000).
- K_T, and K_R and energy loss parameters for the possible configurations – for achieving design criteria (See various references in section 2.3)
- Wave run-up – for determining the freeboard required, where horizontal deck elements need to be incorporated, for example a pedestrian or pier walkway surface is required (Li *et al.*(2013).
- Wave forces on piles – for the structural design of the piled element. (Thomson (2000), Suh *et al.*(2011) & Li *et al.*(2013).
- Bed scour around piles – affects design of the pile elements
- Constructability of piled configurations – from consulting case studies and construction specialists.
- Pile material considerations, such as durability and limitations for construction loads.

2.7 Recent advancements in numerical modelling

The increased attention that piled row breakwaters have received as alternative options over approximately the past two decades also creates the opportunity for new approaches to solve the rather complex environment of energy dissipation through a piled or slotted screen. Schlenkhoff et al (2012) used Particle Image Velocimetry (PIV) in a laboratory and three dimensional modelling (FLOW-3D) to investigate the hydraulic performance of a wave screen (referred to as a permeable breakwater in their paper).

The physical testing was done in a 24m long flume, 0,3 m wide and 0.5m deep in a constant water depth of 0.3m. A piled row with porosity of 50% was tested in all the tests.

The paper concluded that the FLOW-3d model is capable of simulating the key interactions of the hydraulic performance at the wave screen.

The graphical results that can be produced by numerical modelling packages similar to that of FLOW-3D presents very interesting imagery that would certainly be valuable in the sense that

numerical results can be produced at any time step and potentially also animated at any speed for the operator to home in on certain aspects. It is also expected to advance the understanding of the flow intricacies for various configurations. Figure 2-12 indicates an output for a timestep for different input wave parameters.

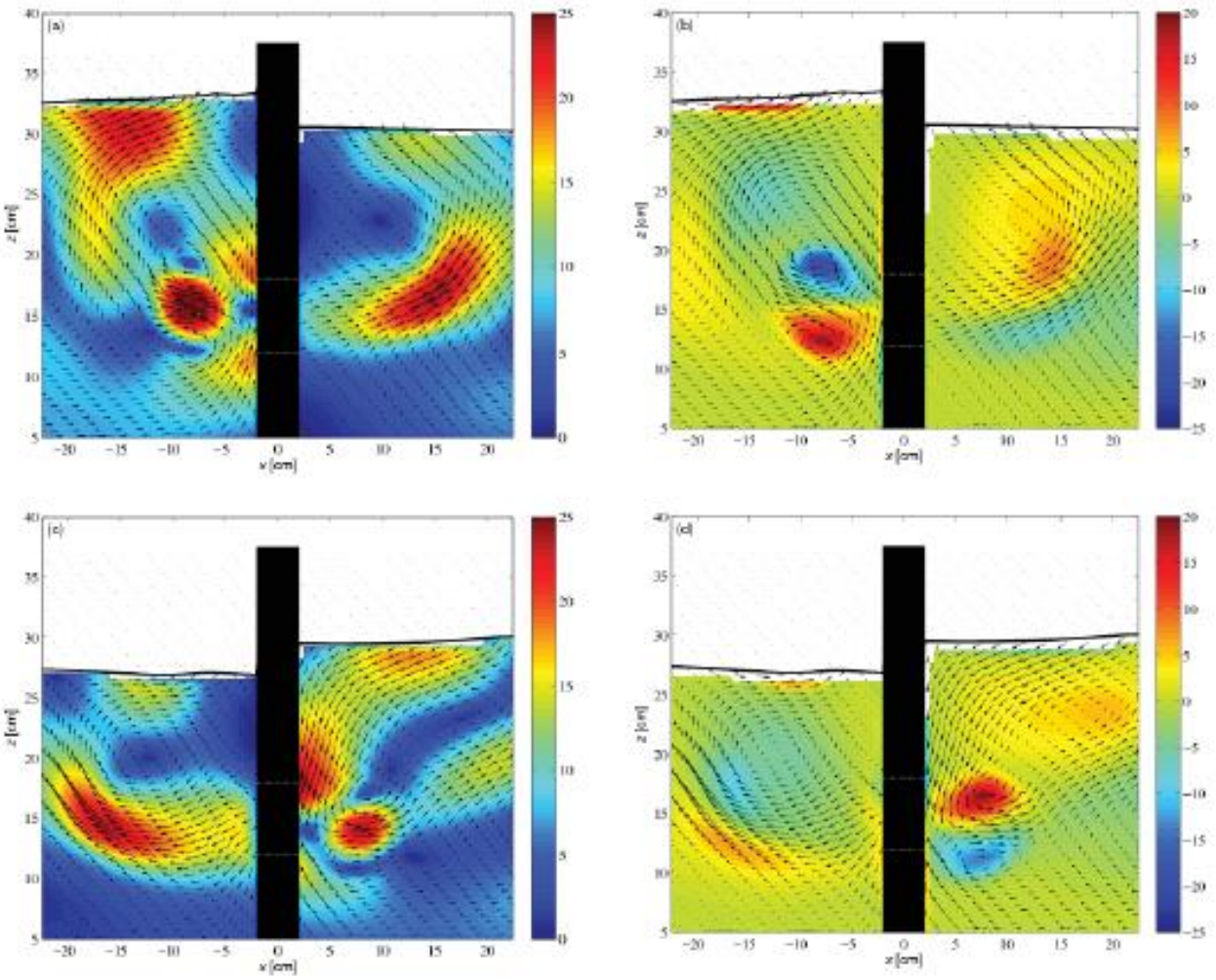

Figure 2-12: An Example of the type of output from velocity magnitude and vectors from FLOW-3D results for four different wave input cases (Schlenkhoff et al, 2012)

3 Physical Modelling

3.1 Introduction to the Physical Model setup

It was decided to undertake the testing of piled breakwater configurations in the large wave flume at the University of Stellenbosch Hydraulics Laboratory. The flume is a 60 meter long, 2 meter wide by 2 meter deep facility equipped with a set of two bottom hinged paddles for generation of waves, which is driven by the HR Wallingford EQ 1026 wave generation system (ref HR WALLINGFORD EQ 1026, 2010). The following sections provide an overview of the available equipment, the selected scale, the set-up and preparations done for the current study and the test programme, as well as the data capturing process.

3.2 Equipment Description

3.2.1 Wave flume

The wave flume was previously fitted with a sloping bed at approximately the mid-length of the basin which provides a gradual slope up to a shallower bed testing area. See figure Figure 3-1 for a cross section of the flume. The tank and beds were surveyed with tape measure and standard levelling equipment to check the levels and dimensions (see section 3.2.2 for photos). More dimensions and survey data for the test bed is included in Appendix A. For the recommended operational water depth of 1.5m the shallow test bed provides approximately 0.4m of water depth. For the purposes of testing required for this paper, the tank was filled to a general depth of more than 1.7m in order to provide a testing depth of between 0.65 m and 0.57 m of water depth.

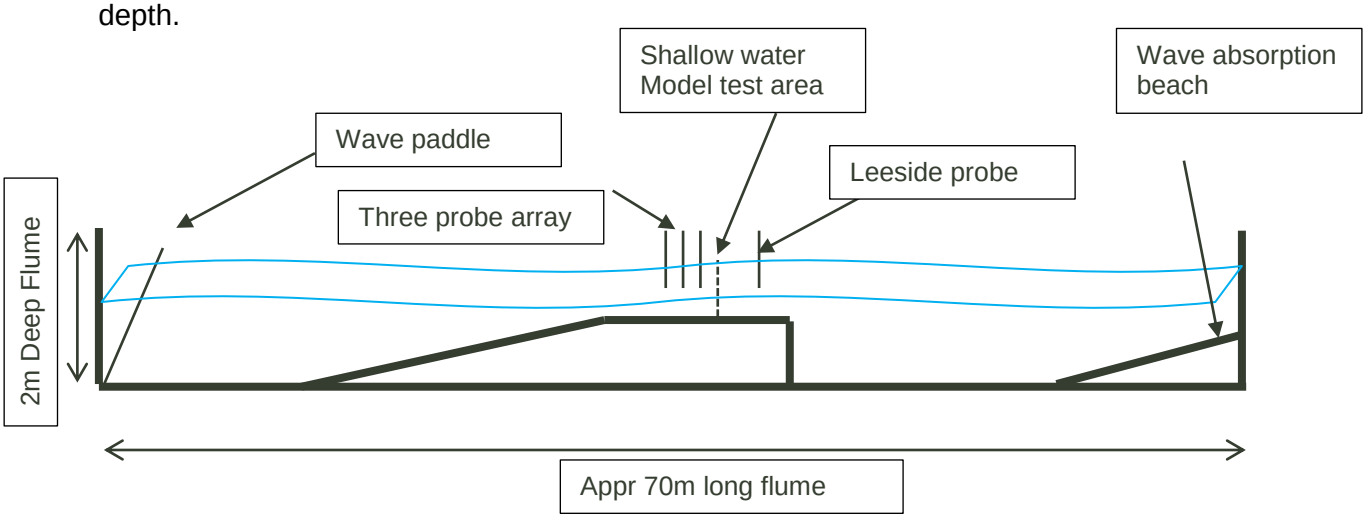

Figure 3-1: Schematic cross section of the flume (Details provided in Appendix A)

Figure 3-2: Side view of wave flume with elevated catwalk

Figure 3-3: View from inside the tank, looking towards sloping section and the shallow test bed in the background

Figure 3-4: Front view on dual bottom hinged wave paddle. Visible on the surface are the resistance probes for the wave absorption system

3.2.2 HR Wallingford Wave Maker

The wave paddle input system is controlled from a PC by means of the HR Wavemaker software suite installed. The input system sends a signal to the remote controlled function generator unit which instructs the wave paddle controls and motor drives. A schematic process flow diagram (see Figure A.2) has been included in Appendix A to show how the system has been set-up. To operate the wave flume and wave generation system, a thorough understanding of the equipment is required in order to not have signal interruptions and unexpected malfunctioning of the wave paddles. Due to the age and condition of the equipment, the set-up and general testing procedures took longer than initially anticipated, but good performance was achieved.

The wave generation capacity is captured by the performance curves shown in Figure 3-5 below. The curves are interpreted for water depths at the wave paddle; in this case the upper curve shown in Figure 3-5 (i.e. water depth at the wave paddle of 1.5m) was the relevant curve to which the testing work was initially designed.

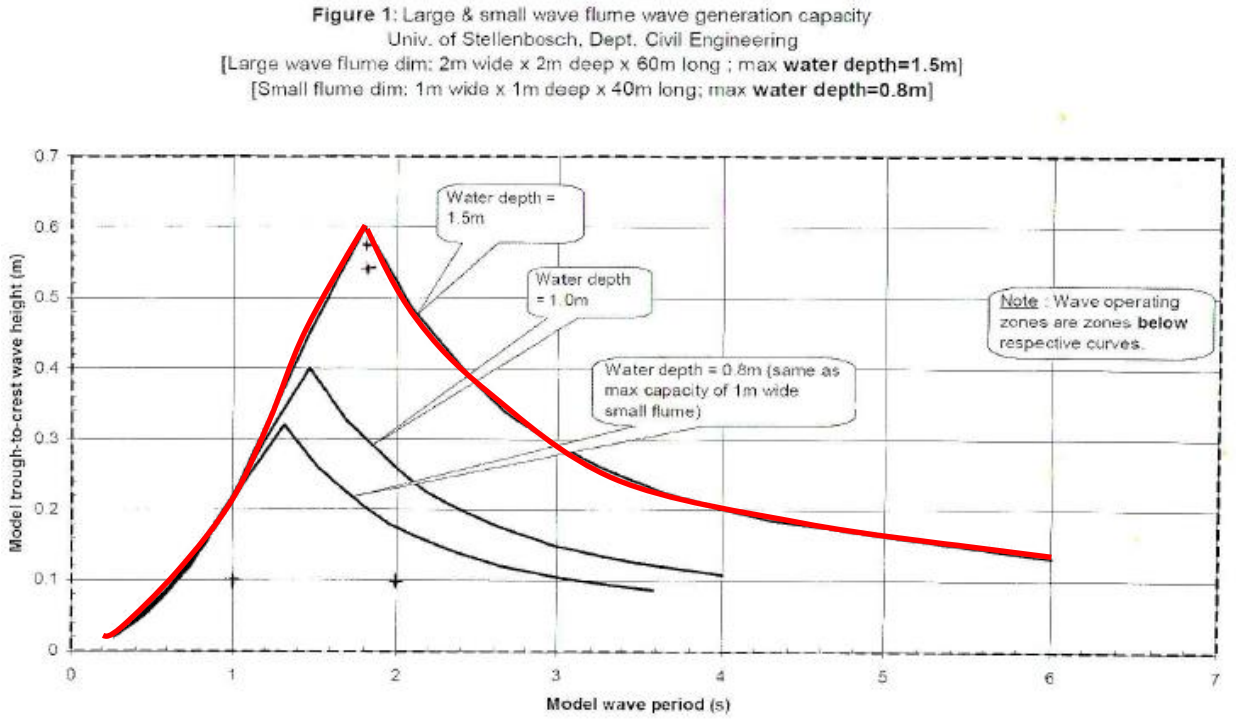

Figure 3-5 Wave performance curve showing wave height capability over wave period, for specified water depths (See red line)

The HR Wavemaker system is able to generate and feed signals for regular and irregular waves, i.e. wave spectra according to JONSWAP spectral rules.

3.2.3 HRDAQ Capturing System

For measuring wave heights in the flume, resistance wave probes were set up which output fed into a HR DAQ data capturing system. This operates completely independently of the wave paddle and related input systems. The calibration and capture sensitivity of the probes could be managed and adjusted from the HR DAQ system..

In order to be able to calculate reflected waves from the piled breakwater model, an array of wave probes had to be set-up. The HR DAQ system requires that a four probe array is utilised, however because of the requirement of transmitted wave heights that also had to be measured, only a three probe array could be utilised (since the available amount of probes is a total of 4). The external data post processing is discussed in section 4. The result of the change in wave probe array setup was both on the testing programme and the model set-up. The reason for this was that a pre-determined set-up of the wave probe spacing had to be used in order to calculate reflection coefficients by the method of least squares (Mansard & Funke, 1980). This resulted in additional time taken upfront in the iterations by the determination of a suitable model scale and also because the post processing had to be done at a later stage at the CSIR in Stellenbosch.

3.3 Model Scale

3.3.1 Scale determination process

This section provides a brief overview of the process undertaken to choose a realistic wave height, wave period and water depth for the prototype cases. Concurrently, the largest possible model scale was determined in order to minimise scale effects while still ensuring the testing was within the model wave generation capacity. In order to relate the testing data to potential sites where small craft harbours or marinas could be located, the scaling of the test was determined through an iterative process. The steps followed were:

- From three potential sites, the local generated wave spectra were estimated by utilising the online toolkit Coastal and River Engineering Support System (CRESS), made available by the Netherlands Ministry of Infrastructure and Environment, Delft University of Technology and UNESCO-IHE.
- The wave height and model dimensions were checked against potential water depths at the proponent sites.
- Information found in literature by (Hughes, 1993) was applied to set up the geometric and kinematic scale factors that would be suitable for the available water depth on the shallow test bed.
- The model scale parameters were then checked against the wave flume depth, and the scaled wave paddle performance graphs (for significant wave height and peak period parameters), to fall within the capabilities of the wave generator. The most important parameter to verify was whether the wave probes could be set-up for this scale and wave input parameters. The probe spacing is briefly discussed in section3.6.1.
- The scaling calculation of the model was repeated for a few possible geometric scaling factors in order to determine a range of valid input wave performance criteria. This was done in order to determine the optimal setup that would not require repetitive reconfiguration of the wave probes between tests where the wave input parameters varied.

The main purpose of the scaling exercise was to target the wave spectra corresponding to the calculated fetch- or depth limited wave spectra at the marina sites. The upper range of the peak period was included to fall within the limits of the wave generator performance graph so that an upper peak period could be investigated for the performance of piled row breakwaters. This was necessary to understand due to the possibility of longer period swell that could be present at the prototype cases.

3.3.2 Potential marina sites

The figures Figure 3-6 to Figure 3-8 contain extracts from Google Earth with the locations of three possible marinas, being the Knysna lagoon in the Western Cape, South Africa, Walvis Bay on the Namibian Coast and Lagos Lagoon in Nigeria. These were considered to provide possible locations, with the Knysna lagoon being the exception in that a marina already exists on the North Eastern section.

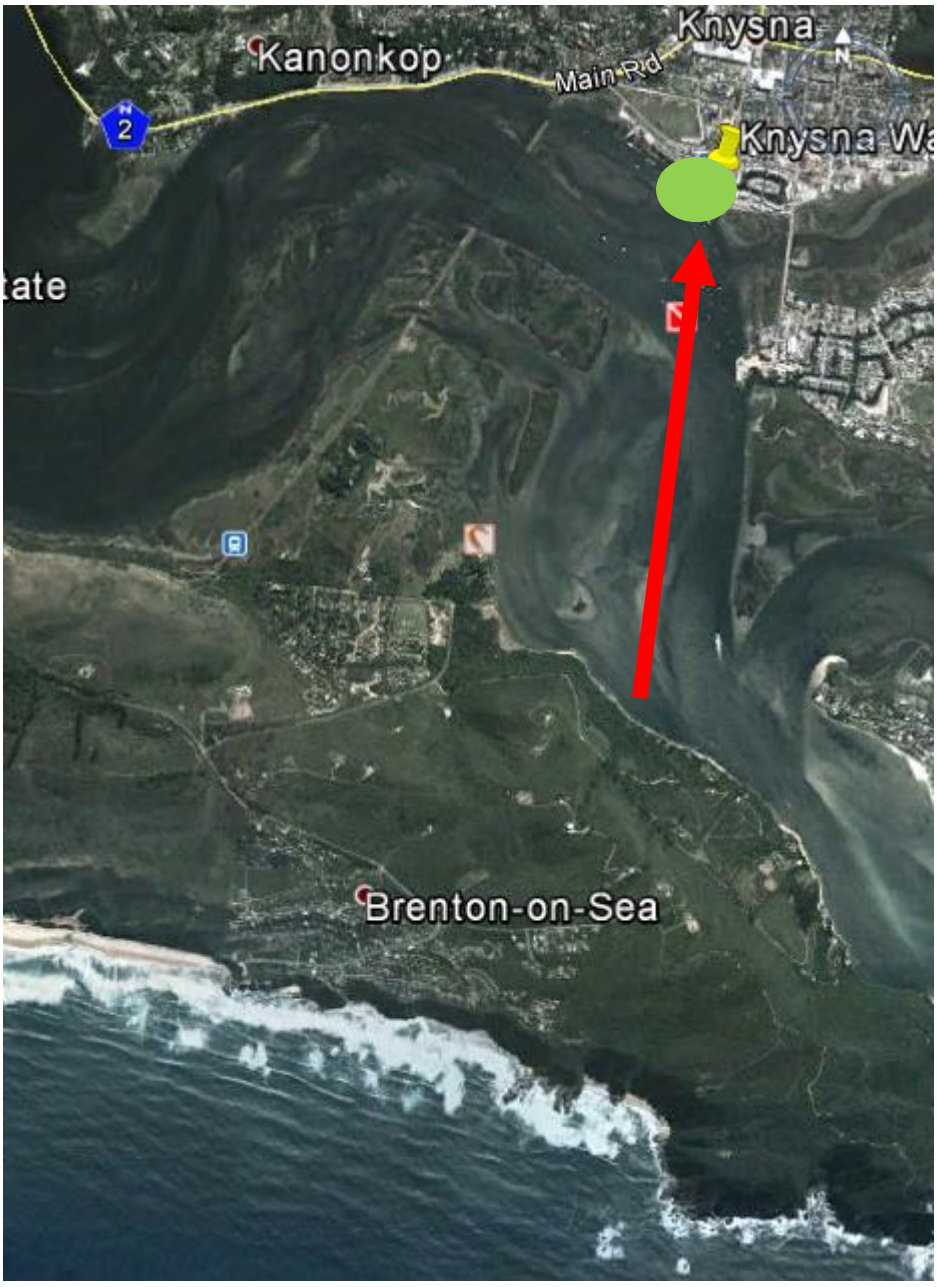

Figure 3-6: Knysna Lagoon, showing the 4 km fetch distance and marina location (Google Earth unlicensed version)

Figure 3-7: Lagos lagoon showing a 12 km fetch distance and proposed marina location (Google Earth version)

Figure 3-8: Walvis Bay (Namibia) indicating fetch distance and the possible marina location

3.3.3 Shallow Water Fetch-limited wave spectra

The calculated wave spectra was done for an assumed extreme one hourly mean wind speed of 25 m/s for all the sites and a water depth of 3m for a fetch distance of 4km. The related wave is listed below in table (Table 3-1) for reference.

Table 3-1: Summary of wave data parameters from the sites

Location	Fetch (km)	Windspeed (m/s)	d (m) (Assumed)	Hs (m)	$T_{P\ (s)}$
Knysna Lagoon	2.5	25	3	0.77	3
Lagos lagoon	14	25	3	0.94	4
Walvis baai.	4	25	3	0.84	4

Although a wind sensitivity studied would be required to determine the return period for design winds, the 25m/s has been selected as a fairly strong wind over five hours for any coastal site, but was kept consistent to illustrate the effect of varying fetch lengths in terms of wave exposure for the various sites.

3.3.4 Model Wave Height & Period scaling

The selected range of wave spectra was done through an iterative process; keeping in mind that time is a limitation on the number of tests and the time taken for modifying the setup in between test runs. The final result after numerous iterations was to set the model scale to 1:5. More tables with probe spacing calculations and model scale calculations have been included in Appendix B.

3.4 Set-up and modifications for testing

3.4.1 Absorption Beach

After the flume was set up to run and before the piled row breakwater test models were installed, the author spent considerable time to develop an absorption beach at the rear of the wave flume in order to minimise the waves reflected back into the test area. Ideally, an additional 3 wave probe array should be used on the leeward side of the test area in order to determine the reflected waves from the rear.

The absorption beach was built with materials that were available in the laboratory. This included model geosynthetic containers (GSC, i.e. small sandbags), a fishing net and model breakwater

armour units. At this stage, the 4 waveprobe array was used to determine the bulk reflection coefficient with the HRDAQ software. Adjustments were made to the absorption beach configuration until the reflection coefficient was between 5 and 15%, depending on the input waves. Figure 3-9: Wave absorption beach showing GSC's, fishing net and packed armour units in the backshows an oblique view of the final absorption beach. The components that were created and that contributed to the efficiency, was as follows:

- Underwater slope from GSC's (roughly at 1:5)
- Fishing net to absorb overtopped waves and induced currents from the overtopping
- Rear screen of armour units to dissipate the remaining waves

Figure 3-9: Wave absorption beach showing GSC's, fishing net and packed armour units in the back

3.4.2 Piled row breakwater test model

Piled row breakwater prototypes were constructed from polyvinylchloride (PVC) domestic downpipe sections. The make-up of the screen had to satisfy the following criteria:

- Water resistant elements, i.e. preferably it should not be susceptible to corrosion or water absorption that could influence the structural or hydrodynamic properties.
- Flexible system to be able to adjust the porosity by adding or removing pile elements.

- Flexible to interchange between round, square and diagonally square sections for testing purposes
- Robust enough to withstand the wave forces and handling during testing.

An example of the initial installation with the round sections is shown below in Figure 3-10. The top bracket clamp system was developed to be flexible, but firm enough to keep the piles fixed in the top position. Although the bracket had some own weight to create downward pressure on the model screen, additional dead weight in the form of concrete blocks were added to ensure the top rail would remain in position. More photos of the model setup have been included in Appendix A.

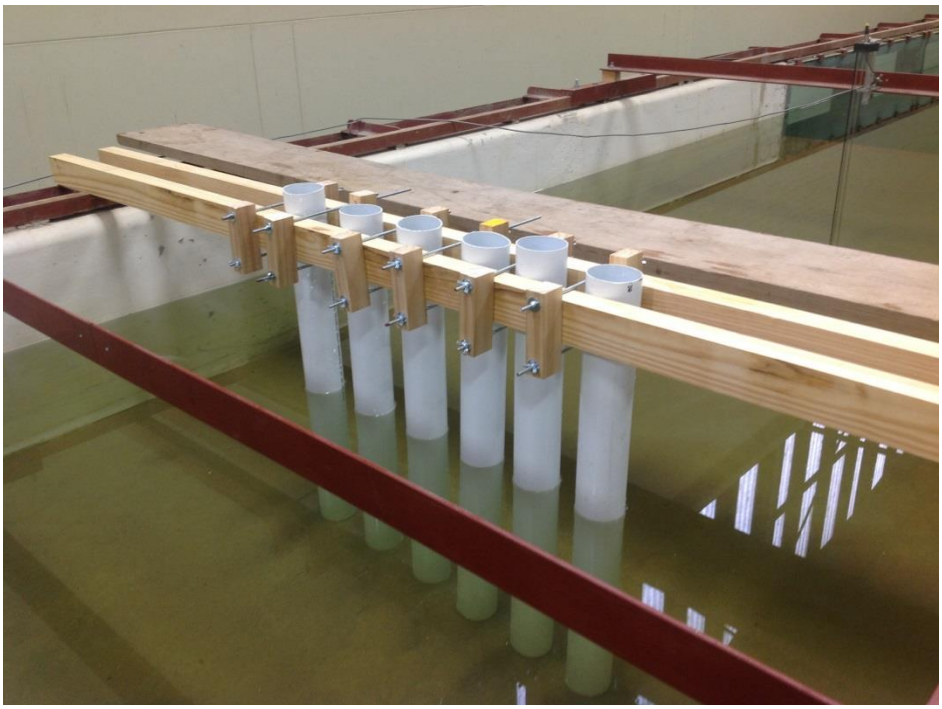

Figure 3-10: Trial installation of few piles to test the installation system

One of the drawbacks for the selected breakwater model system was that due to the commercially available element sizes, the screen could not be setup for the exact same porosities for the different element shapes. For the material that was acquired for this study, there is a limited range of diameters per shape. Although similar porosities across the different shapes could be achieved with partial cross sections on the sidewalls, the aim was to set up a uniform porosity over the length of the model breakwater, and avoid possible local effects on the sides that could impact on the modelling and results.

3.4.3 Modifications after initial tests

After the initial testing was done with a reduced number of piles, the screen was set up for a porosity of approximately 44% in order to investigate the response of the test model under varying wave conditions. It was clear that the wave forces on the piles were of such a magnitude that the bottom end of the piles would not remain in position due to friction only, and a bottom rail was subsequently installed, consisting of a 35mm high angle iron section. Subsequently, the bottom end of all the piled elements were slotted, so as to fit snug onto the bottom mounted rail and thereby providing a restraint at the bottom end of the individual piles and the model overall (See Figure 3-11) .

When the screen porosity was reduced in later tests, the bottom mounted rail had to be refitted with increased number of holding down bolts due to the initial installation that sheared off the holding down bolts. This resulted in some unexpected delays to the testing programme.

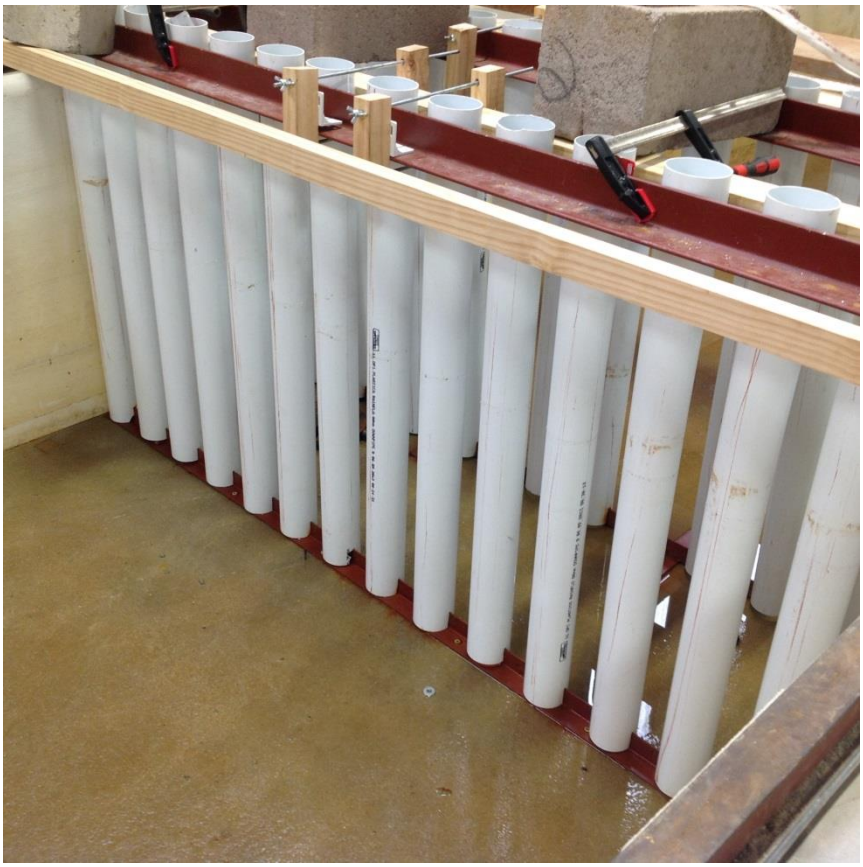

Figure 3-11: Typical installation showing bottom rail anchored to test bed

In addition to the concrete blocks at the top bracket the screen was secured further at the top by friction that was provided by means of general clamps (See Appendix A).

Although the testing programme did not include extensive testing of the double screen, a second model screen was also constructed. The intention was to provide a second screen that could be placed at various locations in relation to the single screen. However, the test programme was not extended to include sufficient testing with the double screen to include this as test data and for analysing.

3.4.4 Challenges with test equipment

The setup and initial trial runs with the wave flume and wave generation system took considerable time to become acquainted with the equipment and the sensitivities of operations thereof.

- The age and condition of the equipment is of concern in that there were several breakdowns and subsequent delays that could not always be traced to exact causes. In many instances the malfunctioning of the wave paddle or the signal generation system seemed to be occurring at random and not related to any steps that could be retraced and avoided. Subsequent to several trial runs to get familiar with the equipment and to fine-tune the absorption beach setup, a total amount of 110 test runs results were retained which represents a fair amount of effort and resulted in a broad database for studying results and conducting validation with previous work, as well as analysis of the current data.

- Although the performance curve for the wave paddle includes low amplitude long frequency waves (for example H_s = 0.05 with T_P = 2.941 s) it appeared that this range of waves was not as smoothly generated as the steeper waves. The reason could be one of many, but the author observed secondary ripples on the lower steepness waves which could be contributed to the drive system. These lower steepness waves were abandoned for the latter part of the testing

- The wave absorption system in the large flume also appeared to not work consistently and the author experienced longer periods of basin calming with the absorption system, as opposed to without the absorption system. For screens with low porosity, the basin took considerable time to calm and this was also then evident from some tests that a pre-existing wave could have been present from a previous test run. This was however

assumed to have a negligible effect on the results as the data capturing and analysis would consider all measured wave energy and from there determine the incident and reflected wave heights.

- Due to a shortage on resistance wave probes, only the post processing of the test data had to be undertaken at the facility of the nearby CSIR in Stellenbosch. However, all the model tests in terms of setting up test runs, data gathering and initial processing was conducted by the author at the Stellenbosch University hydraulics laboratory.

3.5 Test programme

During the setup of the test and initial runs conducted to gain familiarisation with the facility it appeared that the critical path for execution was the waiting period for basin calming, in between tests. Ideally, post processing of completed tests should be done in this waiting period, in addition to preparations of the screen and input parameters for the following test.

From literature, the porosity was selected to not be more than 0.5 as the screens become very inefficient for higher values. From the section discussing scaling, the wave periods and heights were selected. The variables for the testing of round square and diagonal square sections were set as follows, and this resulted in the number of tests conducted (See Table 3-2).

Cross section of pile	Porosities (as %)	f (Hz) [T (s)]	Hs (m)
Round	4%, 20%, 36%, 40% (44%)	0.34, 0.45, 0.596 [2.941, 2.222, 1.678]	(0.05), 0.1, 0.2, 0.3, (0.4)
Square	10%, 25%, 40%	0.34, 0.45, 0.596 [2.941, 2.222, 1.678]	(0.05), 0.1, 0.2, 0.3, (0.4)
Rotated (45 Diag) Square	5%, 48%	0.34, 0.45, 0.596 [2.941, 2.222, 1.678]	(0.05), 0.1, 0.2, 0.3, (0.4)

Table 3-2 Test variables

It must be noted that values in rounded brackets were omitted in some cases where either the performance curve of the paddle could not produce the combination between Hs and Tp, or where overtopping of the structure became a concern for the integrity of the installation. A full set of test runs can be viewed in in Appendix C.

3.6 Data Acquisition

3.6.1 Recording of results

The wave probe array was set up to satisfy scaling as well as processing rules. Appendix B contains the table showing the various spacings considered. According to the method of least squares by Mansard & Funke, the probe spacing has to satisfy the following rules:

i) $L_p/6 < X_{13} < L_p/3$;

ii) X_{13} should not be equal to $L_p/5$ and

iii) X_{13} should not be equal to $3L_p/10$

Where

- The first probe is closest to the wave paddle and the third probe is closest to the breakwater model
- X_{13} = the distance from the first probe to the third probe
- X_{12} = the distance from the first probe to the second probe
- $X_{12} = L_p/10$
- $L_p = \text{TANH}\frac{4\pi 2d}{TP2g} \times 0.5\ T_P{}^2 \frac{g}{2\pi}$

From the worksheet in Appendix B the selected spacing was thus:

X_{12} = 600mm

X_{13} = 1200mm

Figure 3-12 shows the setup of the wave probes, with minor modifications incorporated by the author to reduce turnaround time of probe calibration. Also, due to time constraints it was

decided to select a spacing setup that would not require to be changed between testing of various Tp and Hs.

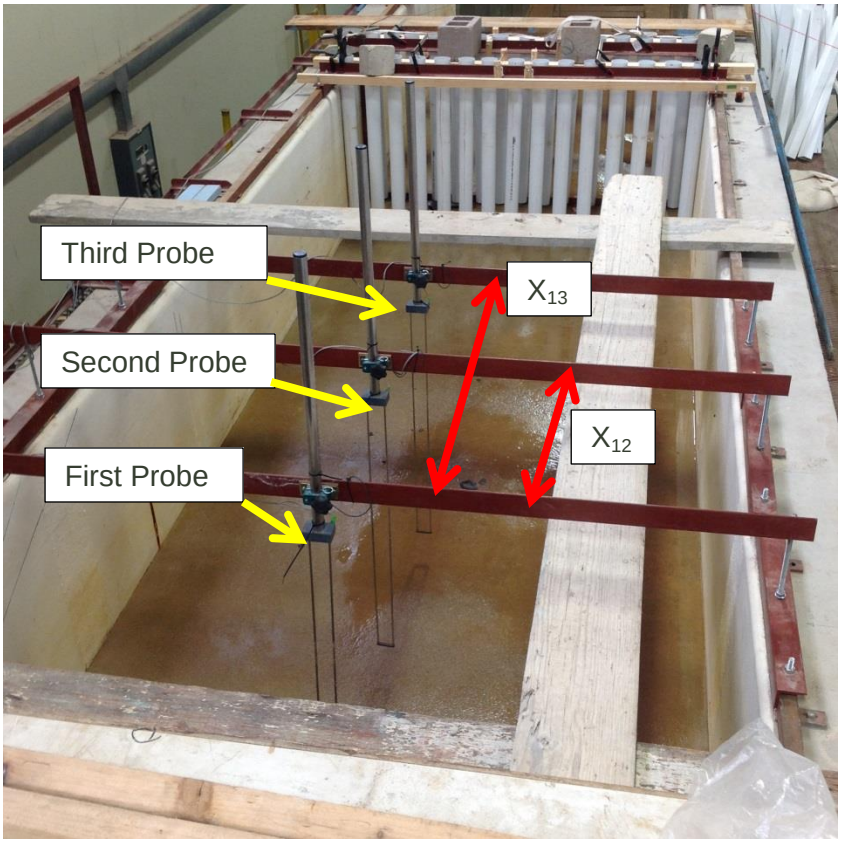

Figure 3-12: Wave probe set-up, with X12 and X13 marked-up and the test screen in the background

3.6.2 Observations during testing

The photos included in Figure 3-13 to Figure 3-18 highlight some observations during the testing as indicated in the titles of the figures.

Figure 3-13: Mild turbulence for high porosity is visible next to the piled row as seen from the seaward side.

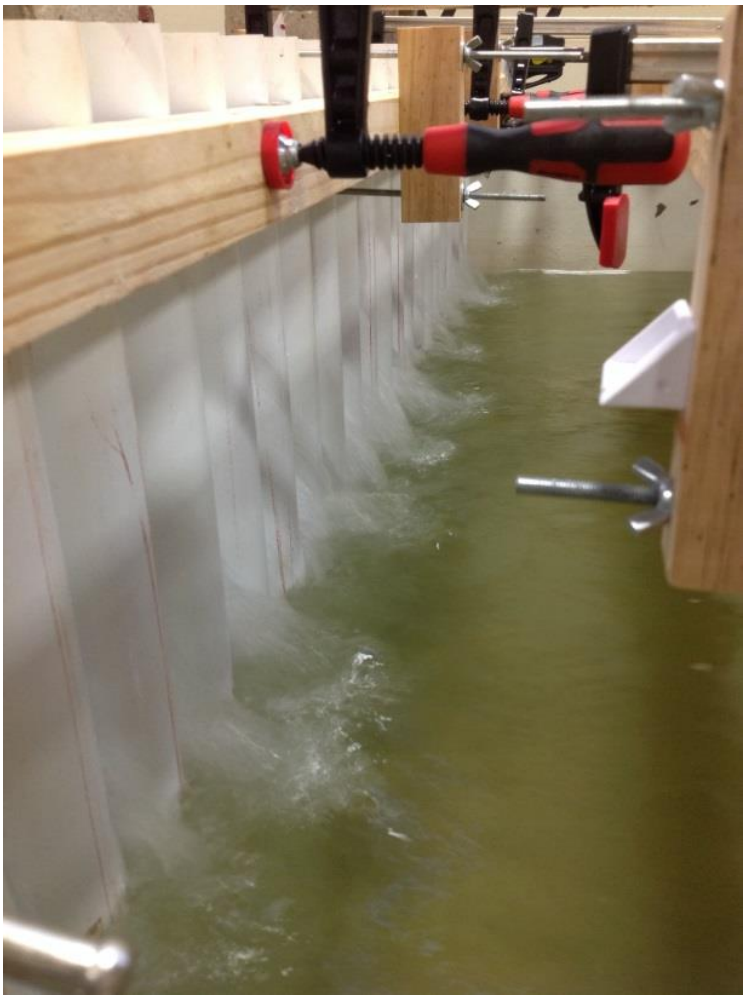

Figure 3-14: Turbulence on leeward side of piled row, during transmission

Figure 3-15: Turbulence on the leeward side after wave has been transmitted.

Figure 3-16: Turbulence around the piled row section for square pile elements shown here as seen from the seaward side.

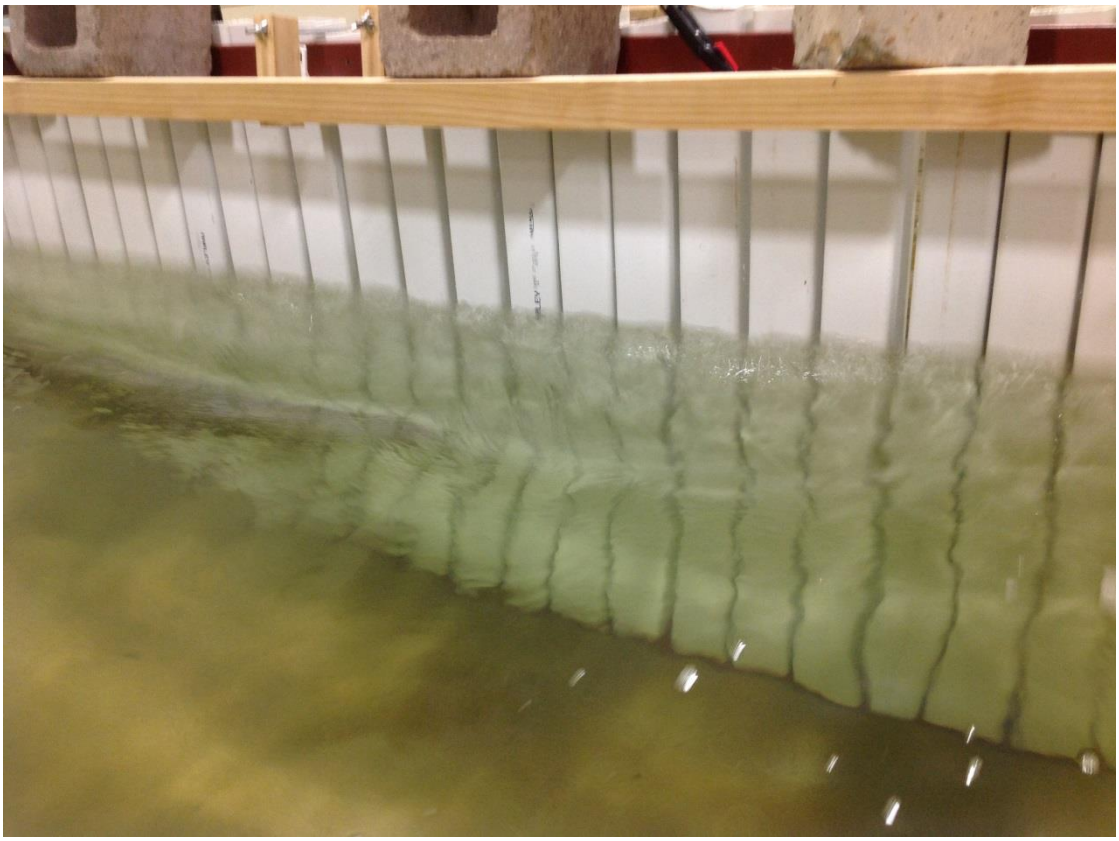

Figure 3-17: For lower porosity, the square piles performed reasonably well.

\

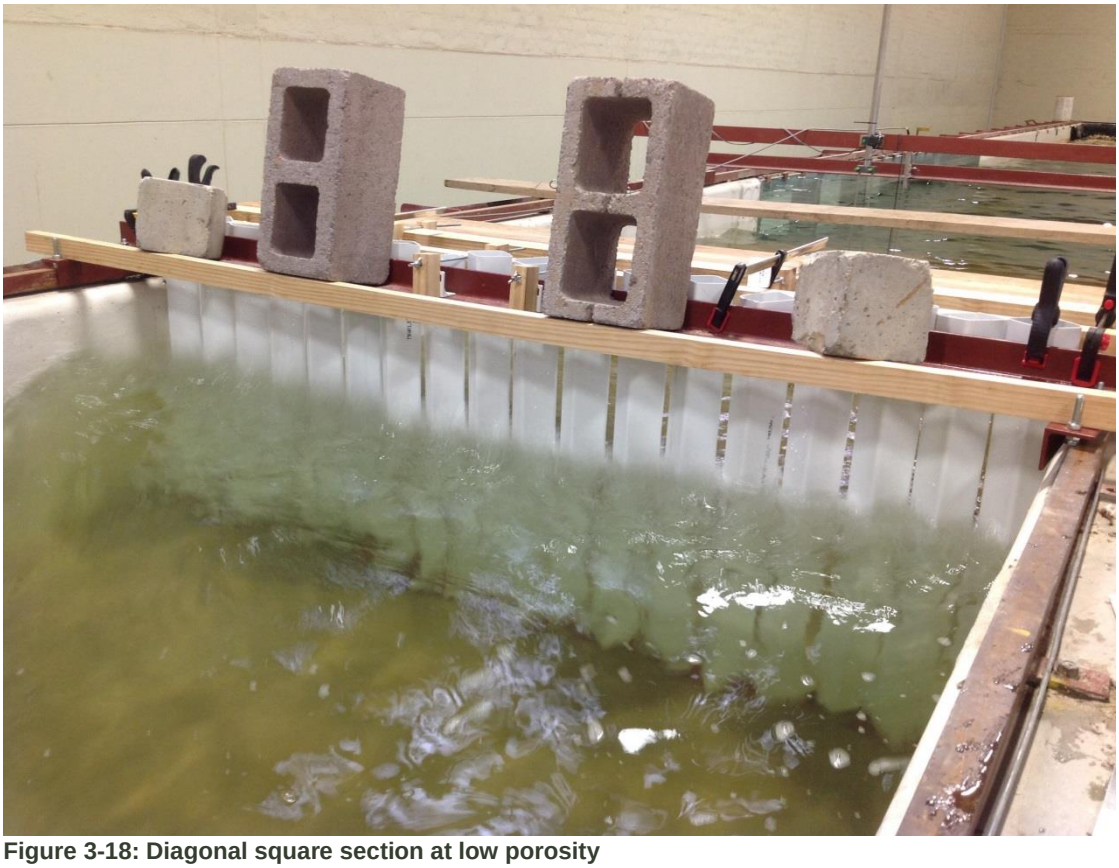

Figure 3-18: Diagonal square section at low porosity

4 Data processing and analysis

The data captured by the HRDAQ system was prepared in spreadsheet format for post processing. Post processing was conducted by the author on a workstation provided by the Coastal & Hydraulics Laboratory at the CSIR in Stellenbosch. The CSIR has developed a coded routine to Mansard and Funke (Mansard & Funke, 1980) that is capable of processing wave probe data for the purpose of calculating wave parameters, reflection and transmission coefficients and presenting the measured data graphically.

Typical output from the post processing was shown in Figure 4-1 to Figure 4-3 below for incident spectra, transmitted spectra and reflected spectra respectively.

These plots were studied individually and the outputs captured to the overall results data base in order to be able to conduct the data summary for the next stages, being validation, analysis and interpretation. More examples of processed output have been included in Appendix C.

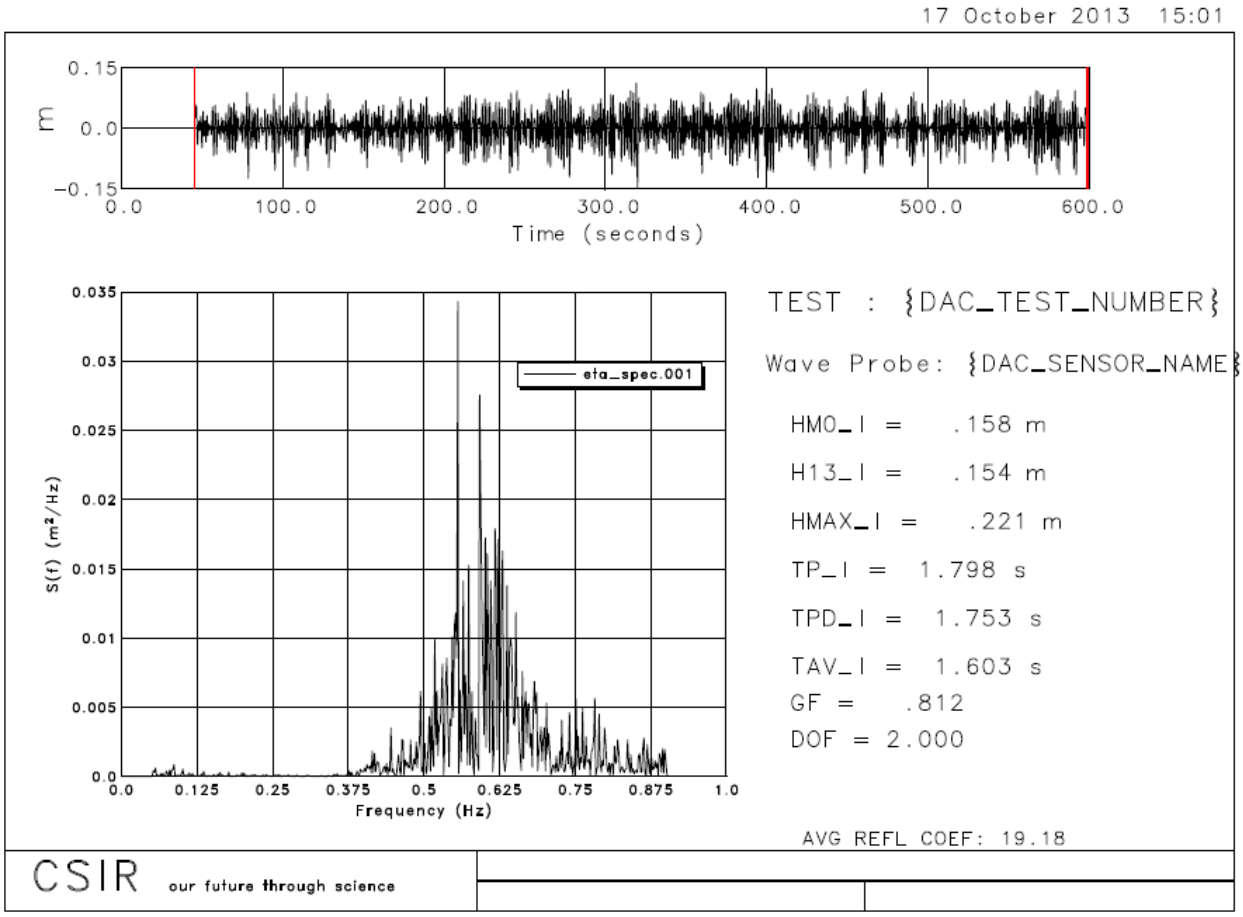

Figure 4-1: Example of processed output for incident spectra

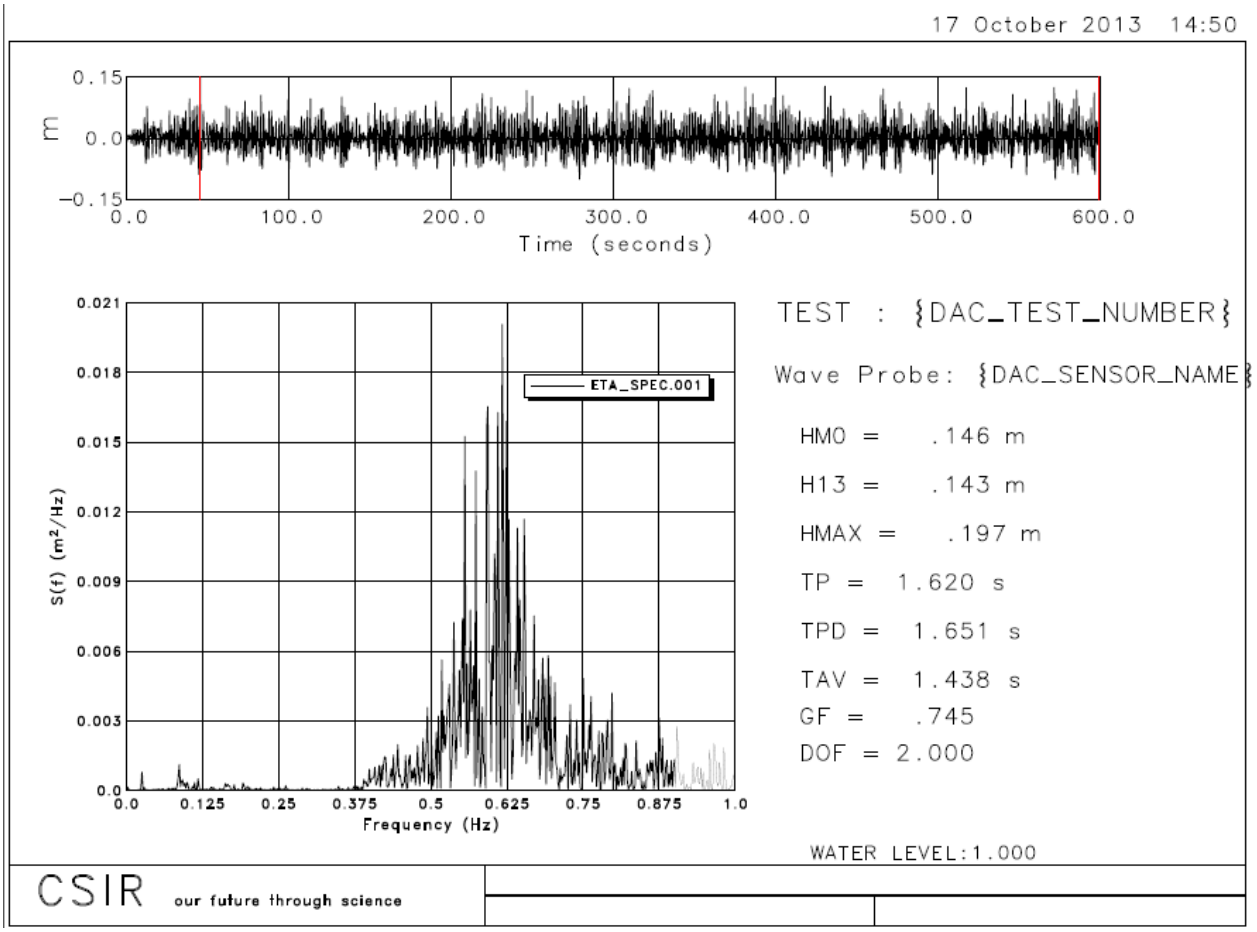

Figure 4-2: Example of processed output for transmitted spectra

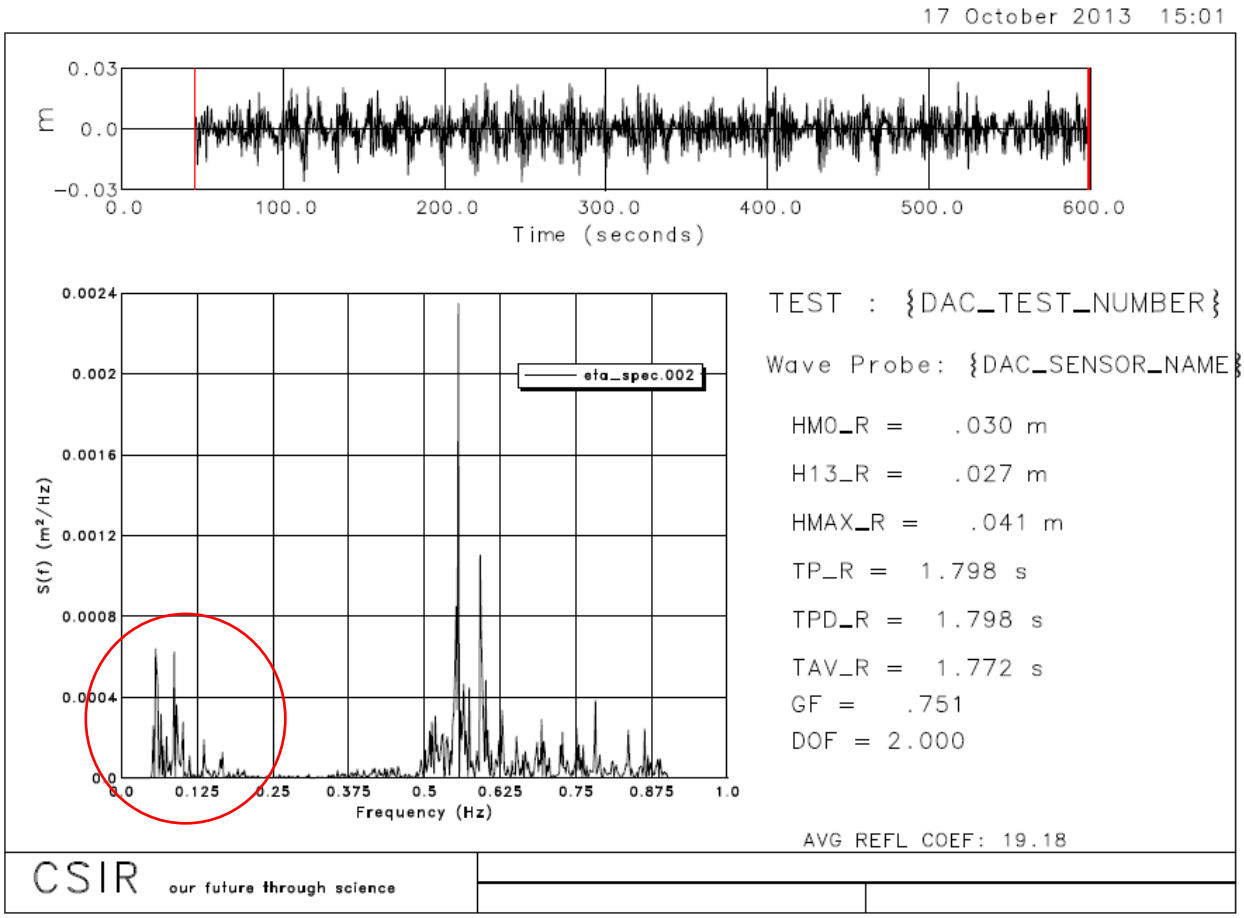

Figure 4-3: Processed output for reflected spectra – note that some residual long wave was present in this test result, indicated by the circle

5 Data Analysis of Results

5.1 Outline of section

Firstly, measured results for the reflection and transmission and energy loss coefficients were compared with the predicted values calculated by empirical equations and also with the data plots available. Following this a parametric analysis of the test data was done, investigating possible dependencies for the performance parameters of the various configurations.

5.2 Validation of recorded data

5.2.1 Data recorded

The complete data set recorded, for circular, square and diagonally square piled elements was initially combined and found to show strong correlation with test results viewed in the literature study. Figure 5-1 to Figure 5-3 below show the derived values for K_T, K_R, K_{EL} and the combined K_T with K_R plots respectively. These initial groupings were developed by plotting the performance coefficients versus the model porosity with no other sub sorting, except for the results obtained from the various pile element shapes.

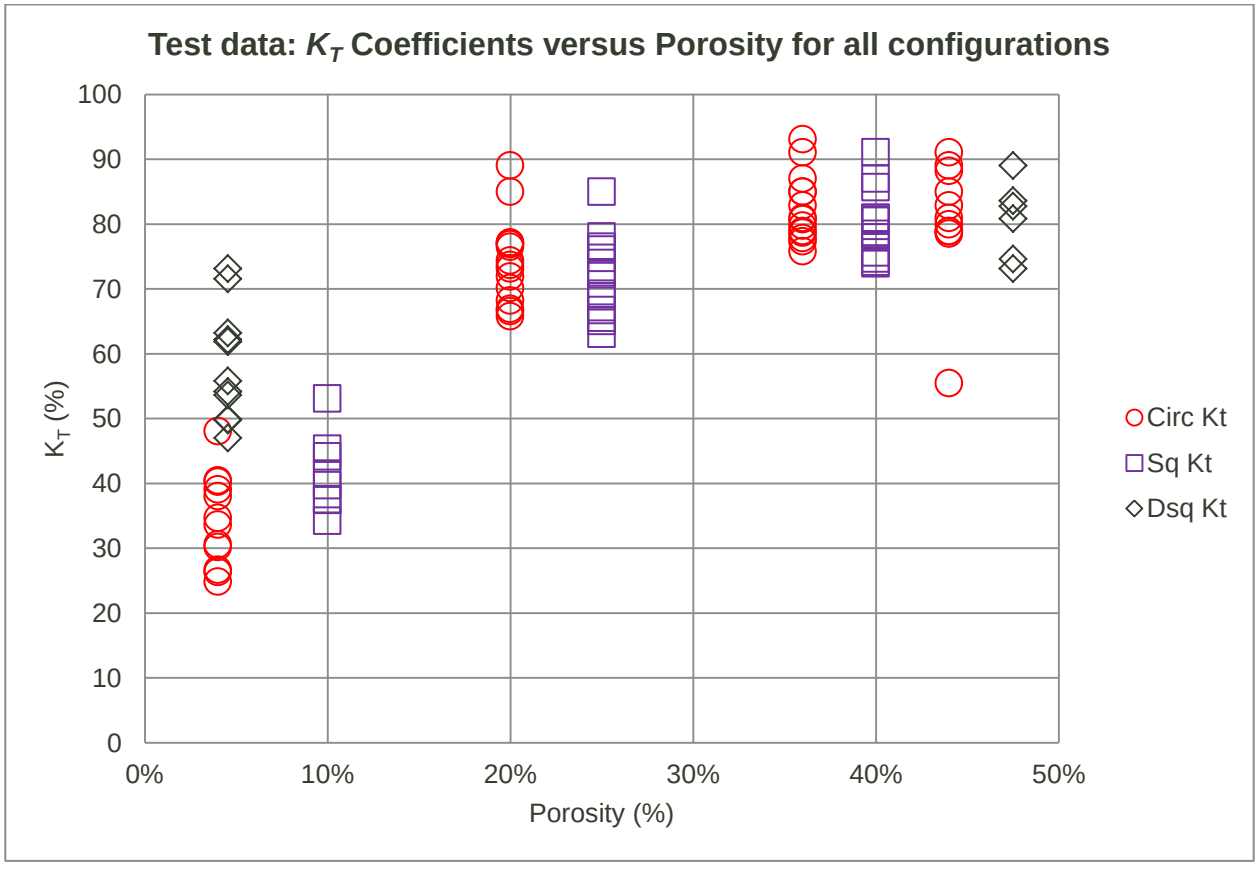

Figure 5-1: Test data: K_T Coefficients versus Porosity for all configurations, for the pile element types

From Figure 5-1 it can be seen that the decrease in porosity of a piled row breakwater generally results in a lower K_T, as can be expected. The apparent bandwidth of results per element type, indicates that there is a strong likelihood that the input parameters have varying impacts on the K_T. Although the screen configuration for each of the different element types could not be accurately constructed on similar porosities, it can be seen that the element types perform differently (refer section 3.4.2.).

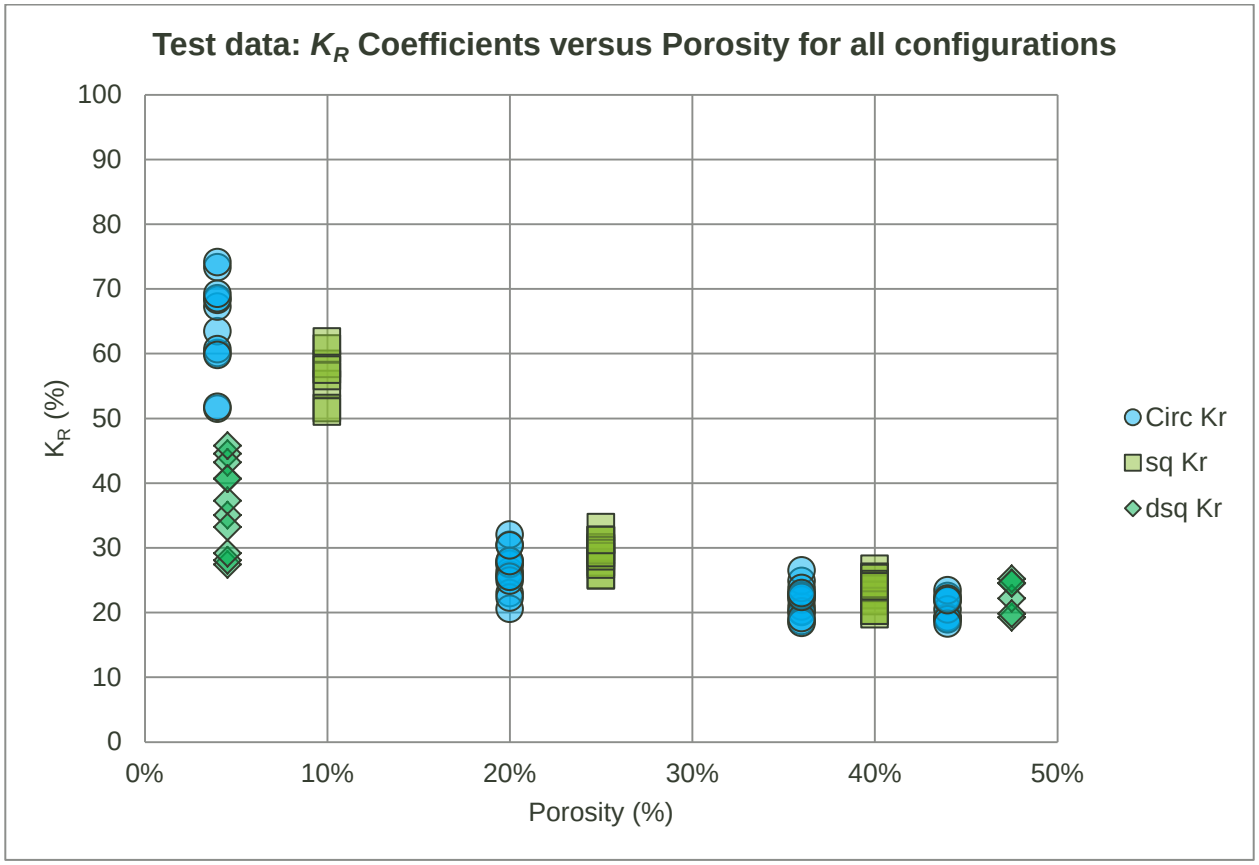

Figure 5-2: Test data: K_R Coefficients versus Porosity for all configurations, for the pile element types

The inverse of K_T is observed on the K_R graph (see Figure 5-2). With a reduced porosity, the reflected waves became higher, which also explains the reduced transmitted wave heights for the same screen porosity.

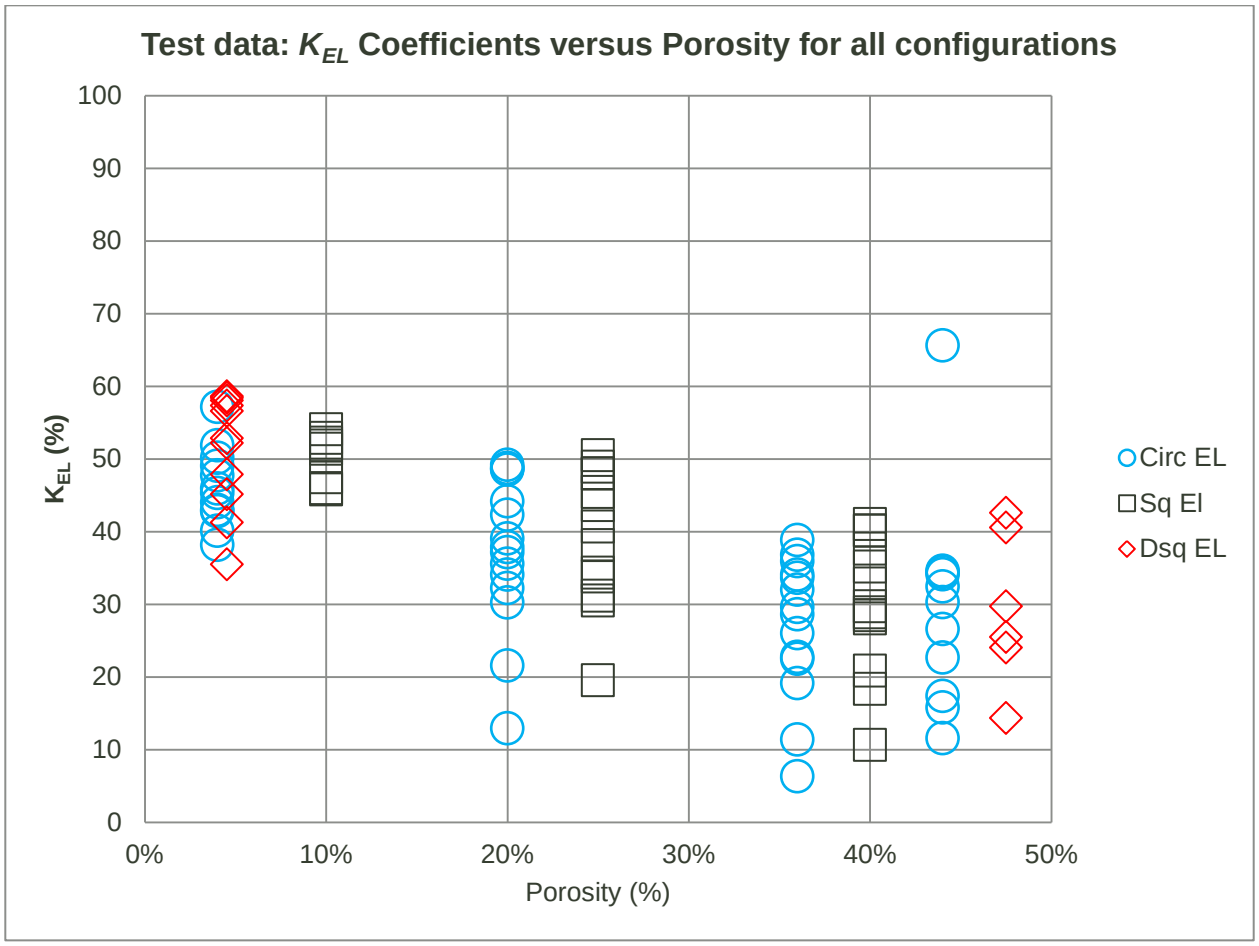

Figure 5-3: Test data: K_{EL} Coefficients versus Porosity for all configurations, for the pile element types

The energy loss coefficient (K_{EL}) is calculated with Isaacson Equation 2-1 and represents a measure of the proportion of incident wave energy flux that is dissipated by the barrier.

Figure 5-4 presents a combined plot for K_T & K_R for the different pile elements. As could be expected, the bandwidth of results per screen porosity setup, for a particular shape, requires further analysis and understanding. This is undertaken in section 5.3.

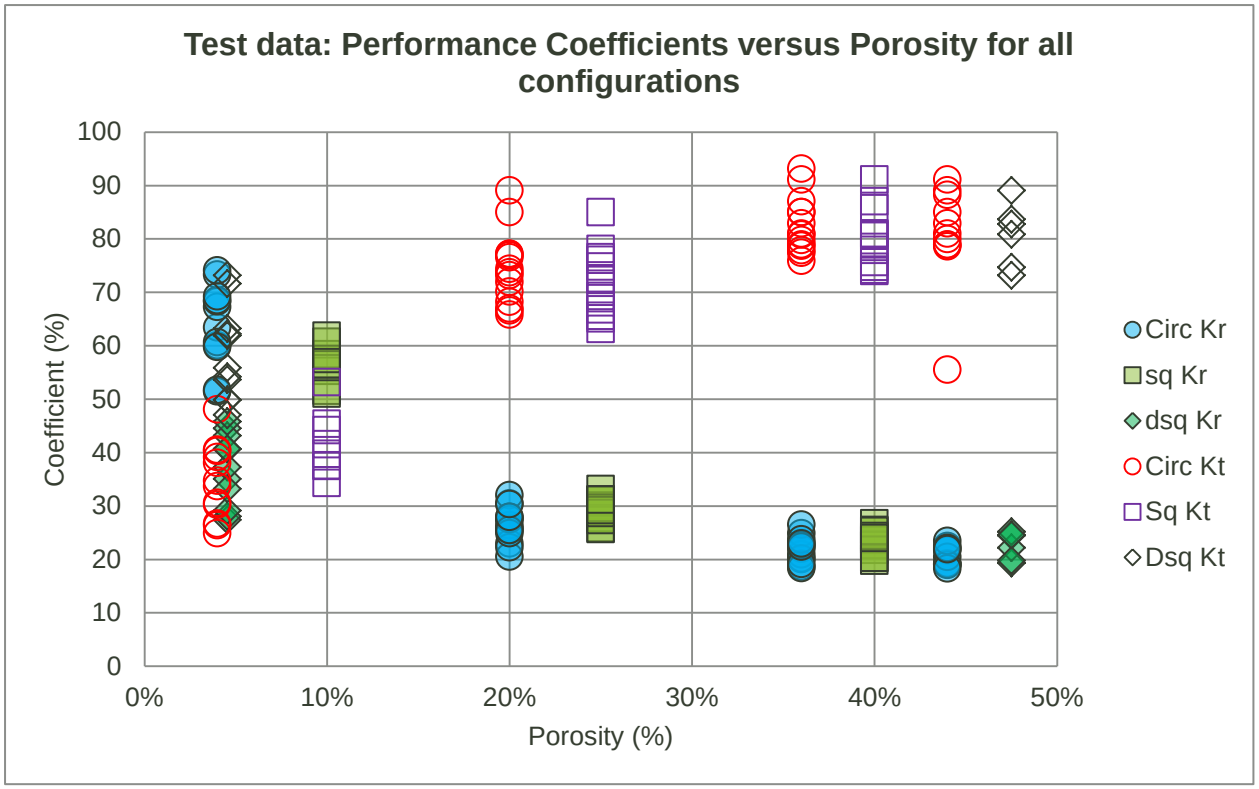

Figure 5-4: Test data: Performance Coefficients versus Porosity for all configurations

5.2.2 Available empirical formulae from literature

From the literature study, the equations by Thomson (2000) and those of Mei and Kriebel presented in Suh (2011) were used to develop predicted values. The formulae retained for the purpose of predicting performance coefficients for the model tests are presented in section 2.3 and listed as equations 2-1 to 2-6: The values from these equations have been incorporated in the graph plots Sections 5.2 and 5.3 as follows

- Equation 2-2 and Equation 2-3 after Thompson (2000) abbreviated as GT in figures (Transmission Coefficients for the two Thompson equations are denoted as "PrGT Kt1" and "PrGT Kt2" respectively)
- Equation 2-4 and Equation 2-5 after Mei (1989) abbreviated as Mei in figures (Reflection and Transmission Coefficients as per Mei equations are denoted as "Pred Mei Ct" and "Pred Mei Cr" respectively)
- Equation 2-6 and Equation 2-7 after Kriebel (1992) abbreviated as Kri in figures (Reflection and Transmission Coefficients as per Kriebel equations are denoted as "Pred Kri Kt" and "Pred Kri Kr" respectively)

Figure 5-5 shows the predicted value ranges for the exact input parameters that were used in the testing, although for clarity the recorded results have been omitted from this graph.

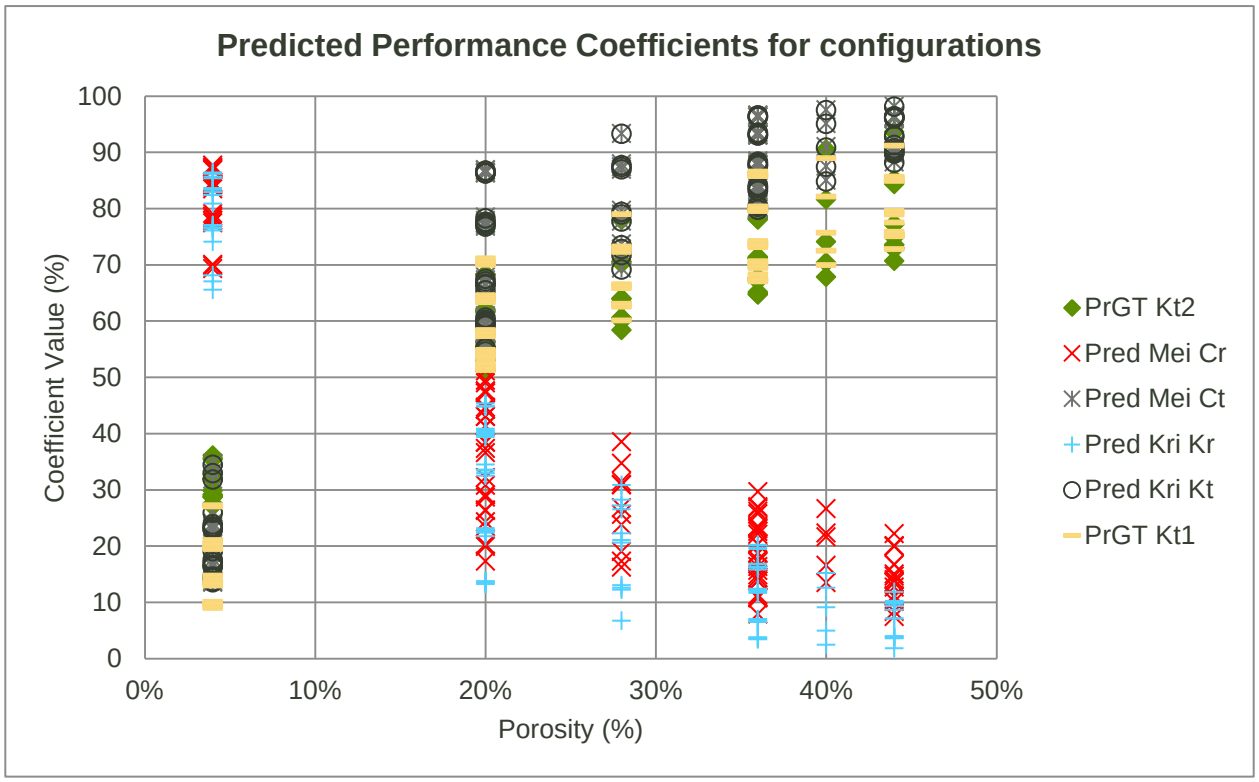

Figure 5-5: Predicted Performance Coefficients for configurations

In the analysis section of this thesis (see section 5.3), these predicted values were used for comparison with the recorded results.

The following sets of graphs indicate the predicted values compared to the current test results. For the purpose of understanding the bandwidths observed in the results graphs in the aforementioned section, data was further grouped in terms of well-known dimensionless parameters (CEM, 2006) whether or not current research and previous studies data sets have strong correlations. The following fields were chosen from previous work to do this validation.

- K_T & K_R versus H/L or (see Figure 5-6 & Figure 5-7)
- K_T & K_R versus $d/g/T^2$ (see Figure 5-8 to Figure 5-11)

These two groupings presents a simple way of doing the validation of the data sets for both wave height (Hm0) and wave period (Tp) dependent parameters.

These plots were developed for the circular pile element results only, although a more detailed comparison between the various pile element types is undertaken in section 5.3.

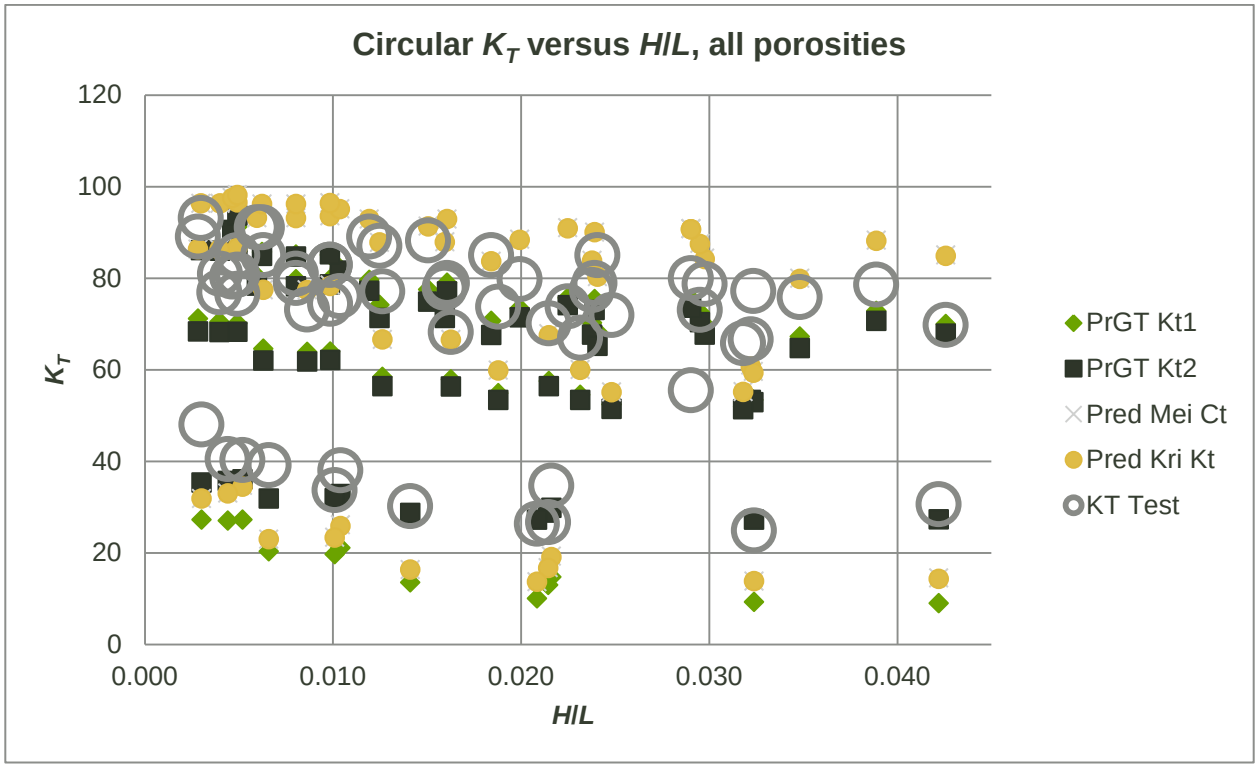

Figure 5-6: Circular K_T versus H/L, all porosities

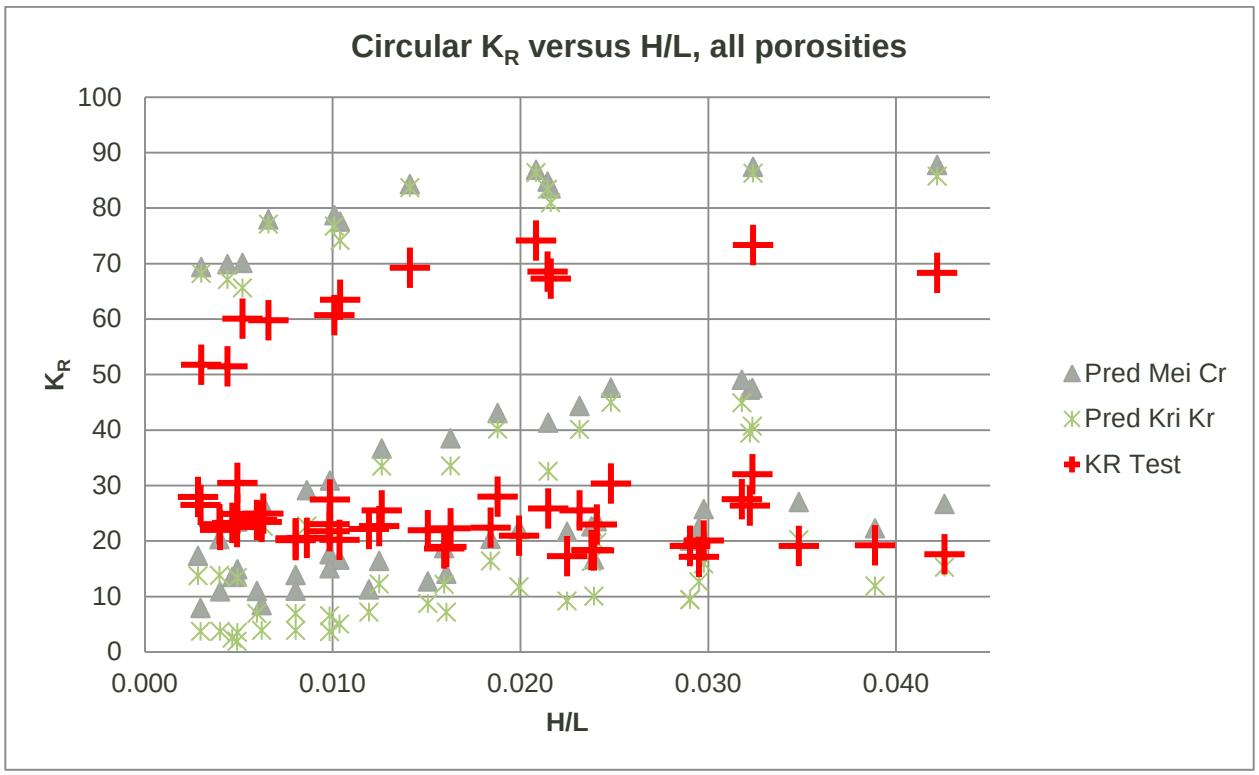

Figure 5-7: Circular K_R versus H/L, all porosities

From Figure 5-6 and Figure 5-7 the results still evidently appear to be split into bandwidths. However, these bandwidths still correlate well with the predicted values from the equations used. Furthermore, the results of the lower porosity tests appear to show more sensitivity to wave steepness. The increased reflection and reduced transmission at higher steepness values indicates this sensitivity quite clearly.

By comparison, it was noted that the results were valid for different ranges of H/L for these equations. This could have contributed to various possible anomalies, such as differences in the test set-up, generalisation of the cross section of the equations and the data and also possibly the method of deriving the equations could have been based on truncated data sets. In most cases, there is strong correlation with equations put forward by Thomson (2000) for K_T varying correlation between Mei and Kriebel (according to Suh *et al.*, 2011) and some over estimation of K_R for the higher values. This is therefore expected to be the result of a difference in the method or data sets for the lower porosity tests.

Figure 5-8 to Figure 5-11 accommodates a breakdown of a test setup in terms of the model porosity to enable a better comparison of resolution.

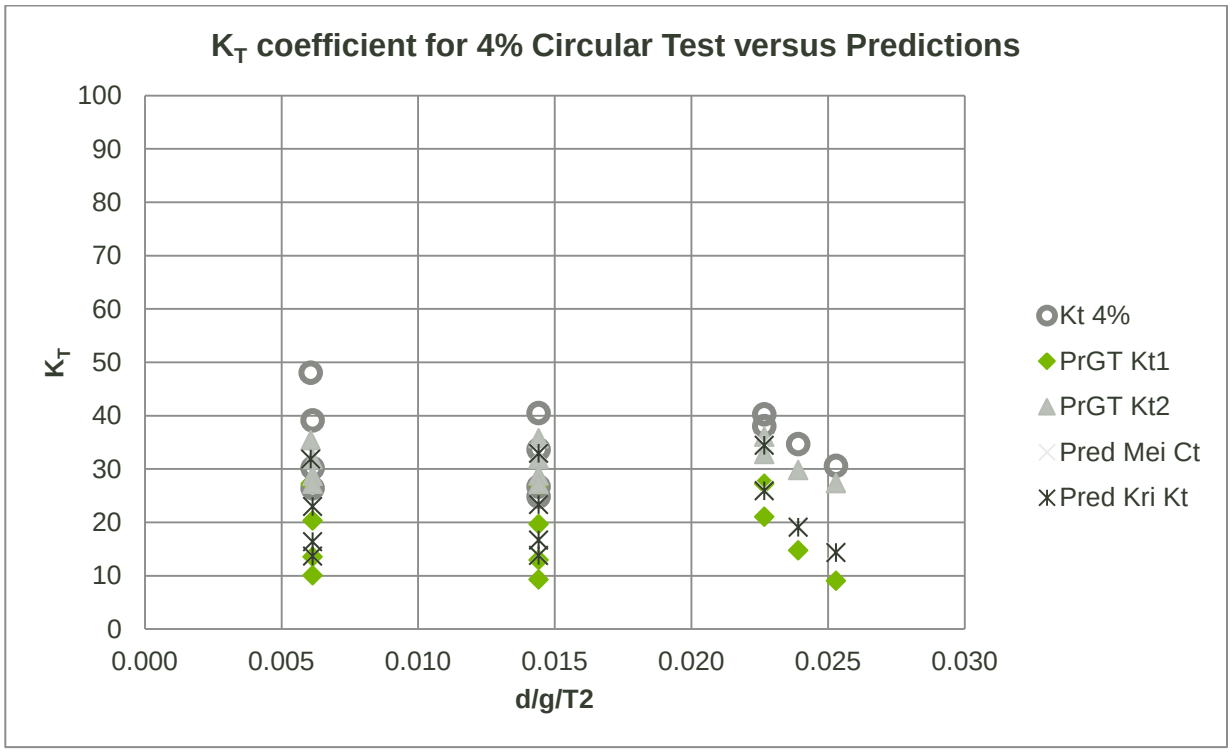

Figure 5-8: K_T coefficient for 4% Circular Test versus Predictions

Figure 5-8 shed more light on the outcome in the case of lower porosity, where the predicted values in most cases were lower than the measured values, although in the author's opinion these were still within range.

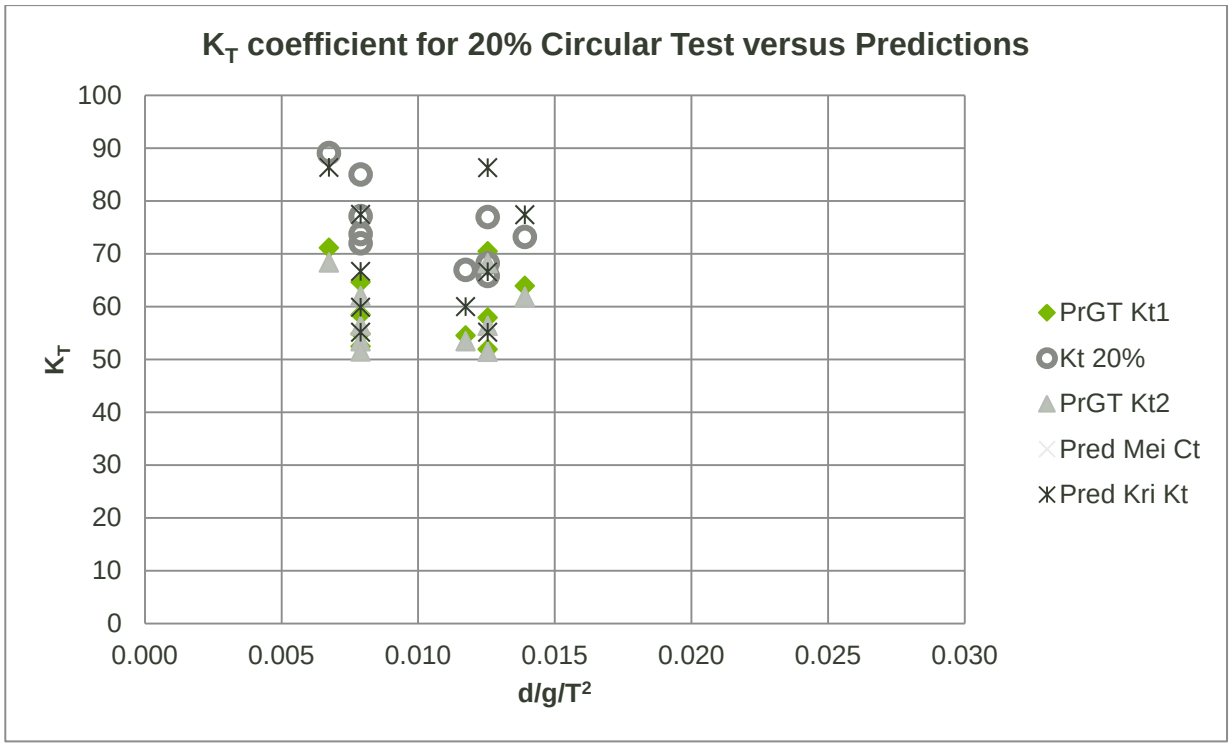

Figure 5-9: K_T coefficient for 20% Circular Test versus Predictions

For a porosity of 20% the best correlation was found to be between Kriebel (in Suh, 2011) and Thomson (2000). The same observation was made for Figure 5-10.

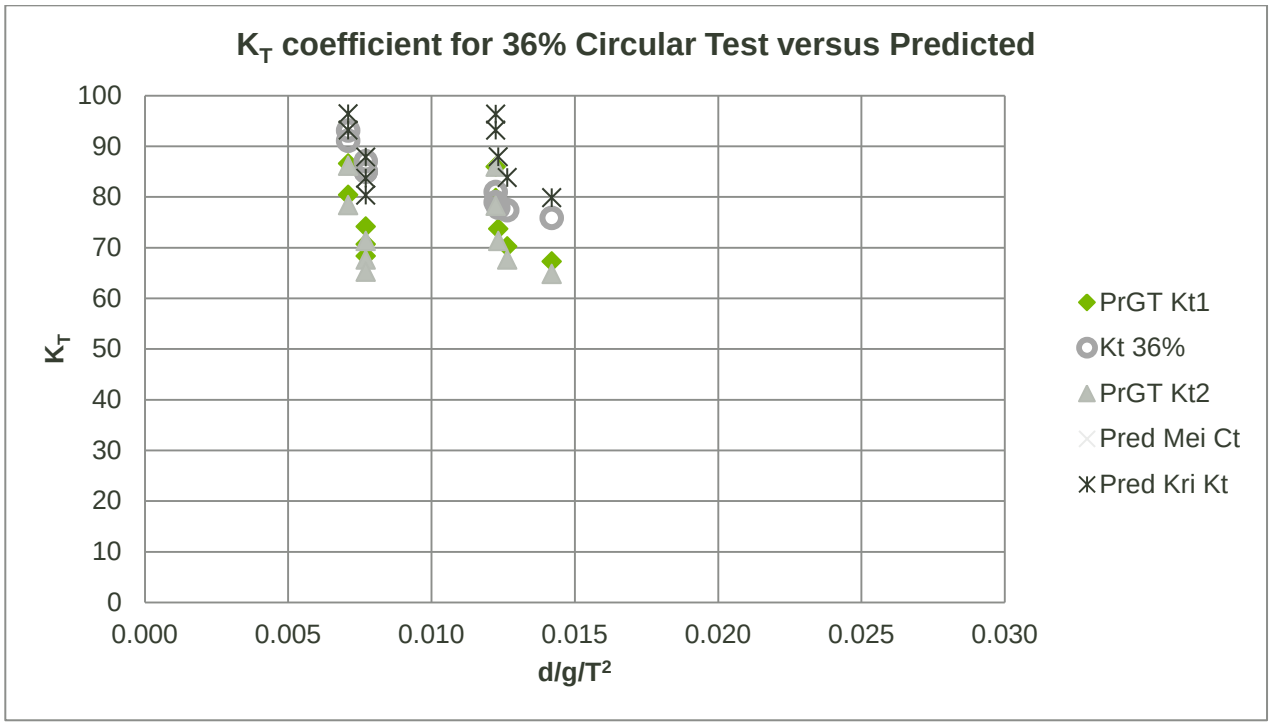

Figure 5-10: K_T coefficient for 36% Circular Test versus Predicted

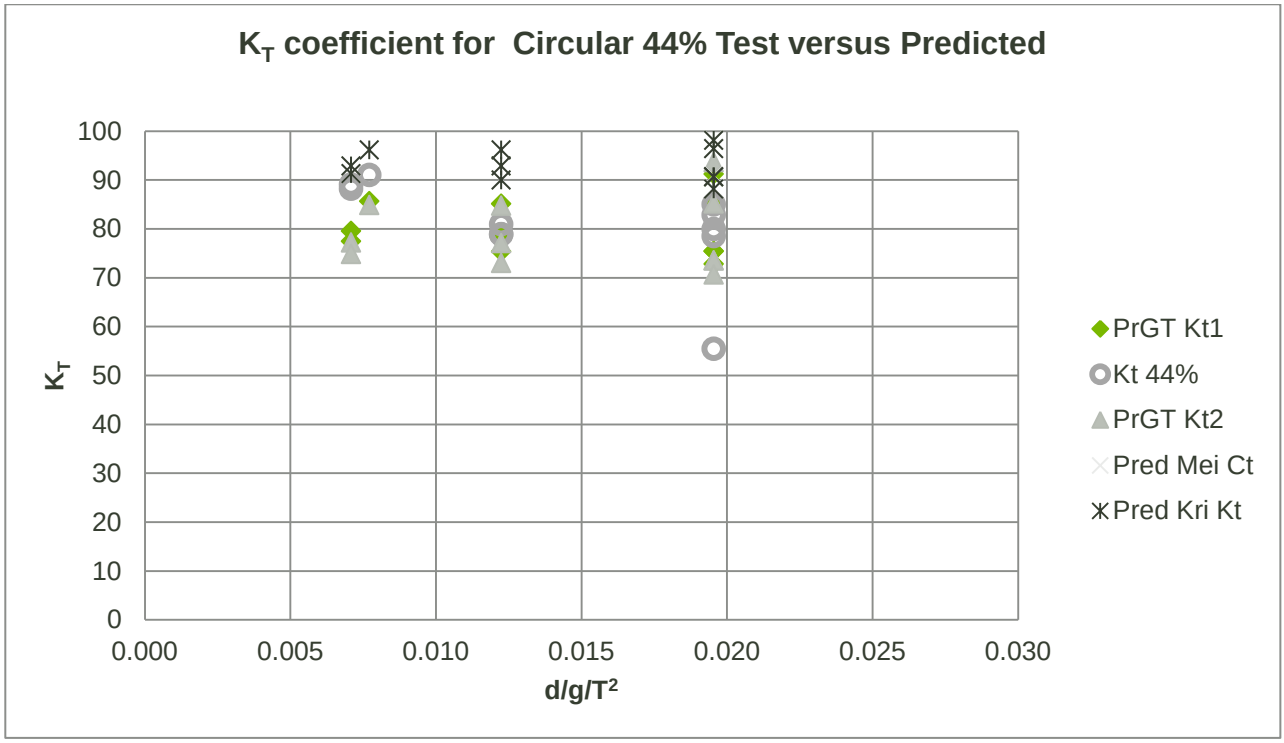

Figure 5-11: K_T coefficient for Circular 44% Test versus Predicted

The 44% porosity test results corresponded well with the range close between the two equations from Thomson (2000).

It was deduced from the foregoing comparative plots that the test result data had a very good fit with the predicted values.

5.2.3 Overlaid graphs

For some of the equations sourced in the literature study, no explicit solution could be developed from the equations provided, or in certain cases (See Allsop & Hettiarachchi, 1988) the published performance coefficients were produced from previous testing. The test results from this thesis were overlaid so that they could be compared with previously published data. Although the scales might appear warped, the following graphs with overlaid backgrounds were developed in order to observe whether the test results of this thesis are within the range of previous work.

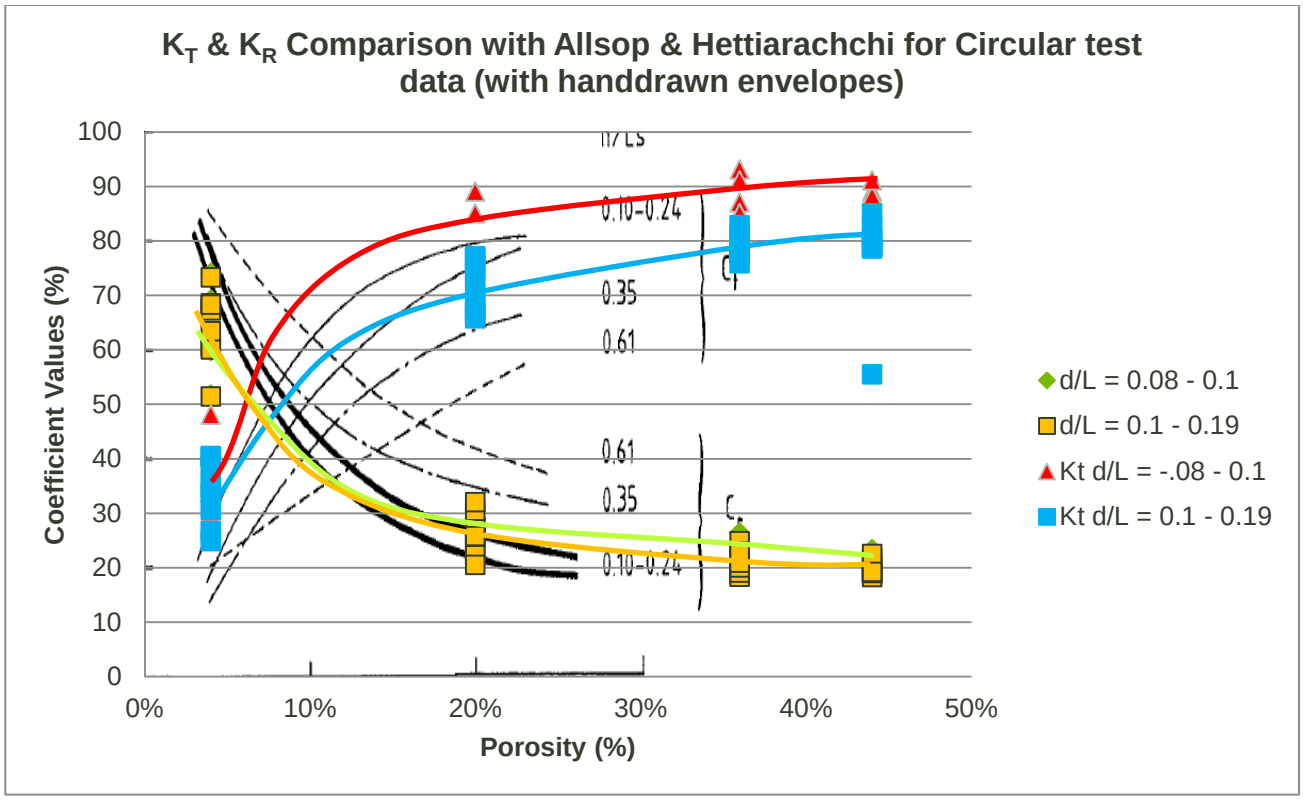

Figure 5-12: K_T & K_R Comparison with Allsop & Hettiarachchi for Circular test data

From Figure 5-12 it was concluded that the overlay presented a fair correlation between the test results and the graph by Allsop.

Suh *et al.* (2011) developed a relationship between a friction parameter *Y* and the ratio of (*e t*) / *d*. The overlay of the processed results onto a combination of data produced by Suh *et al.* is

presented in Figure 5-13. It is noted that this comparison yielded acceptable results compared to previous work.

Equation 5-1: Friction parameter equation following Suh (2011)

$$\gamma = 0.0584\left(\frac{rb}{h}\right)^{-0.7}$$

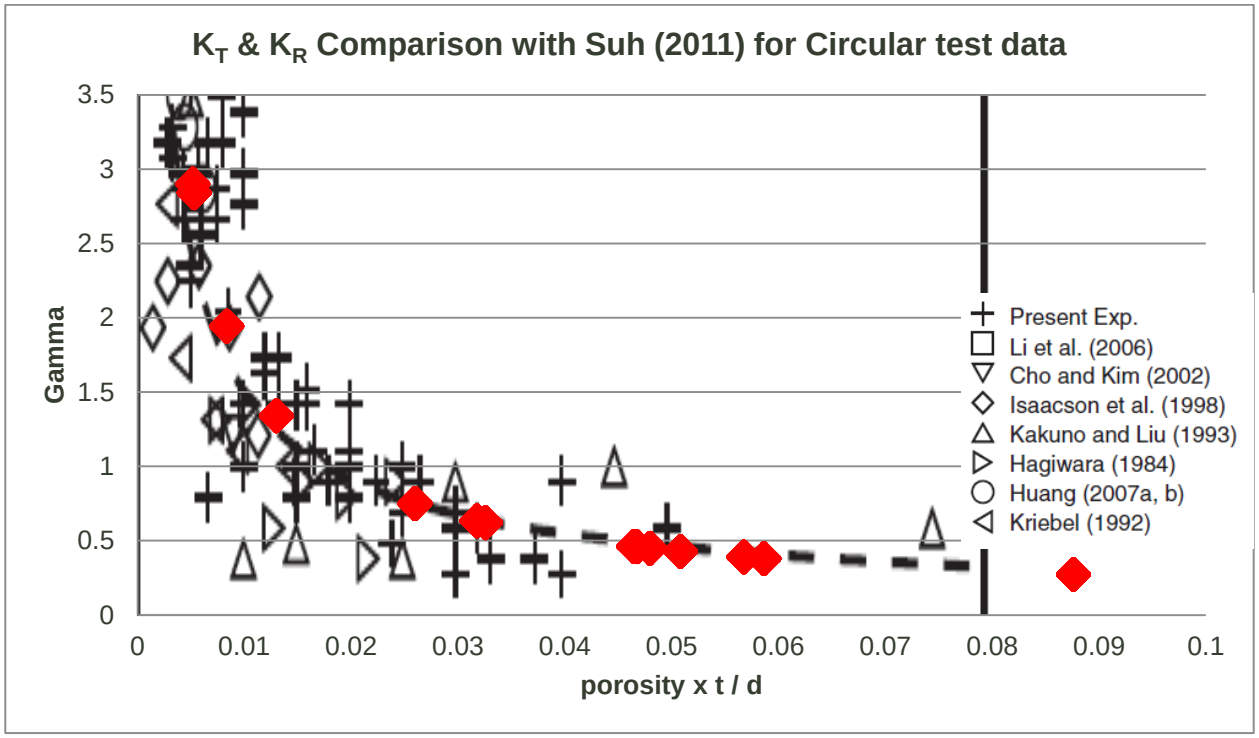

Figure 5-13: K_T & K_R Comparison with Suh (2011) for Circular test data

5.2.4 Conclusion on Validation

From the comparisons and overlays presented it was concluded that the current test data correlates well with previously published empirical equations and test data. The analysis of the results in the following section will revisit some of the empirical equations, so as to present an additional backdrop to the current test results.

5.3 Analysis of recorded data

Results from the post processing were captured and further processed in an EXCEL spreadsheet format. Inspection of the data resulted in only two records being questioned as being out of range when compared with other results and the expected trends and these two records were therefore omitted from further analysis.

The following dependencies were studied and are presented in this section in the following order, under allocated headings with Table 5-1 in section 5.4 providing a summary of the outcome:

- Particle velocity over relative depth for H/L
- Particle Velocity versus H/L
- K_T versus Tp – circular sections
- K_R versus Tp – circular sections
- K_T versus Hm0 – circular sections
- K_R versus Hm0 - circular sections
- K_T versus $d/g/T^2$ - circular sections
- K_R versus $d/g/T^2$ - circular sections
- K_T versus kd - circular sections
- K_R versus kd - circular sections
- K_T versus H/L - circular sections
- K_R versus H/L - circular sections
- K_R versus H/L x e
- K_R versus H/L/e
- Coeff versus d/L, for porosity - all shapes (instead of kd)
- Coeff versus Hs/L, for porosity - all shapes (instead of ka)
- Coeff versus H/d, for porosity - all shapes
- K_R versus H/L compare shapes with similar porosity
- K_R versus H/L compare shapes with similar nr of piles

Observations for the results compared have been included in between the sections and a short discussion is offered in the following section.

5.3.1 Wave particle velocity (all porosities, all shapes)

From the literature review it was seen that the velocity potential formed the basis of many of the equations. In this section, the results were interrogated in respect of the calculated maximum horizontal (V_U) and vertical wave particle velocities (V_W) to investigate the relationships. This calculation was done with the equations as per CEM (2008) for transitional waters. For the purpose of this analysis, wave particle velocities were plotted for maximum values over relative depth and wave steepness. See Figure 5-14 and Figure 5-15 for plots over *d*/*L* and *H*/*L* respectively.

$$V_u = \frac{H}{2} \times \frac{gT}{L} \frac{\cosh\left(2\pi \frac{(z+d)}{L}\right)}{\cosh\left(\frac{2\pi d}{L}\right)} \cos\theta$$

Equation 5-2: Horizontal wave particle speed calculation (CEM 2008)

$$V_w = \frac{H}{2} \times \frac{gT}{L} \frac{\sinh\left(2\pi \frac{(z+d)}{L}\right)}{\cosh\left(\frac{2\pi d}{L}\right)} \sin\theta$$

Equation 5-3: Vertical wave particle velocity (CEM 2008)

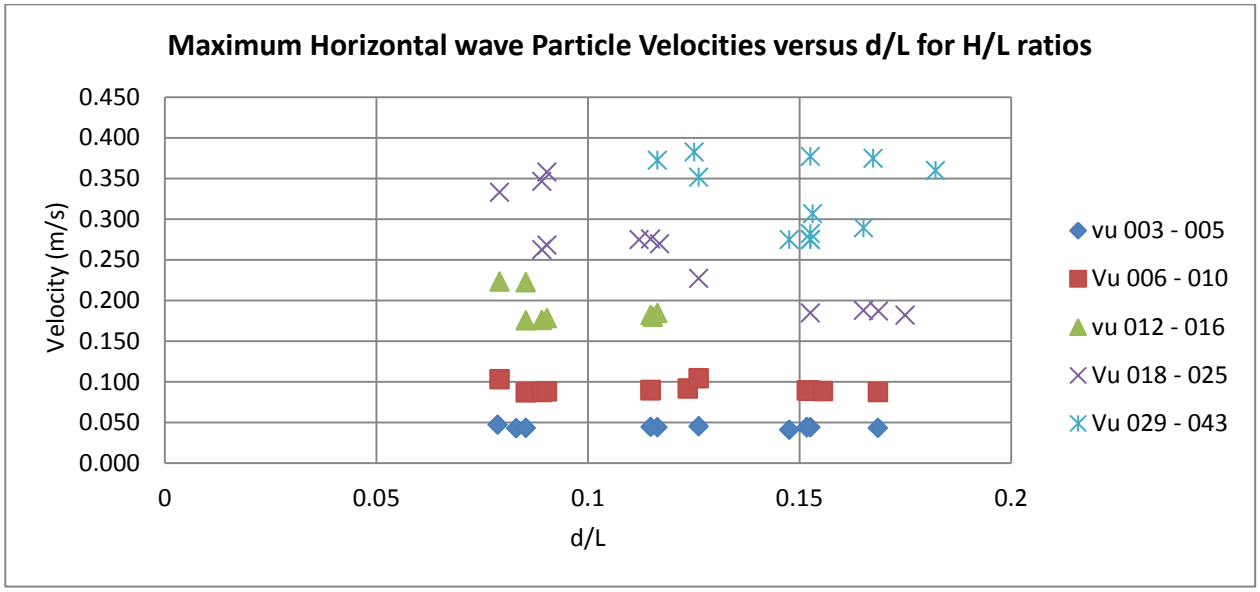

Figure 5-14: Maximum horizontal wave particle velocities versus d/L for H/L ratios

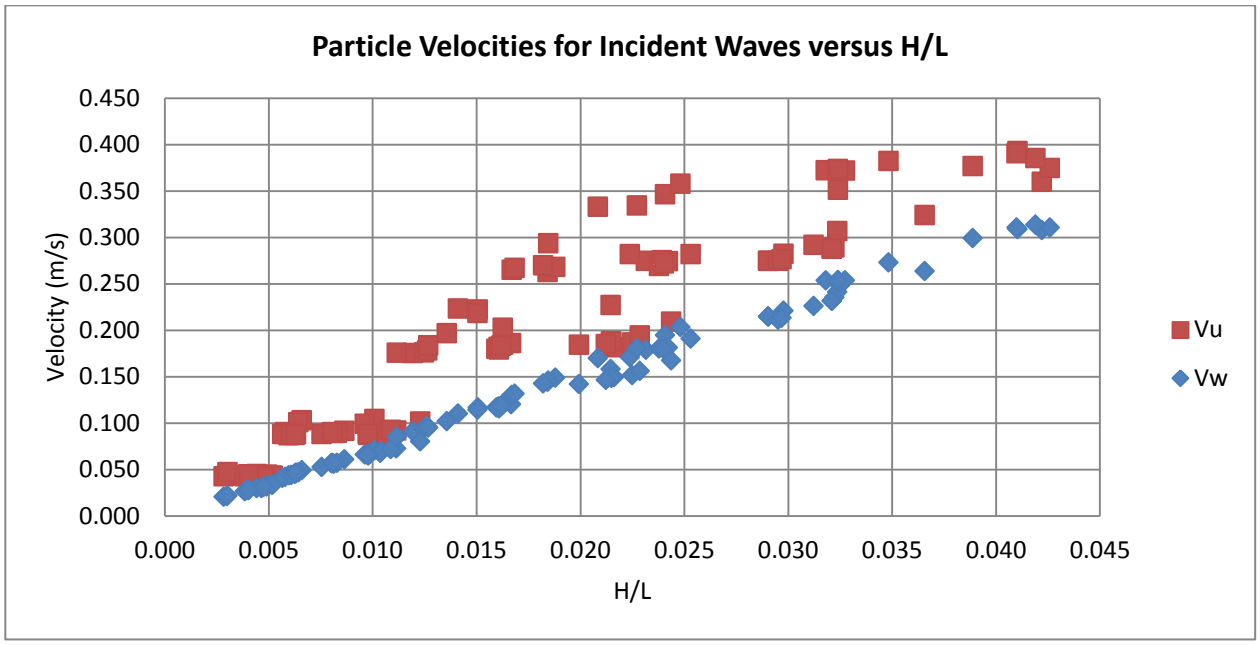

Figure 5-15: Maximum horizontal (V_U) and vertical (V_W) wave particle velocities for incident waves versus H/L

As no relationship is clear from the comparison to with *d*/*L*, the *H*/*L* graph was the only valuable comparison. The increase in particle velocity (both V_U and V_W) with increased wave steepness is of particular interest as further analysis graphs will show relationships of transmission and reflection coefficients over wave steepness. In results from the literature, the increased velocities resulted in higher energy losses, possibly due to increased turbulence at the wave screen.

5.3.2 Wave Period (circular piles only)

From Figure 5-16 and Figure 5-17 the dependency of K_T and K_R on wave period was not conclusive. No relationship is deduced from this analysis.

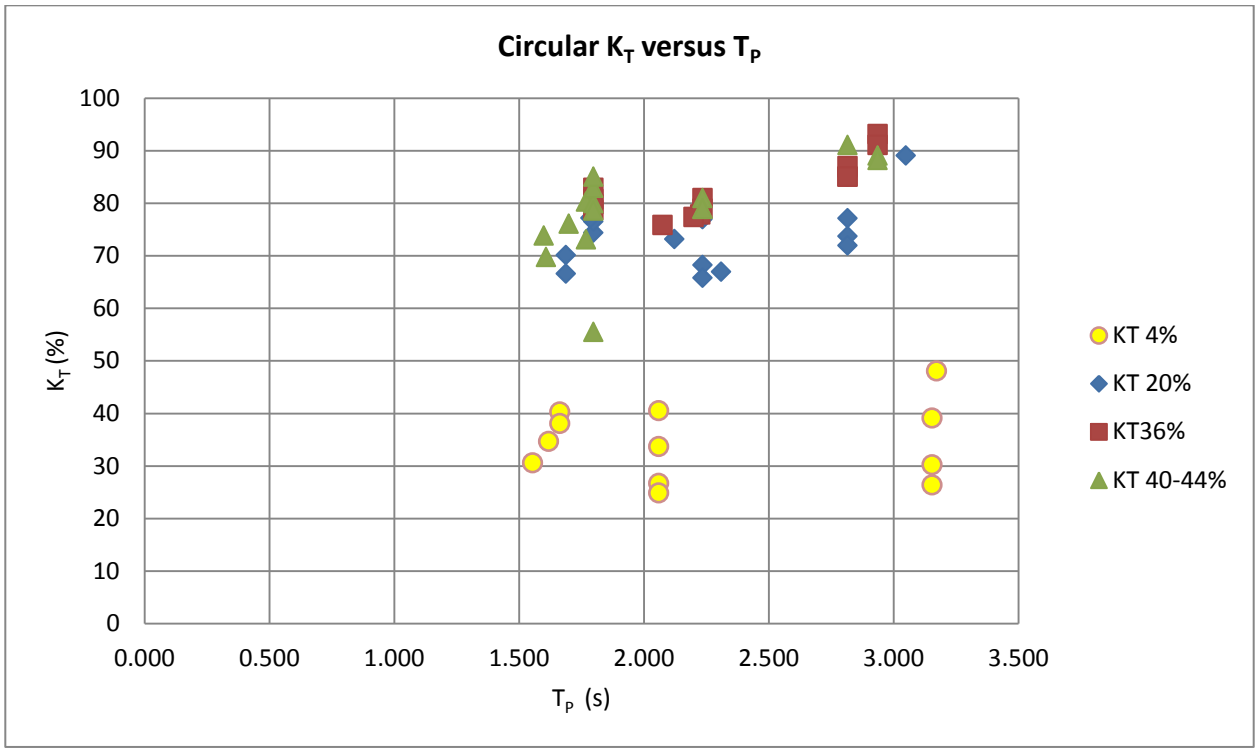

Figure 5-16: Transmission coefficient versus T_P for circular pile elements

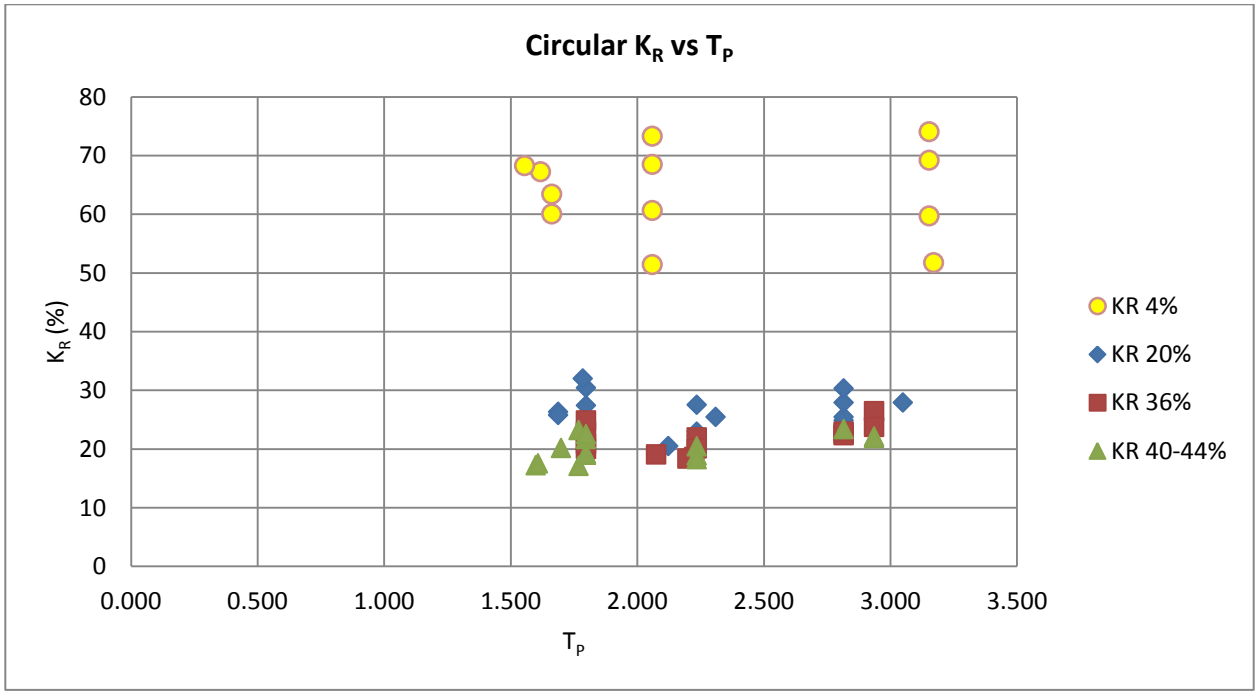

Figure 5-17: Reflection coefficient versus T_P for circular pile elements

5.3.3 Wave Height (circular piles only)

Comparisons of KT and K_R over the incident wave height have been produced and plotted in Figure 5-18 and Figure 5-19. From these graphs it was observed that for low porosities transmission is slightly reduced and reflection is increased with increasing wave height. It is not possible to determine any dependency with the higher porosities.

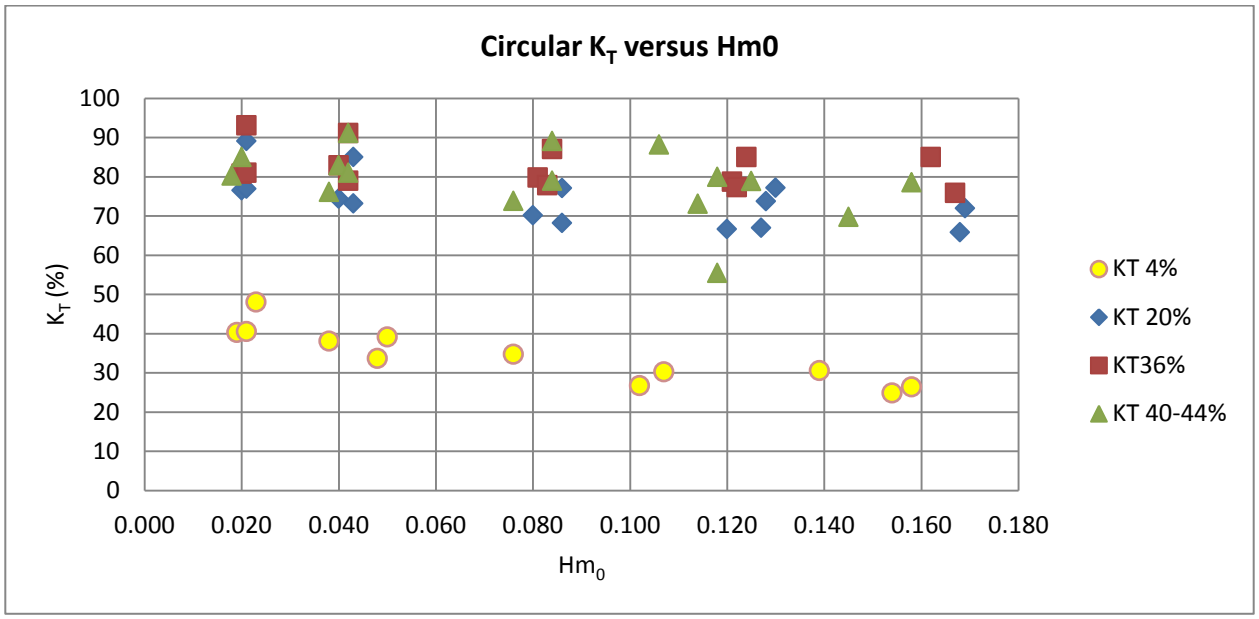

Figure 5-18: Transmission coefficient versus Hm_0 for circular pile elements

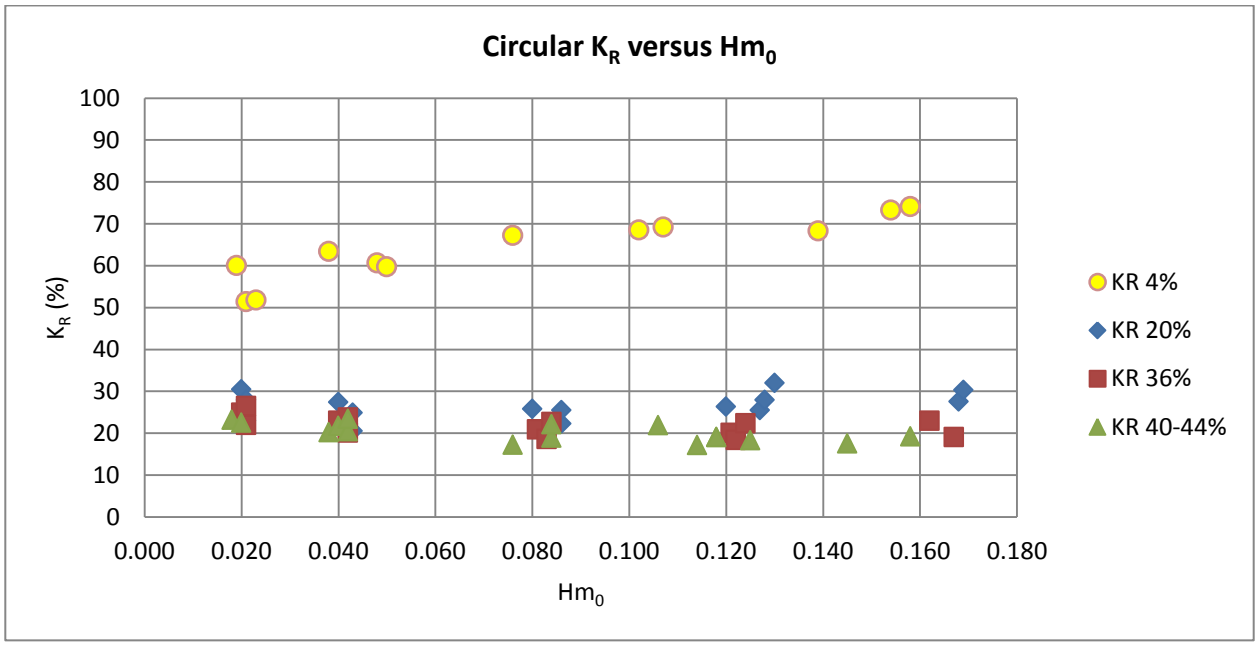

Figure 5-19: Reflection coefficient versus Hm_0 for circular pile elements

5.3.4 d/g/T^2 (circular piles only)

This parameter is popular for wave data analysis as it involves depth and period influenced values. However, when studying the graphs there is no strong dependency over the range of results (See Figure 5-20 and Figure 5-21).

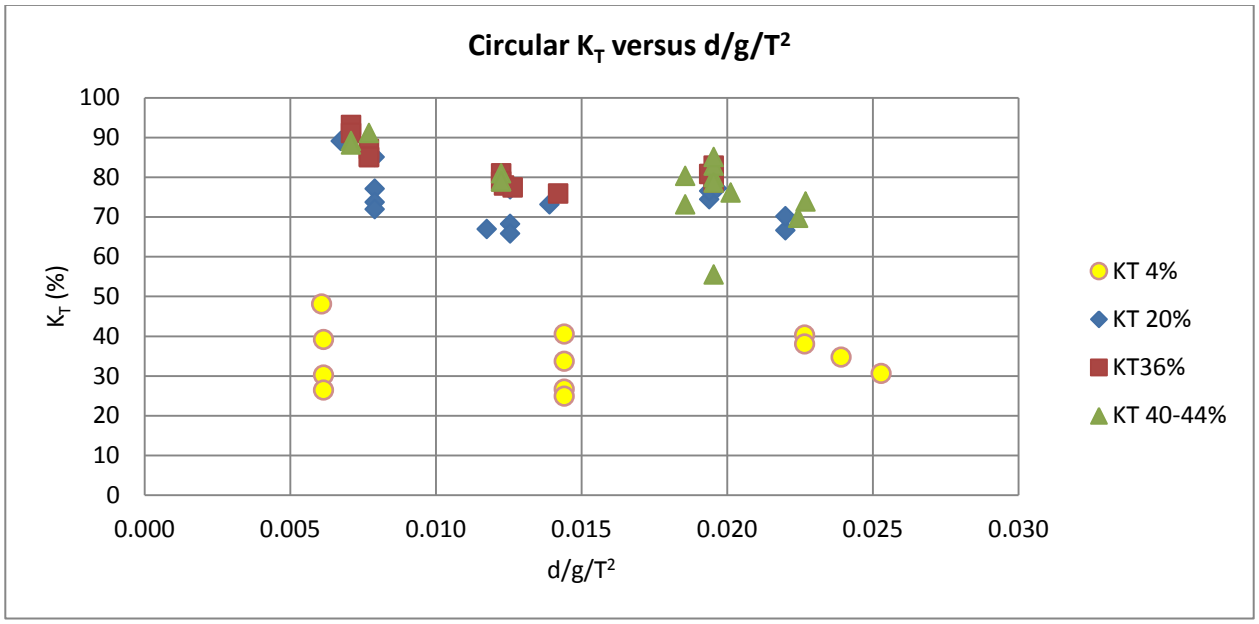

Figure 5-20: Transmission coefficient versus d/g/T^2 for circular pile elements

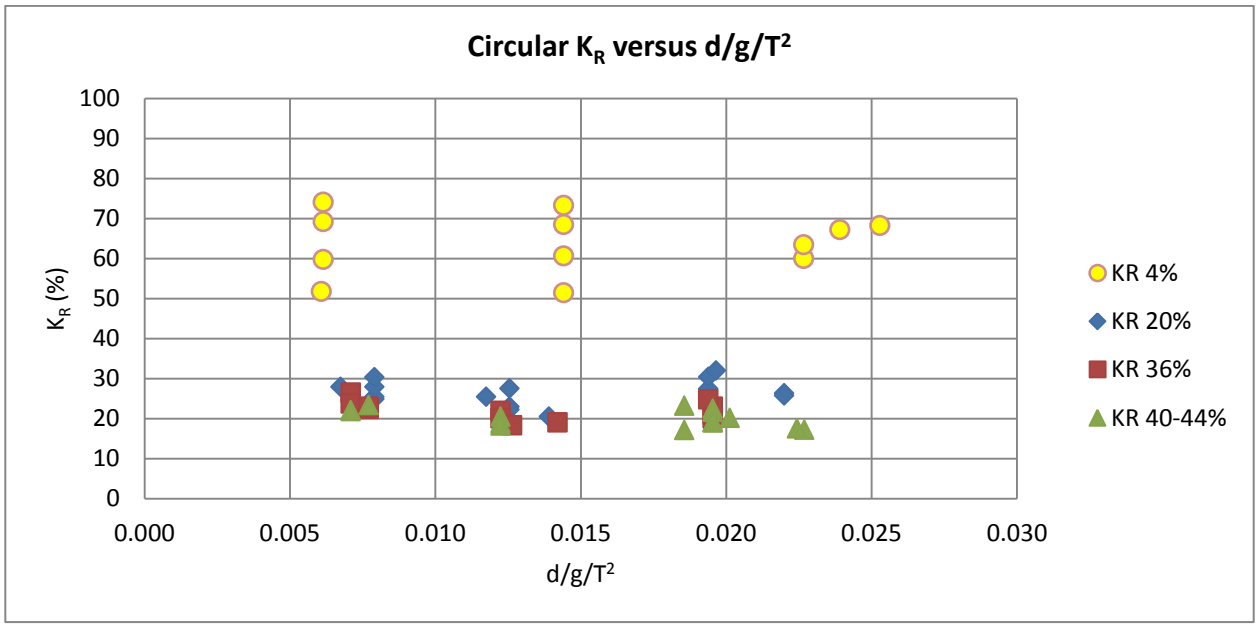

Figure 5-21: Reflection coefficient versus d/g/T^2 for circular pile elements

5.3.5 kd (circular piles only)

The wave parameter multiplied by the water depth is often used to investigate wave parameters or sets of results. From Figure 5-22 and Figure 5-23 no conclusions can be drawn other than that the coefficient values for K_R and K_T appear more sensitive for lower porosities.

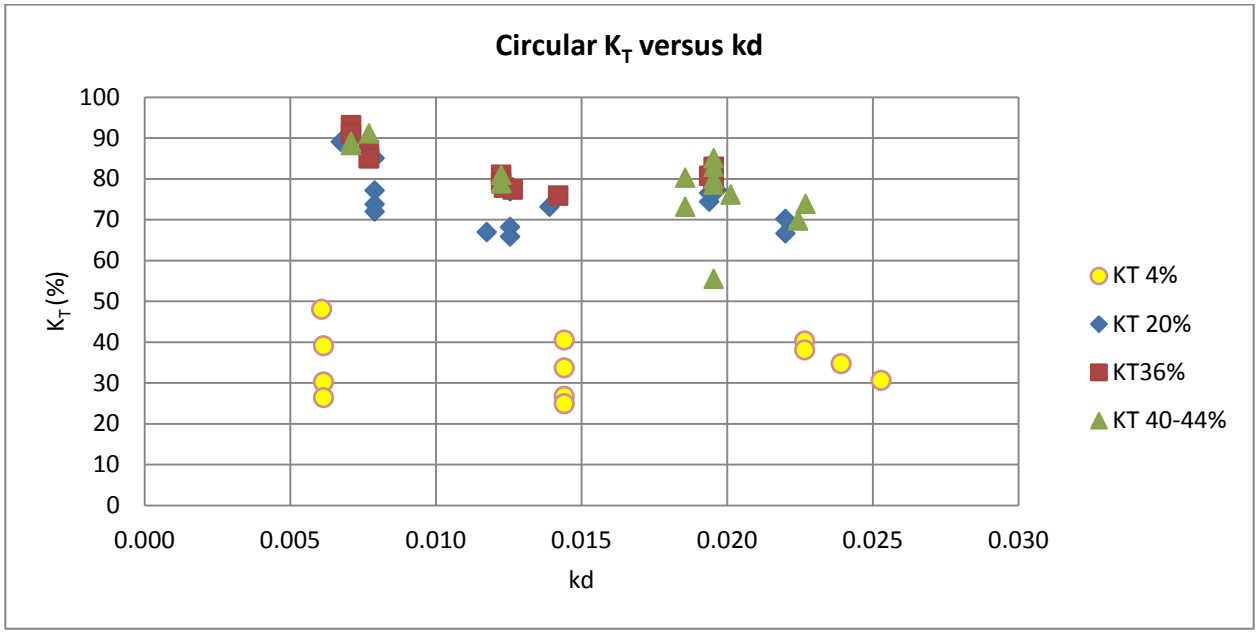

Figure 5-22: Transmission coefficient versus kd for circular pile elements

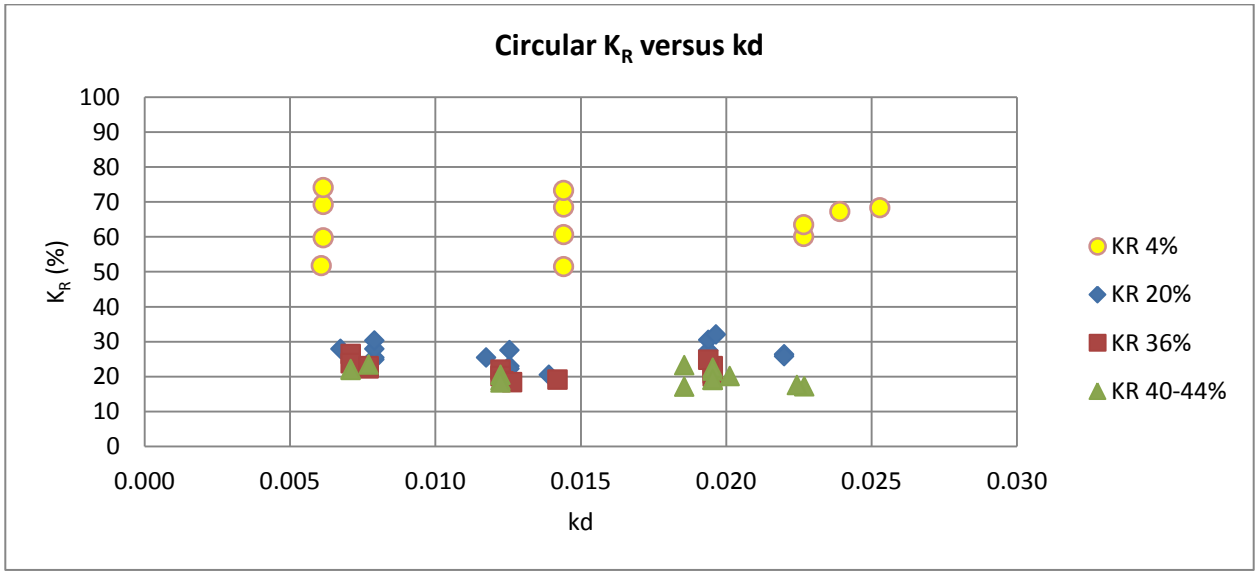

Figure 5-23: Reflection coefficient versus kd for circular pile elements

5.3.6 H/L (between pile element types)

The comparison of pile element types in terms of wave steepness is presented in Figure 5-24 and Figure 5-25. The spread of results again points to the varying sensitivity per pile type as porosity decreases. For the lower porosity values, the circular piles are most sensitive, thereafter the square piles and the least sensitive are the diagonal squares.

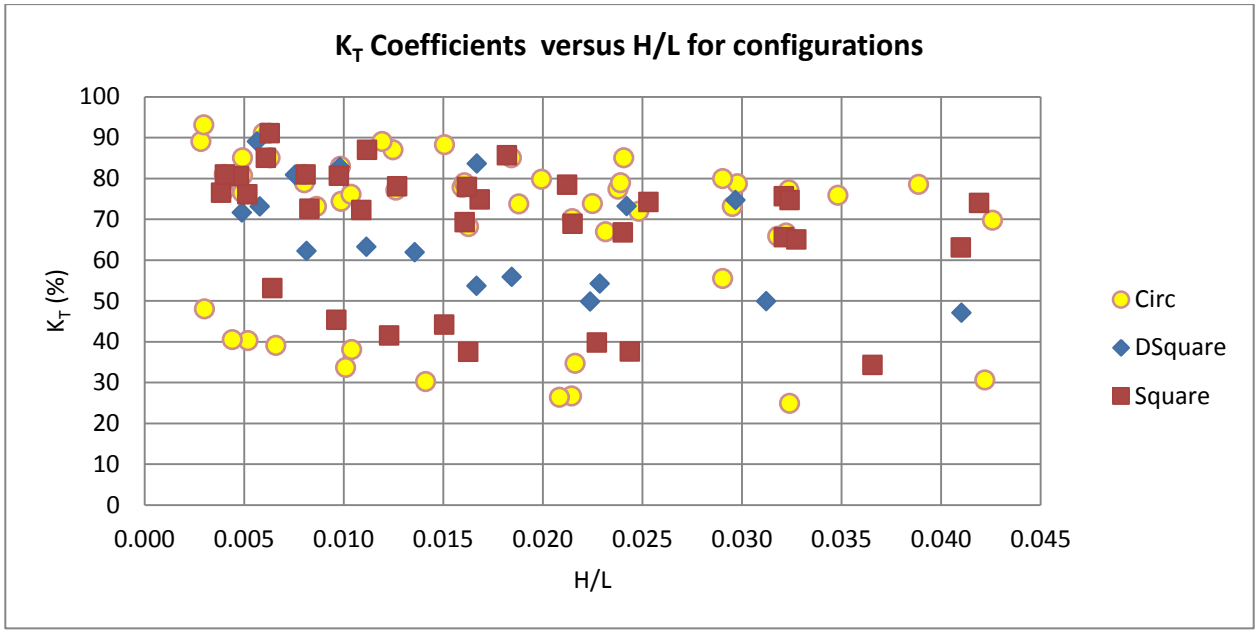

Figure 5-24: Transmission coefficient versus H/L comparing different element shapes

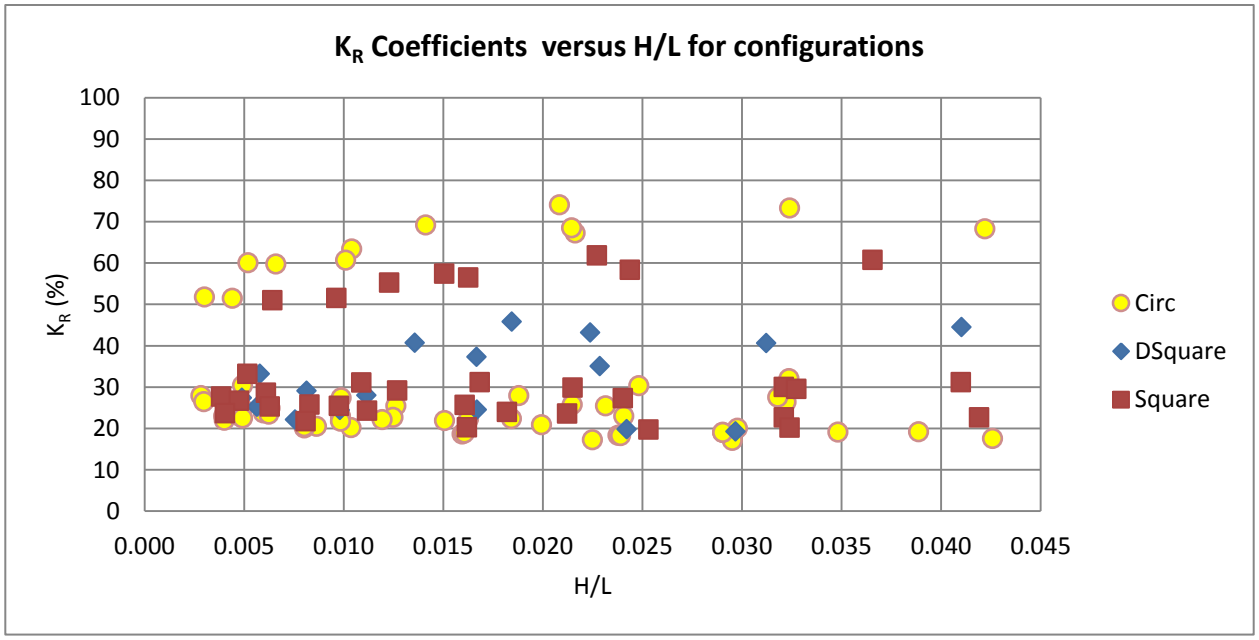

Figure 5-25: Reflection coefficient versus H/L comparing different element shapes

5.3.7 H/L x e

As some literature made mention of the steepness times the porosity ratio, it was tested in this study, but from what can be seen in Figure 5-26 this did not yield a useful comparison. No relationships were further investigated.

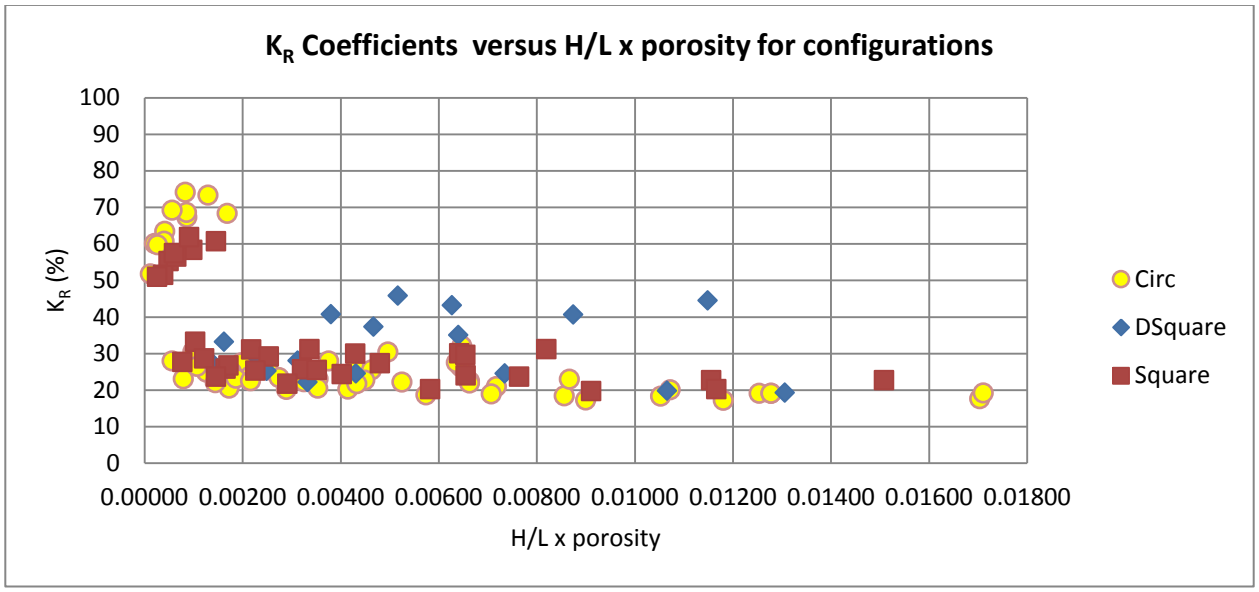

Figure 5-26: Reflection coefficient versus H/L x e comparing different element shapes

5.3.8 H/L/e

Wave steepness divided by porosity was investigated for one instance only (similar to the comparison for steepness x e), but the resulting plot in Figure 5-27 did not present more clarity on steepness combined with porosity.

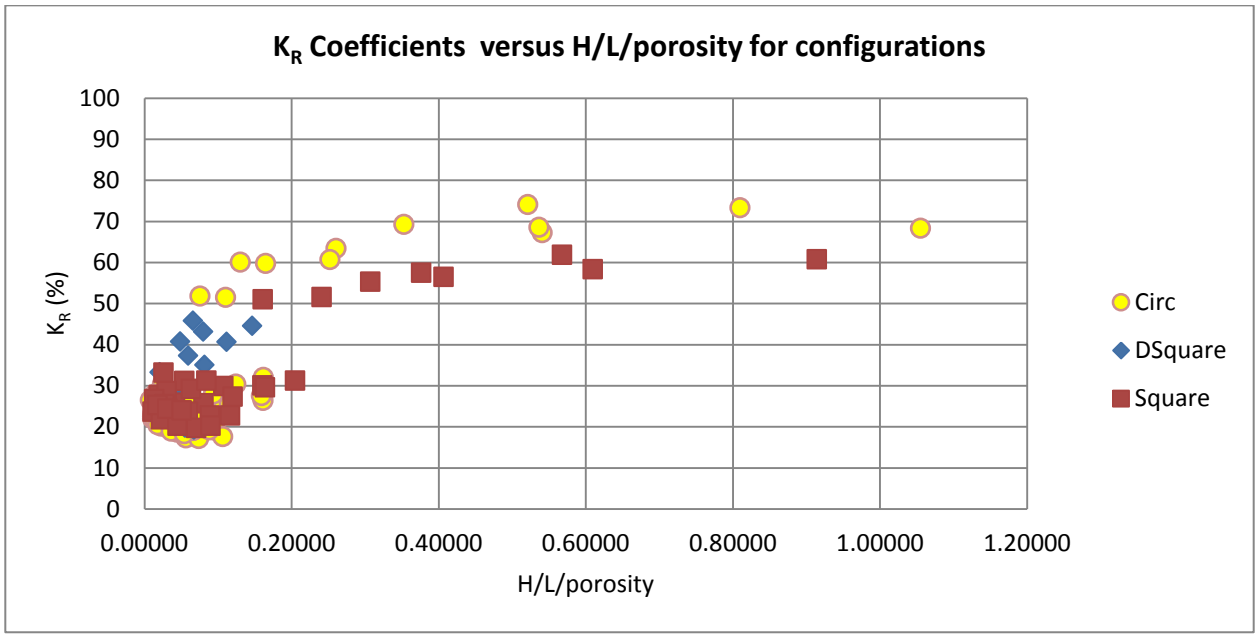

Figure 5-27: Reflection coefficient versus H/L/e comparing different element shapes

5.3.9 Circular piles: d/L for varying porosities

In this section, Figure 5-29 to Figure 5-31 represents a more detailed comparison of the relationship between reflection and transmission coefficients over relative depth (d/L) as well as incorporating predicted values for the coefficients. The only possible relationship identified is that the sensitivity of the coefficients at lower porosities is confirmed. As for the comparison with predicted values, the transmission coefficients have strong correlation with those predicted by Thomson and also by Kriebel. The reflection coefficient from the test data seem to correspond with Mei and Kriebel's predicted values. The trends presented by the d/L plots have strong correlation with the kd plot in section 5.3.5, as could be expected.

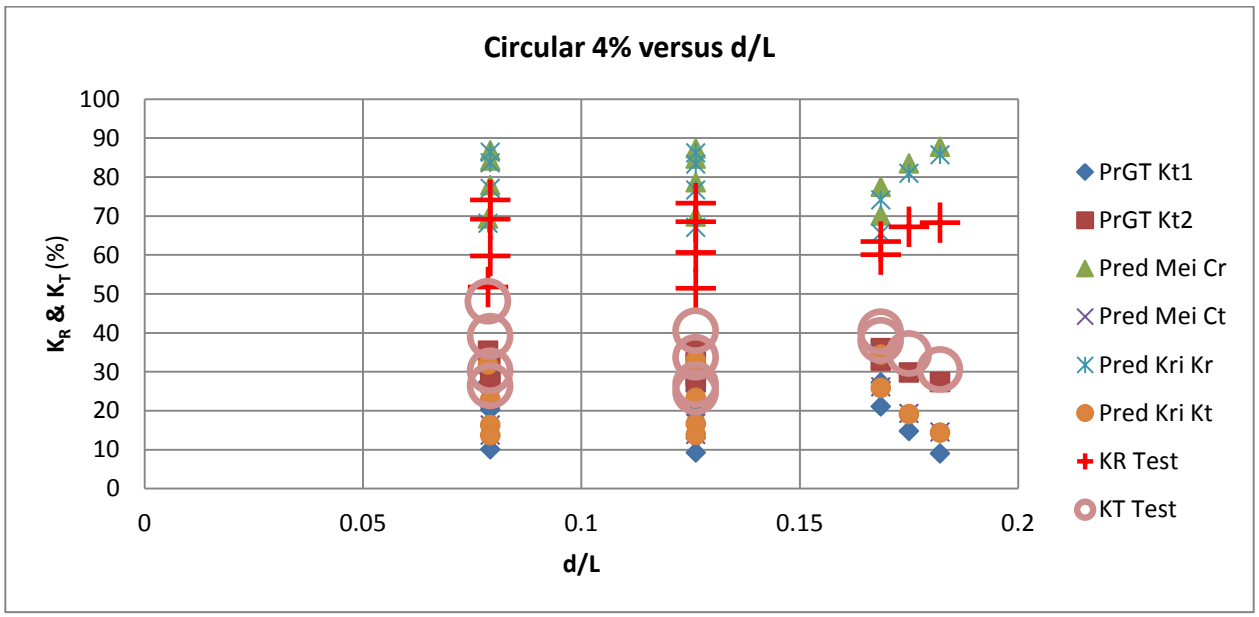

Figure 5-28: Coefficients for Circular piles, 4% porosity versus d/L including predictions

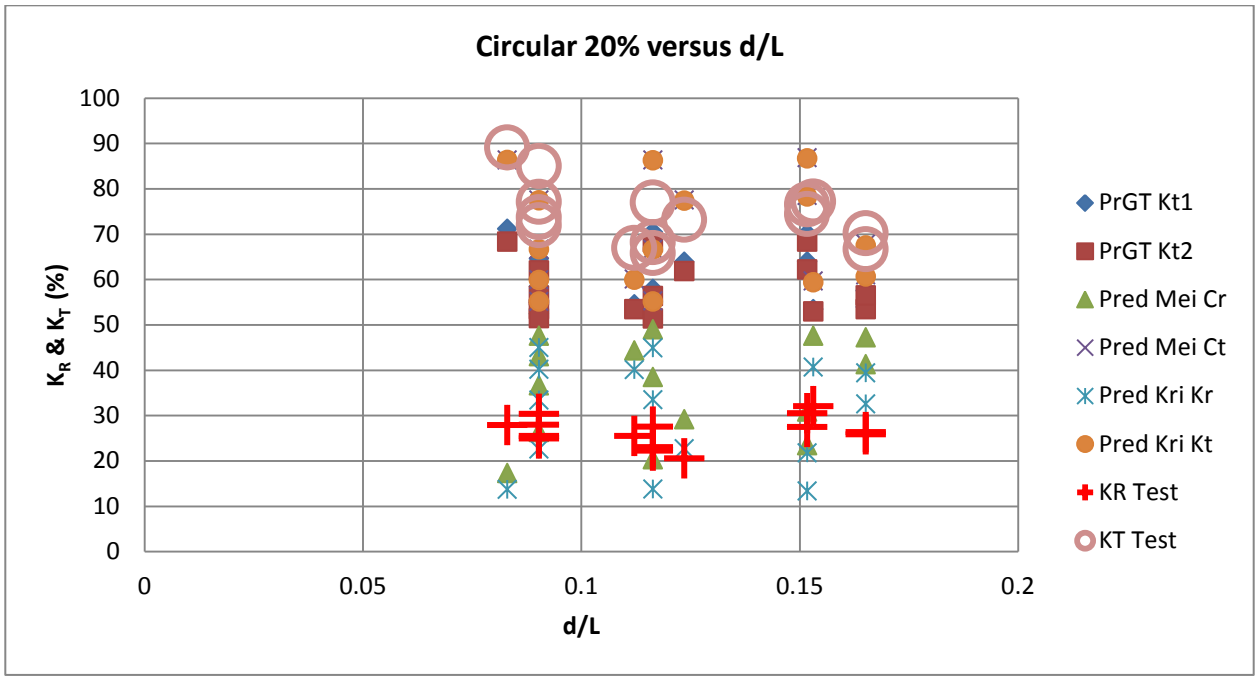

Figure 5-29: Coefficients for Circular piles, 20% porosity versus d/L including predictions

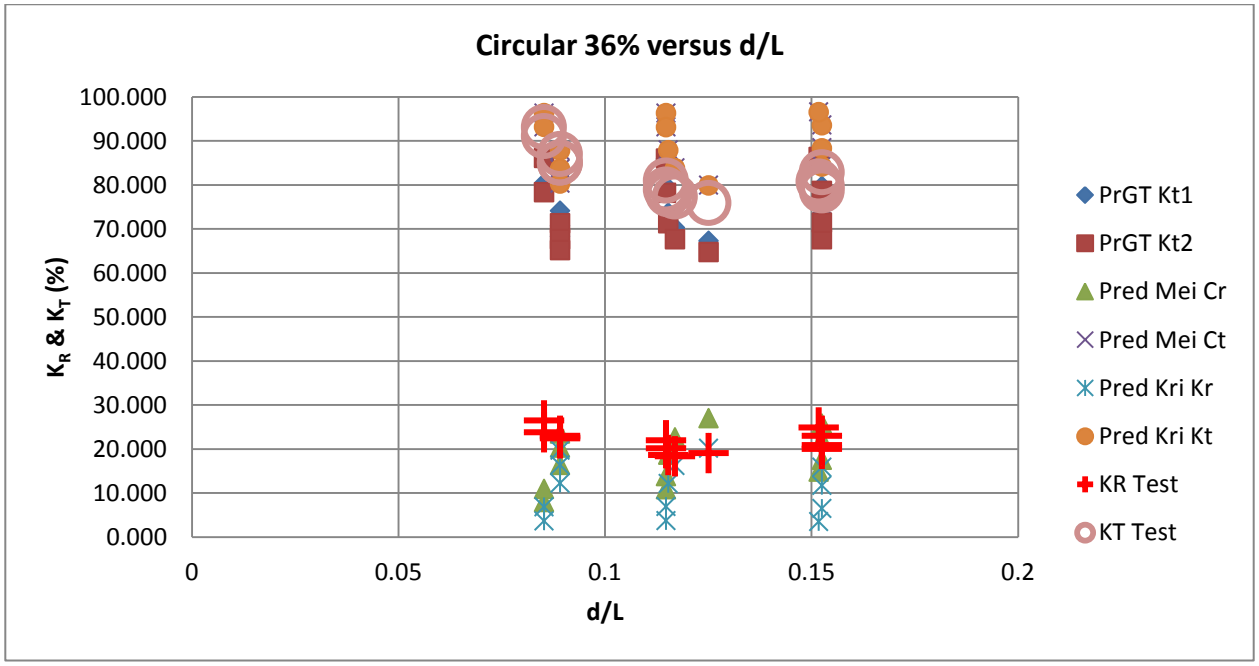

Figure 5-30: Coefficients for Circular piles, 36% porosity versus d/L including predictions

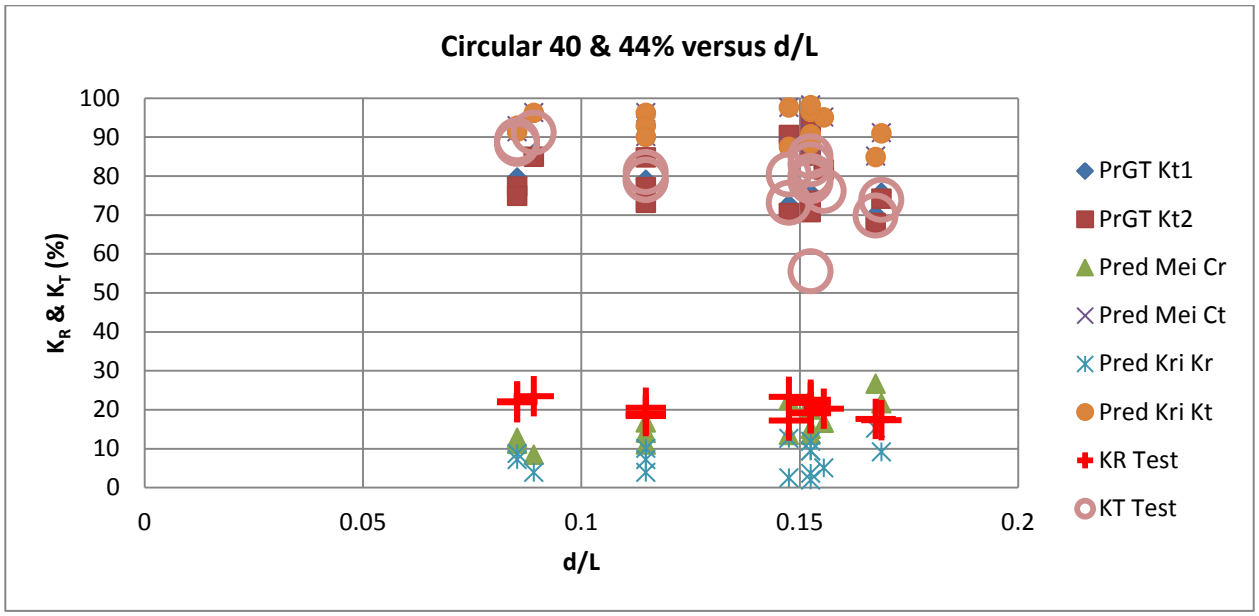

Figure 5-31: Coefficients for Circular piles, 40% & 44% porosity versus d/L including predictions

5.3.10 Diagonal square piles: Coefficients versus d/L for varying porosities

In this section, Figure 5-32and Figure 5-33 represents a more detailed comparison of the relationship between reflection and transmission coefficients over relative depth (d/L) as well as incorporating predicted values for the coefficients. No conclusion was reached on the dependency of coefficients over relative depth. As for the comparison with predicted values, the transmission coefficients are generally higher and the reflection coefficients were generally lower than the predicted values.

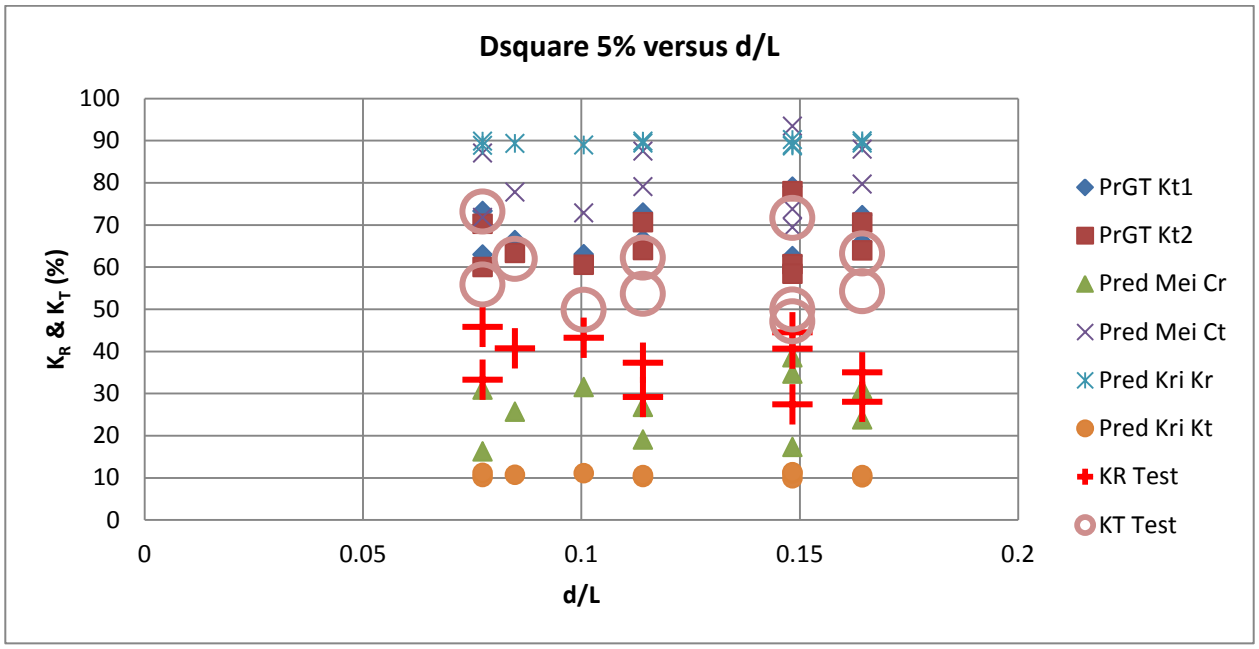

Figure 5-32: Coefficients for diagonal square piles, 5% porosity versus d/L including predictions

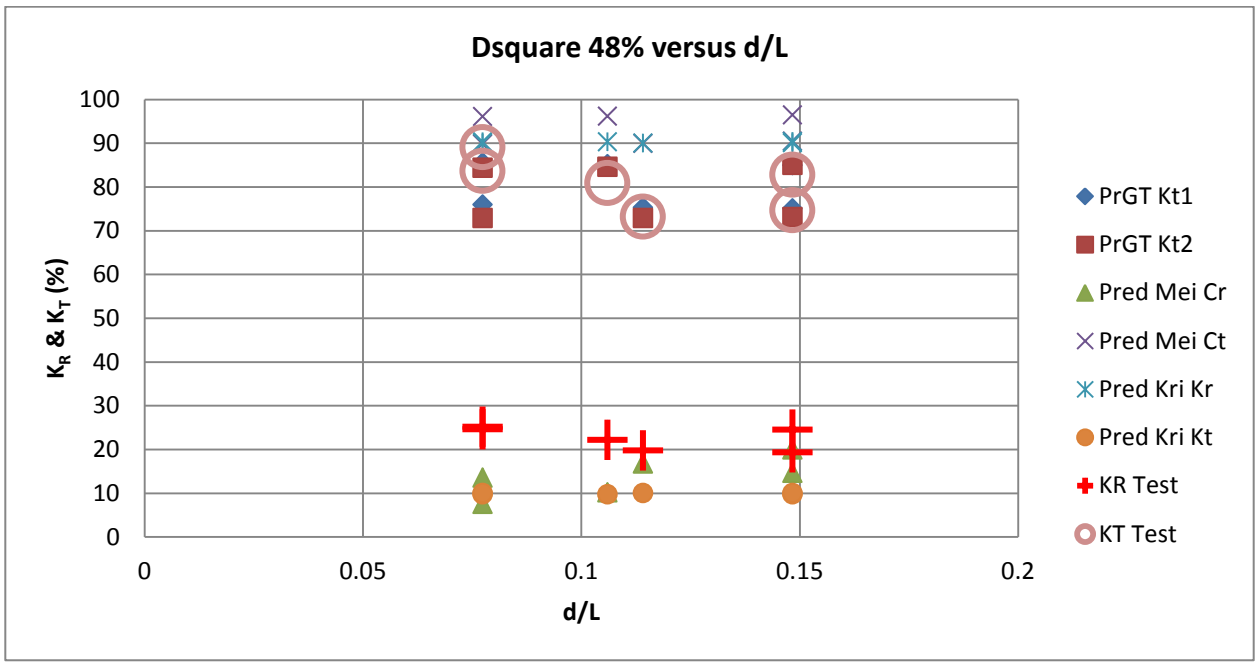

Figure 5-33: Coefficients for diagonal square piles, 48% porosity versus d/L including predictions

5.3.11 Square piles: Coefficients versus d/L for varying porosities

In this section, Figure 5-34 to Figure 5-35 indicate no dependency of transmission and reflection coefficient on relative depth. As for the comparison with predicted values, the transmission and reflection coefficients are generally higher and lower respectively.

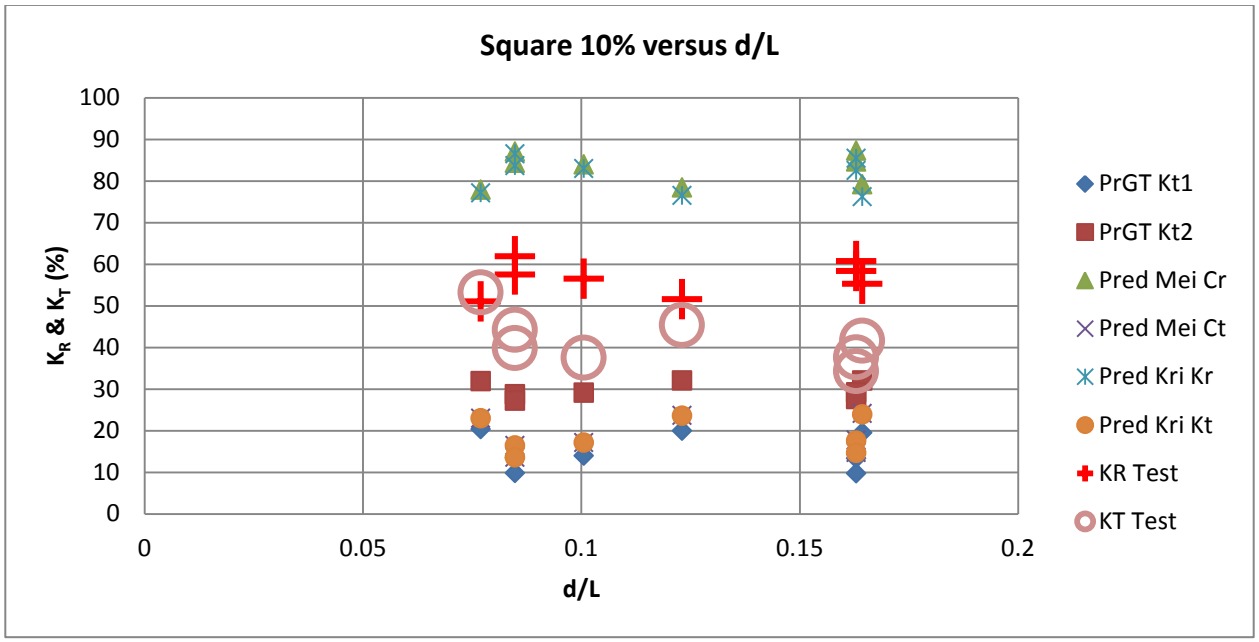

Figure 5-34: Coefficients for square piles, 10% porosity versus d/L including predictions

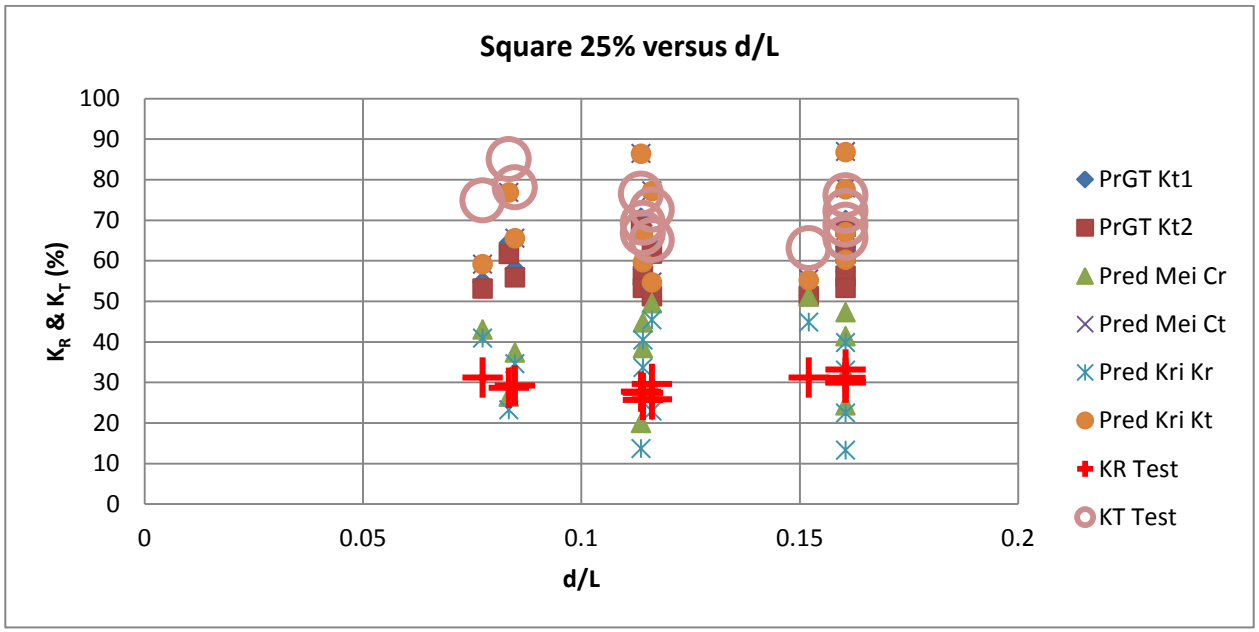

Figure 5-35: Coefficients for square piles, 25% porosity versus d/L including predictions

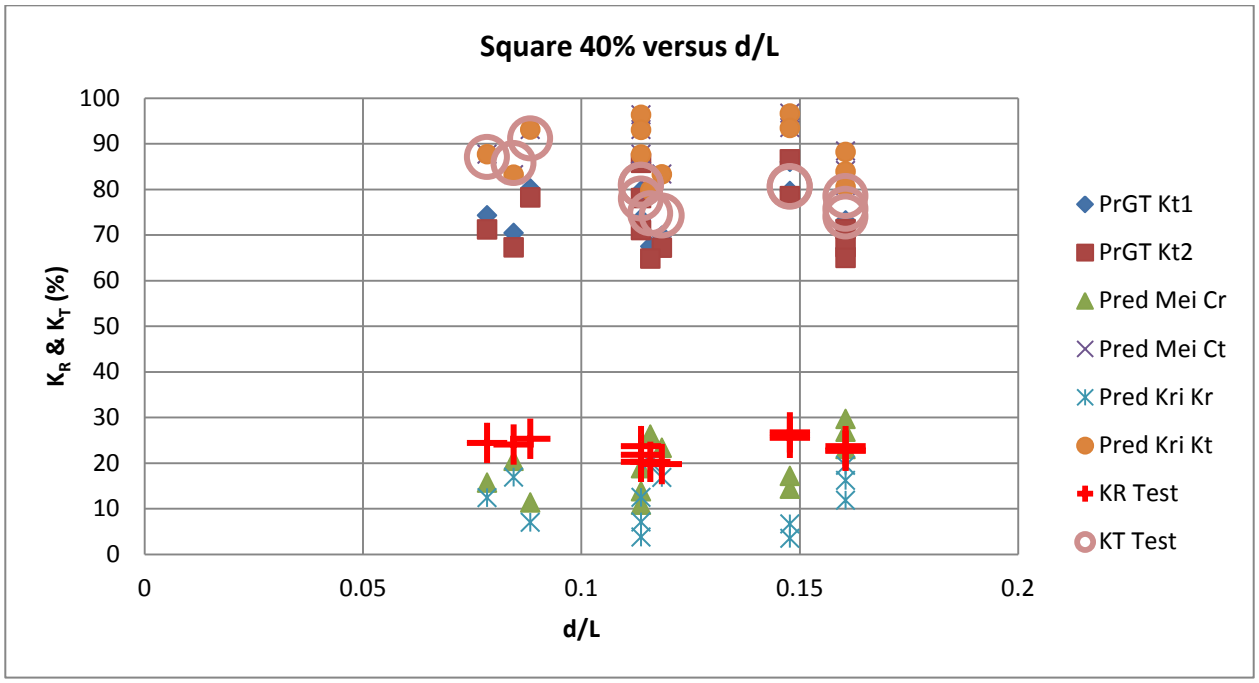

Figure 5-36: Coefficients for square piles, 40% porosity versus d/L including predictions

5.3.12 Circular piles: Coefficients versus H/L for varying porosities

The dimensionless parameter H/L or wave steepness has shown some relationship to the transmission and reflection coefficients in earlier sections. In Figure 5-38 to Figure 5-40 the transmission coefficients are in general higher than predicted and the reflection coefficients lower than predicted. For the lower porosities, there is some dependency that can be observed in that transmission reduces and reflection increases with increased wave steepness.

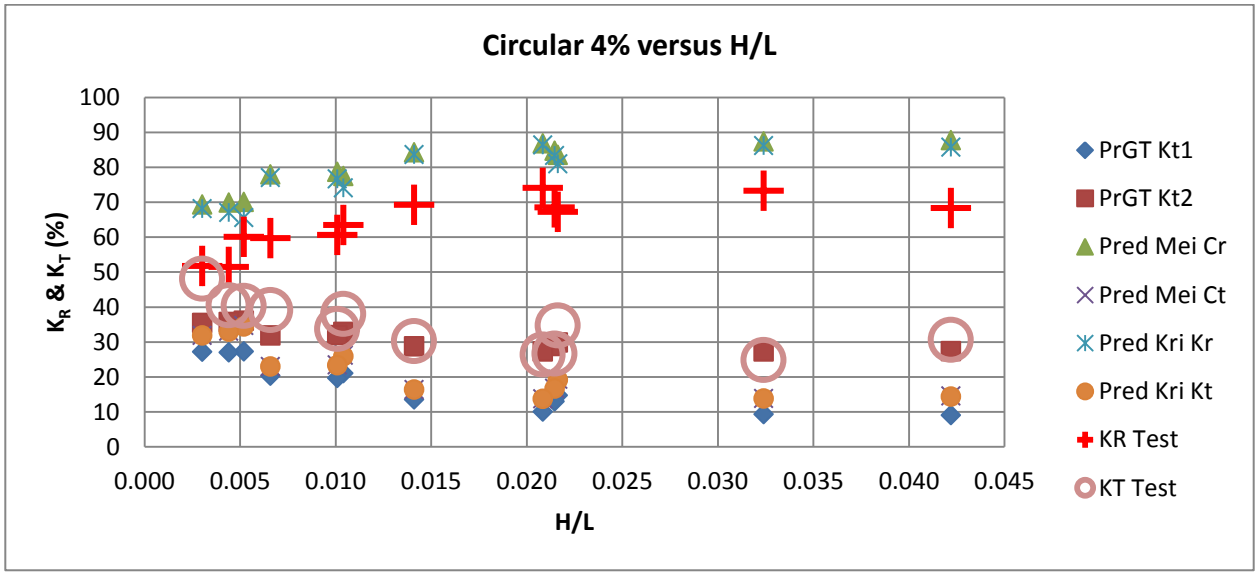

Figure 5-37: Coefficients for circular piles, 4% porosity versus H/L including predictions

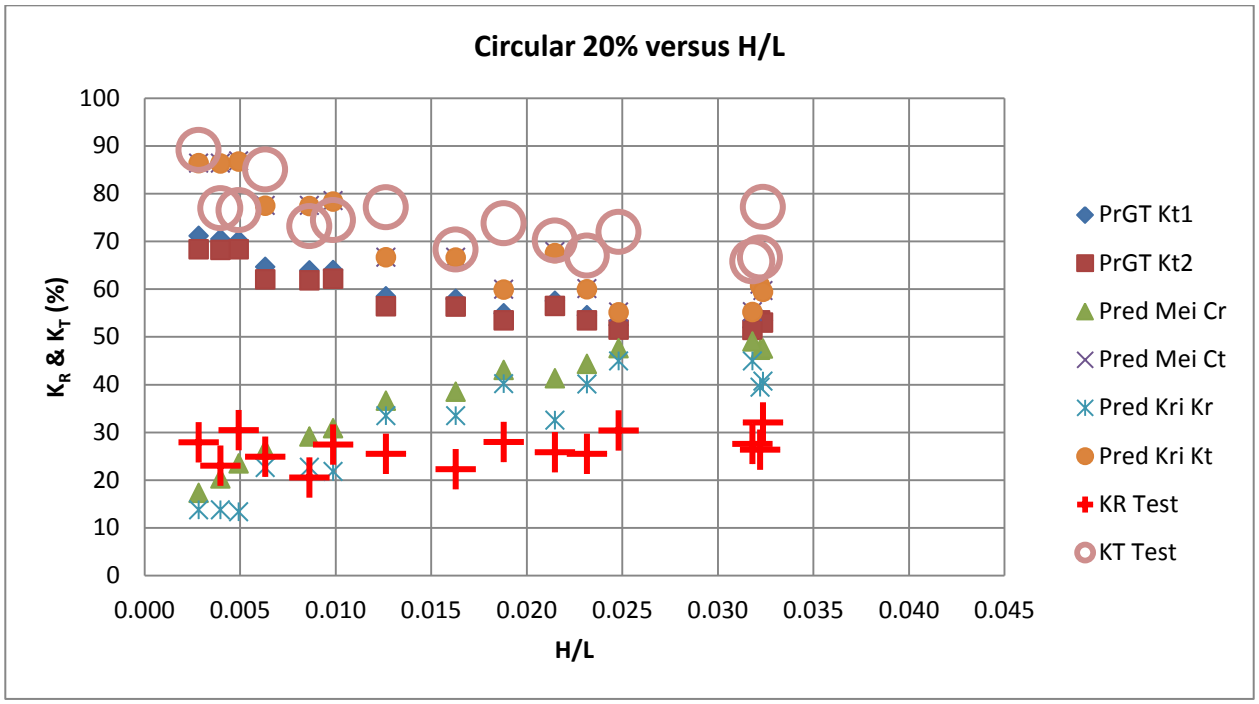

Figure 5-38: Coefficients for circular piles, 20% porosity versus H/L including predictions

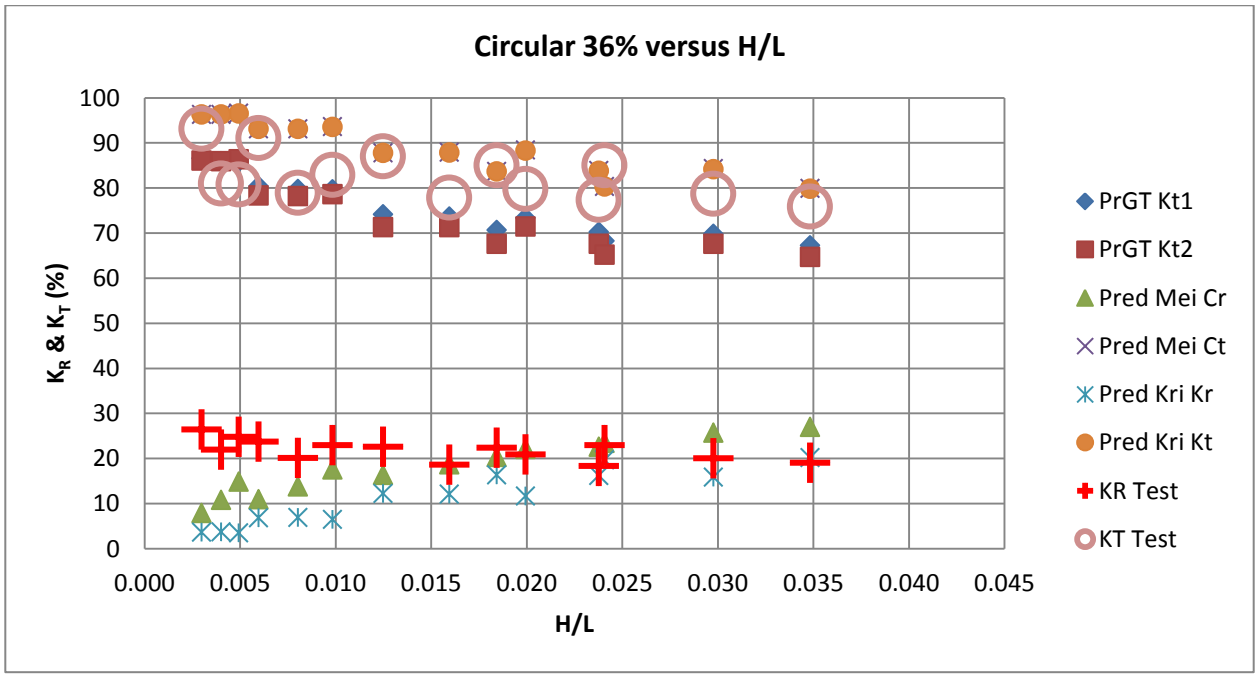

Figure 5-39: Coefficients for circular piles, 36% porosity versus H/L including predictions

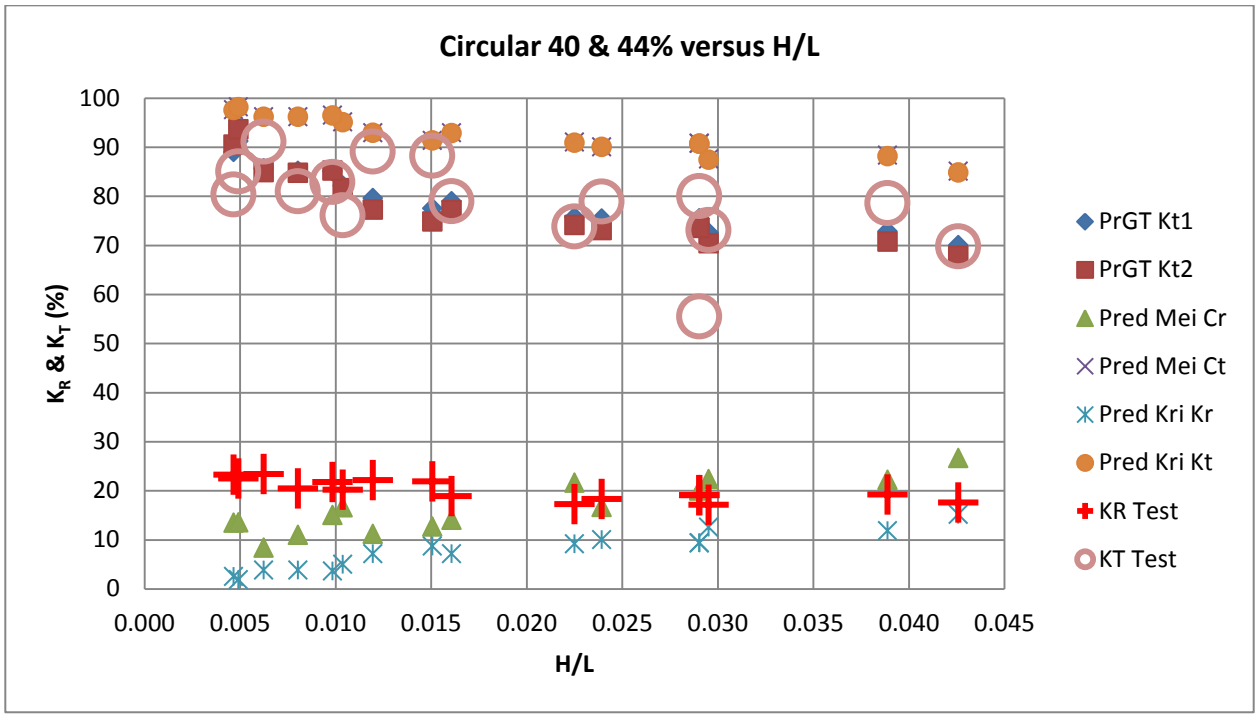

Figure 5-40: Coefficients for circular piles, 40% and 44% porosity versus H/L including predictions

5.3.13 Diagonal square piles: Coefficients versus H/L for varying porosities

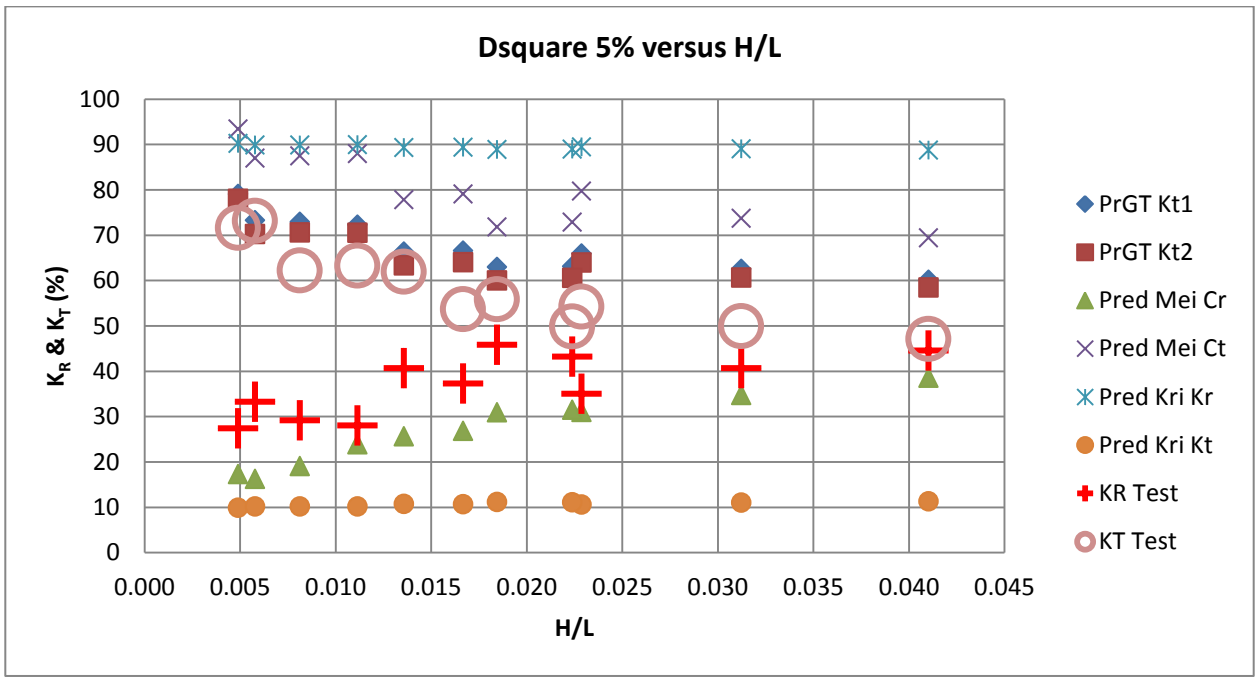

Figure 5-41: Coefficients for diagonal square piles, 5% porosity versus H/L including predictions

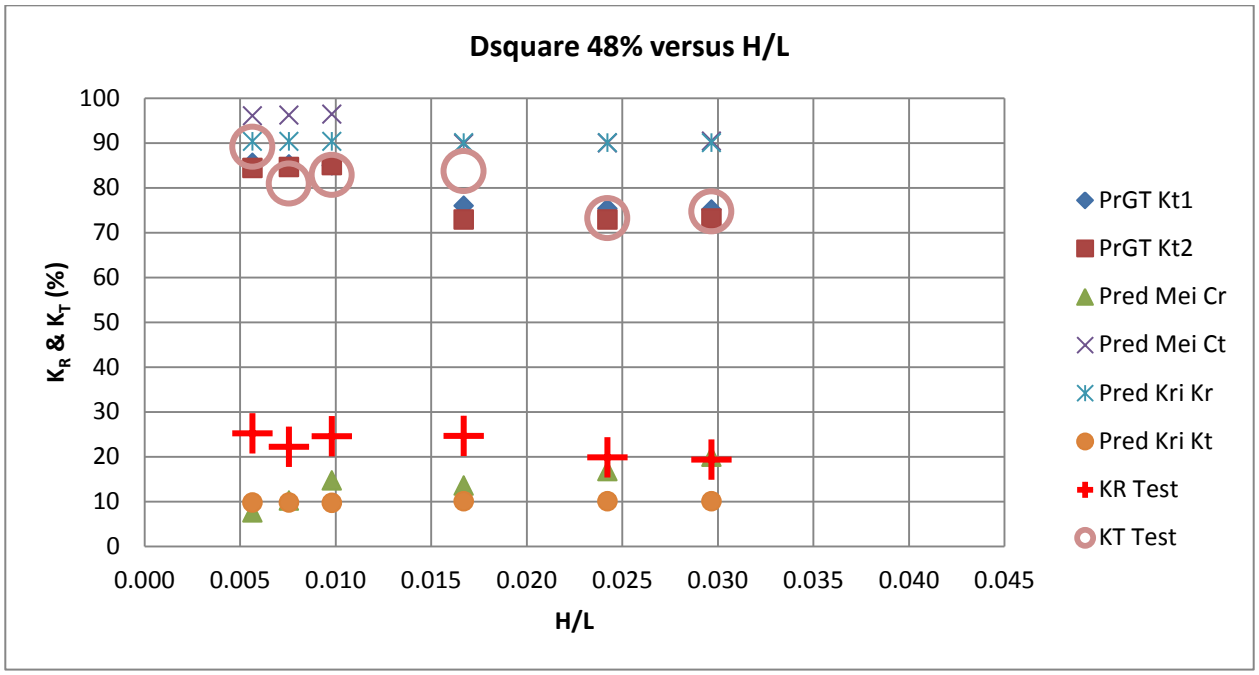

Figure 5-42: Coefficients for diagonal square piles, 48% porosity versus H/L including predictions

5.3.14 Square piles: Coefficients versus H/L for varying porosities

Figure 5-43 to Figure 5-45 shows similarities with the circular sections for the lower porosities, in that the screen transmission and reflection coefficients are reduced and increase, respectively, with increased wave steepness. Compared with the predicted values, the values from the test data are lower for reflection and higher for transmission values respectively.

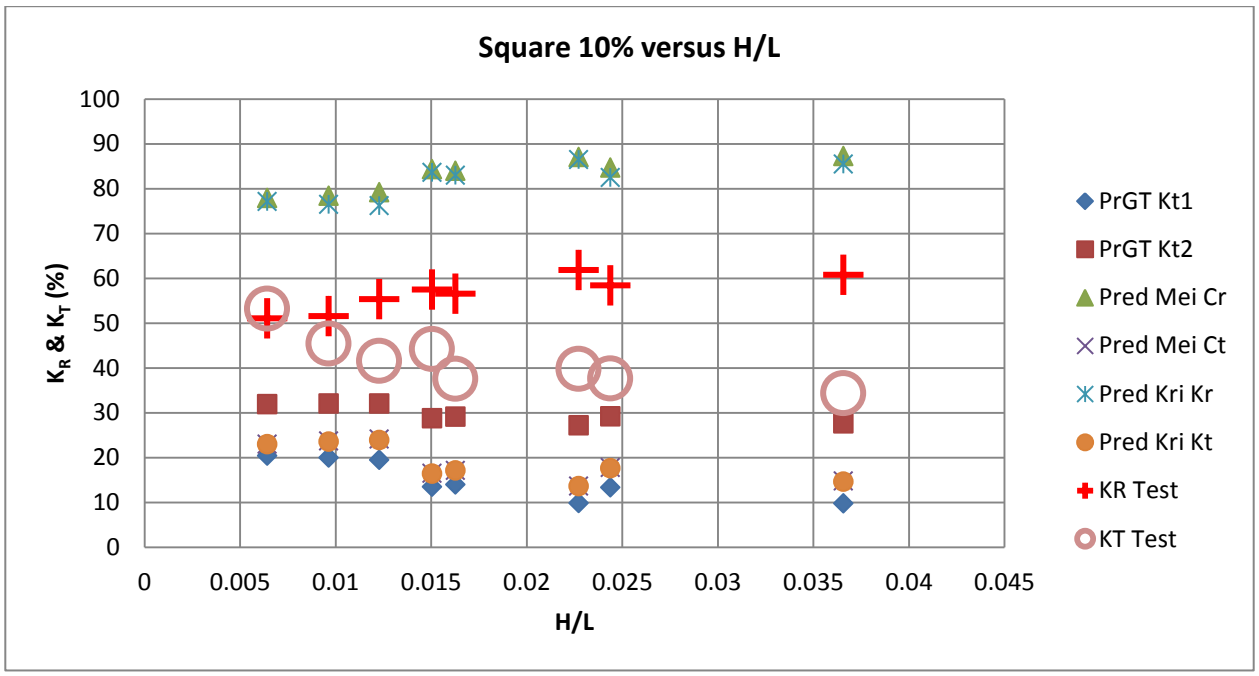

Figure 5-43: Coefficients for square piles, 10% porosity versus H/L including predictions

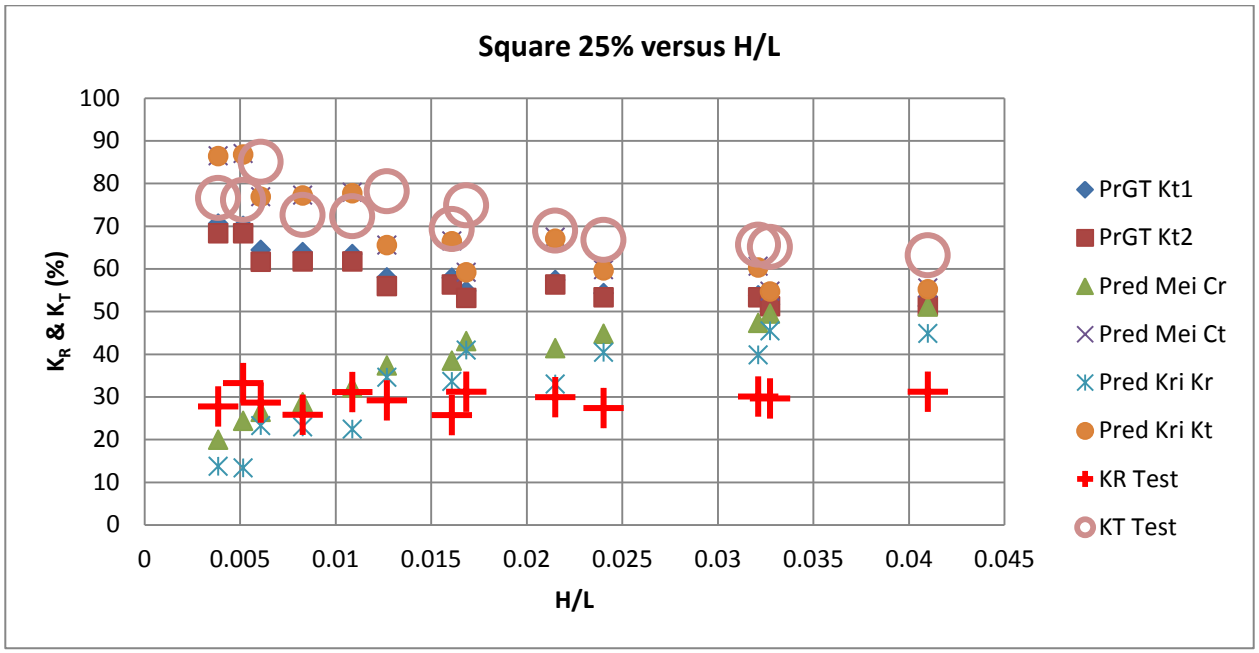

Figure 5-44: Coefficients for square piles, 25% porosity versus H/L including predictions

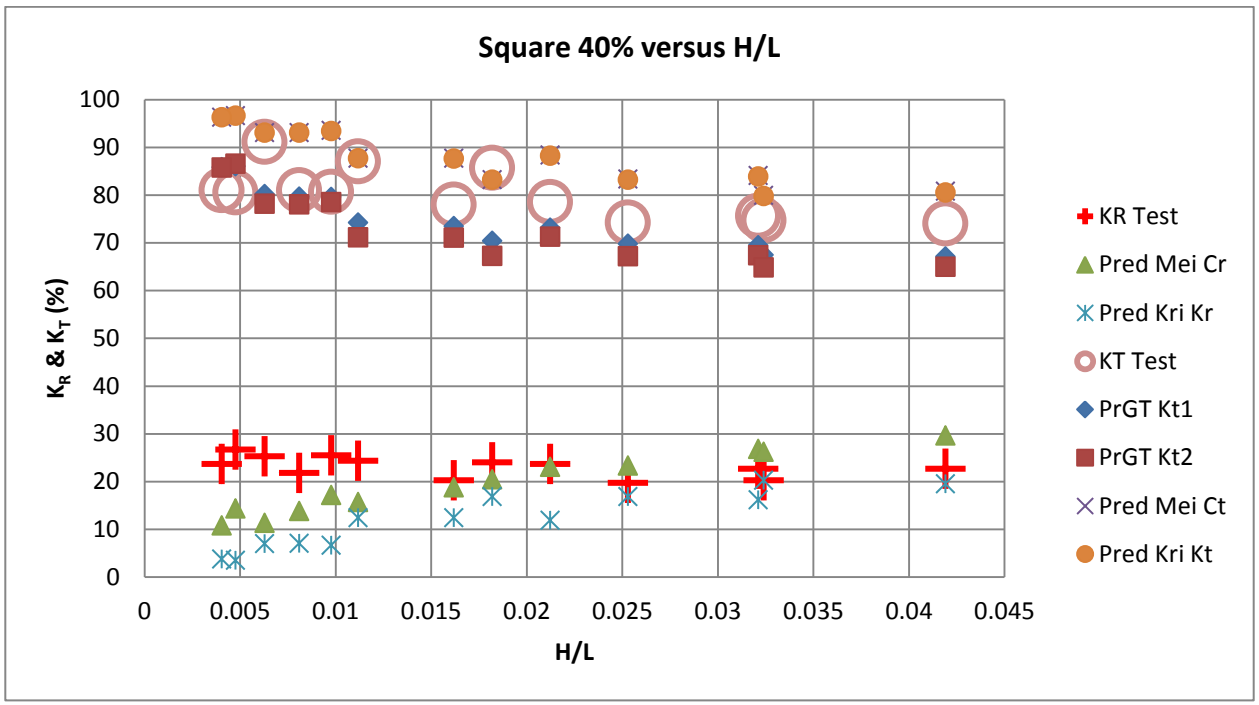

Figure 5-45: Coefficients for square piles, 40% porosity versus H/L including predictions

5.3.15 Circular piles: Coefficient versus H/d for varying porosities

When dividing H/L by d/L one is left with H/d which was presented only for circular sections with varying porosities in Figure 5-46 and Figure 5-47. This ratio did actually yield some trends for the lower porosity values. Increased reflection and reduced transmission was noted with increased H/d values.

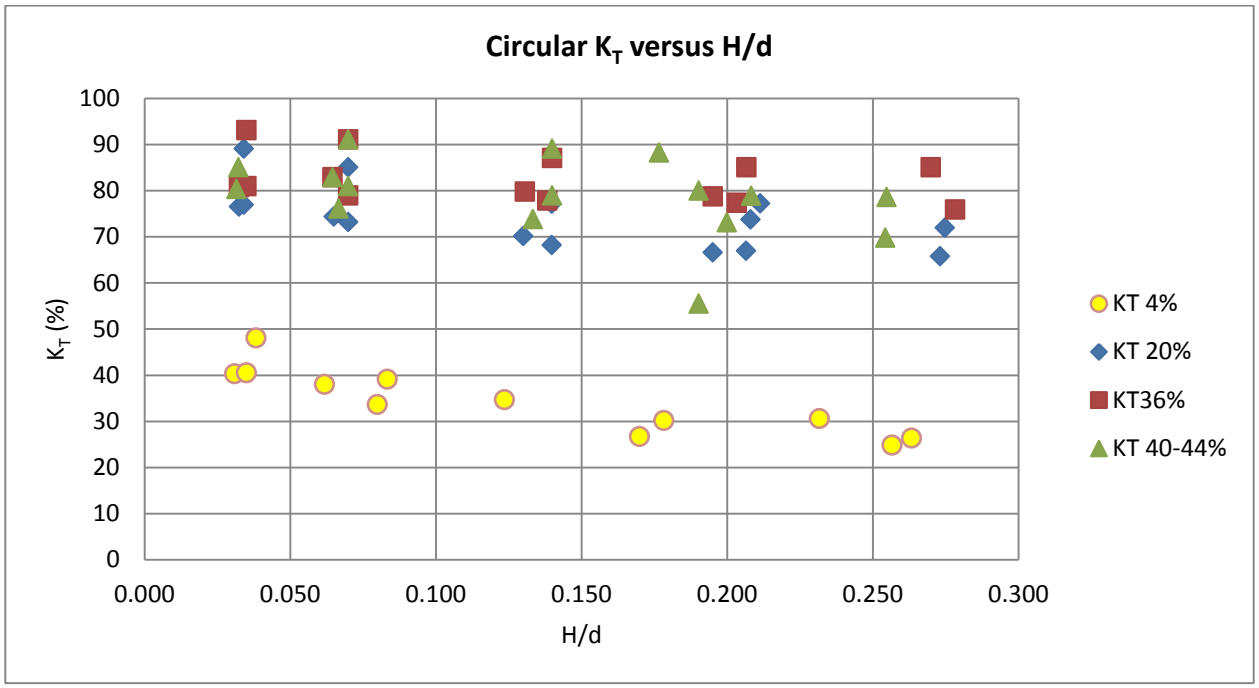

Figure 5-46: Transmission coefficient versus H/d for varying porosities

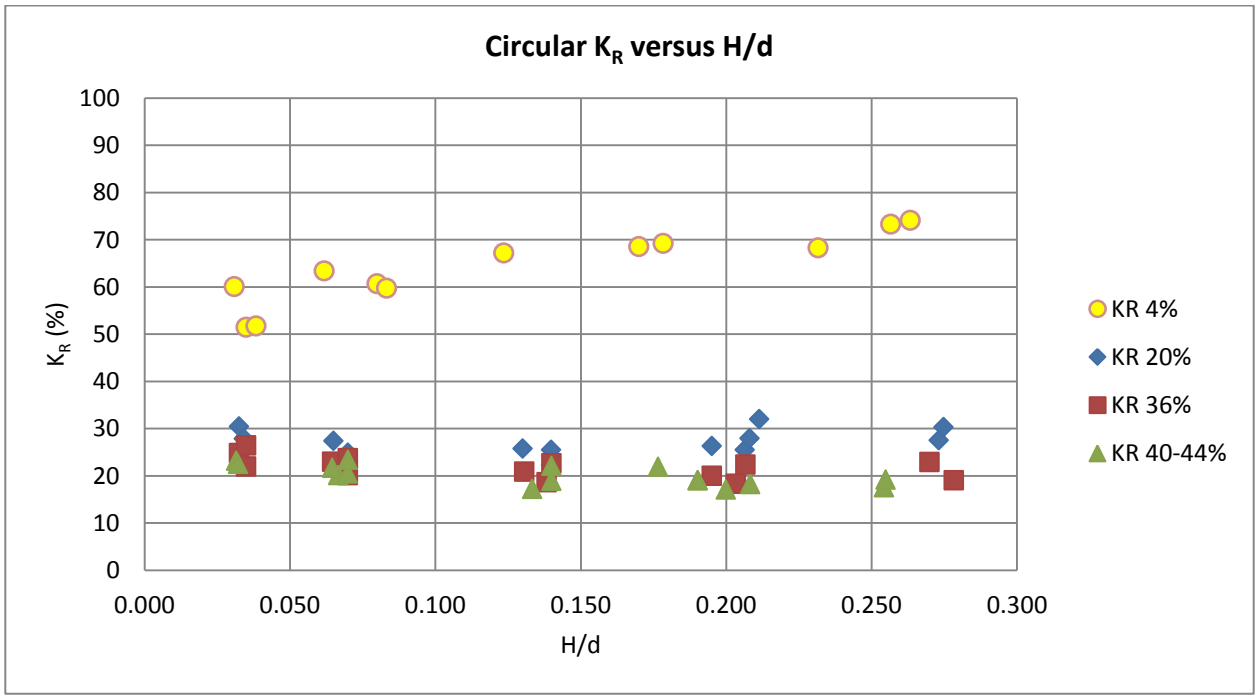

Figure 5-47: Reflection coefficient versus H/d for varying porosities

5.3.16 Circular piles: Reflection coefficients versus H/L for low porosities

For the purpose of comparing the types of pile elements more directly, the reflection coefficients for the lowest porosity for each of the shapes were compared.

If the highest performing shape could be viewed as the highest reflection achieved, then the circular piles seem to yield the better results, although it should be noted that the tests could not be set up with exactly the same porosities between the piles given the fixed width that varied for the sections that had to fit into the overall width. It would be premature to do a ranking on the comparative performance of the respective shapes based on this value only. However, throughout the results the circular and square elements performed best and the diagonal elements were less responsive at the lower porosities, although the coefficient values at higher porosities compared well with predicted values.

It should be noted that the same porosity was achieved with fewer piles in the case of the diagonal piles, compared with the number of piles required for circular and square elements.

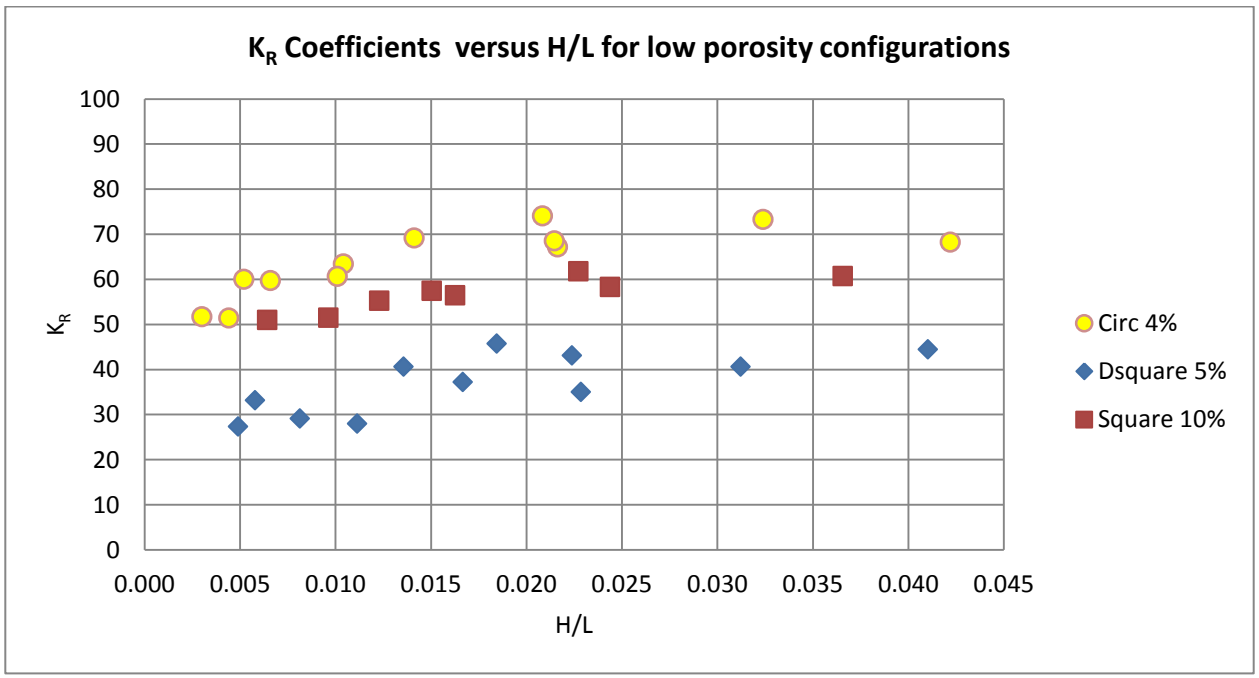

Figure 5-48: Reflection coefficient versus H/L for low porosities

5.3.17 Circular piles: Reflection coefficients versus H/L for similar number of piles

To compare the amount of materials used, rather than the porosity, which is a ratio based on the percentage gaps between elements in elevation, the following graph (See Figure 5-49) compares coefficients for configurations between the shapes where the criterion was to select the closest matching number of vertical piles as opposed to the derived percentage.

It is interesting to note the outcome as the diagonal square elements seem to perform quite well in this instance, with the circular and square elements in a separate grouped bandwidth. It also appears that this difference is accentuated at higher wave steepness.

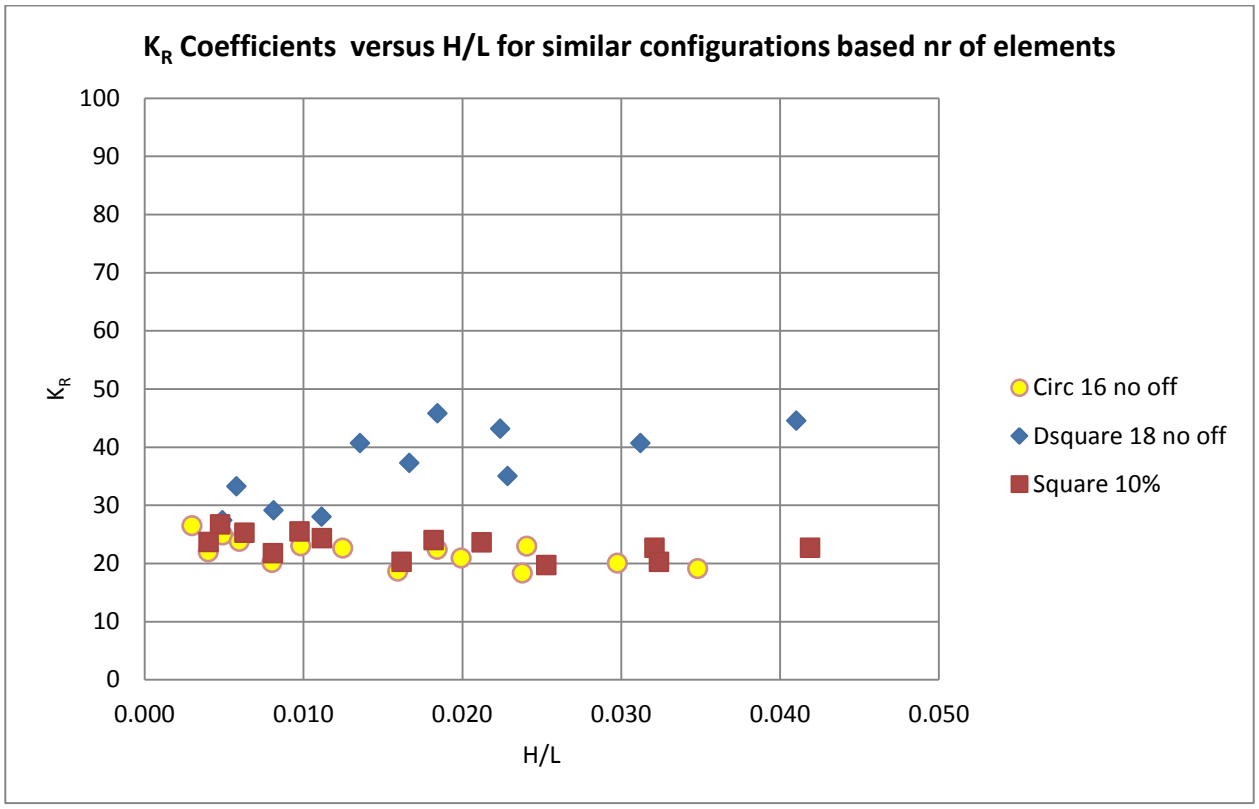

Figure 5-49: Reflection coefficient versus H/L for varying porosities

5.4 Summary Discussion on Data Analysis

Various relationships were tested to investigate dependencies between various input and performance parameters. A summary of the relationships that could be identified is contained in Table 5-1.

The most interaction was found to occur with low porosities (below 10%) with dependencies on several parameters not being clear enough to draw conclusions. However, the trends of coefficients over wave steepness were found to yield some clear dependencies. The most

valuable observations were obtained from the wave steepness plots, and it was also shown that particle velocity was increased for an increase in wave steepness. As wave steepness increases, the reflection from the model breakwater increased while the transmission through the model breakwater decreased.

To compare the element types, it is important to keep in mind that the material used to obtain certain porosity could be the most important aspect when considering possible alternatives, as this would directly relate to matters of finance and time when considering implementation. In general, for a given breakwater porosity, the circular elements were most efficient followed by the square elements and least efficient was the diagonal squares. However, for a fixed quantity of material, i.e. for a fixed number of piles, the diagonal squares performed the best in terms of the highest reflection and lowest transmission respectively for a given input wave.

Table 5-1: Summary of data analysis

Report Section	Dependencies investigated	Relationship or Dependency from graphs
5.3.1	Particle velocity over relative depth for H/L	None
	Particle Velocity versus H/L	Increased particle velocity for increased H/L
5.3.2	K_T versus Tp – circular sections	None
	K_R versus Tp – circular sections	None
5.3.3	K_T versus Hm0 – circular sections	Reduced transmission for increased Hm_0
	K_R versus Hm0 - circular sections	Increased reflection for increasing Hm_0
5.3.4	K_T versus $d/g/T^2$ - circular sections	None
	K_R versus $d/g/T^2$ - circular sections	None
5.3.5	K_T versus kd - circular sections	Grouping in apparent bandwidth. No trend visible.
	K_R versus kd - circular sections	Grouping in apparent bandwidth. No trend visible.
5.3.6	K_T versus H/L - circular sections	Some trend visible in bandwidths. Detailed analysis undertaken in 5.3.12 – 5.3.14
	K_R versus H/L - circular sections	Some trend visible in bandwidths. Detailed analysis undertaken in 5.3.12 – 5.3.14
5.3.7	K_R versus H/L x e	None
5.3.8	K_R versus H/L/e	None
5.3.9 – 5.3.11	Coeff versus d/L, for porosity - all shapes (instead of kd)	Grouping in apparent bandwidth. No trend visible.
5.3.12 – 5.3.14	Coeff versus Hs/L, for porosity - all shapes (instead of ka)	Transmission reduced & reflection increased with higher steepness
5.3.15	Coeff versus H/d, for porosity - all shapes	Increased reflection and reduced transmission for increase in H/d
5.3.16	K_R versus H/L compare shapes with similar porosity	circular and square elements performed best and the diagonal elements were less responsive
5.3.17	K_R versus H/L compare shapes with similar nr of piles	Diagonal squares performed best, and increased the gap for higher wave steepness

6 Curve fitting with test data

For the purpose of contributing to the value of the empirical equations identified, the data that was analysed in section 5.3 was further analysed for identifying potential trends and curve fitting. Although no sophisticated method was used for the curve fitting, the MS EXCEL functionality allows the operator to test different type of regression functions, whether linear, polynomial, logarithmic, and exponential or log normal.

The dependency selected for doing curve fits, was the wave steepness for the lowest porosity set-up per pile element shape. In order to select the best fit, the visual fit was inspected for the best functions, and the best fit was then selected based on the geometry of the curve as well as the comparison of the R^2 values of the statistical fit.

It is noted that there are significantly more sophisticated methods of determining empirical equations, such as SYSTAT (Thomson, 2000) which could develop multi-term polynomials with variable coefficients. It is therefore important to note that the curves and functions put forward in this thesis are valid only for similar input parameters and these should not be extrapolated to other values of the test parameters, without studying their context in this study and the assumptions made.

For the various shapes of piled elements, the following set of equations is presented as published contribution to literature (see Table 6-1). The full set of graphs with fitted curves and equations have been included in Appendix C.

Table 6-1: Equations for fitted curves & R2 values

Element Shape	Porosity	Equation	R^2
Circular	4 %	K_T = -7.475 * ln(H/L) + 1.3476	R^2 = 0.7835
Circular	20 %	K_T = -6.234 * ln(H/L) + 47.062	R^2 = 0.5799
Square	10%	K_T = -9.803 * ln(H/L) + 0.9494	R^2 = 0.8446
Diagonal Square	5%	$K_T = 24203 * (H/L)^2 – 1759(H/L) + 79.358$	R^2 = 0.9222

7 Application of test results to possible marina sites

7.1 Area of application

The physical model testing incorporated the predetermined input parameters (i.e. water depth, pile element configurations and wave parameters) from potential sites as shown in section 3.3. This section aims to apply the test data to potential sites where protected shallow water marinas could be developed.

This thesis focussed on the hydraulic performance of piled row breakwaters, although for the selection of an alternative concept in engineering practice several other considerations need to be included in the evaluation of the possible concepts as pointed out in section 1.4.1. However, for the selection of the type and setup of piled row breakwater sub-options, given that possibilities exist to vary the overall porosity and the type of piled elements, this thesis has presented a useful comparison when considering certain options.

For the purpose of developing an effective marina concept, the basin tranquillity in terms of a maximum allowable wave height would be determined based on the expected design vessels. The calculated transmitted waves for that particular site would then be used to test the concept of the proposed marina. The transmitted wave height would therefore be viewed as a measure of performance. The effectiveness of the marina layout and its components would take into consideration the cost required (in this case the required material quantity) to achieve the target tranquillity. This would vary for various pile breakwater configurations and pile element shapes and spacing.

During concept evaluation stage, it would be advisable to calculate the tranquillity for a range of porosities for the design conditions in order to optimise the design for material required versus performance. The number of piles included and a mass per unit meter length should be included as a measure of the material required, as a basis for comparison

To determine whether the configurations that were tested could be applied as effective breakwaters for marinas, the basin tranquillity of the potential sites has been estimated from the test data from this thesis.

The following sections were aimed at applying the evaluation of concept options to a possible project application. Firstly, suitable conditions for marinas were summarised from technical references (see Section 7.2) in terms of wave height. Section 7.3 then reports the test of the pile configurations to derive the transmitted wave heights for comparison with suitable berthing conditions. A short discussion is presented in Section 7.4 on the application of the test data.

7.2 Basin Tranquillity for Prototype Marina

From the potential marina sites selected, the maximum water depth per site was limited to 3m at low tide, as this was also the corresponding limit of water depth that the physical testing could consider. Therefore, the design vessel sizes were selected to correspond with this depth, including a 10% allowance for underkeel clearance for safe berthing.

A selection of indicative vessel sizes has been sourced from previous projects and represent the range of sizes that could be required to be hosted in the potential marina (see Table 7-2). From this table, all vessels with a draught of less than 2.7m would be able to use the marina. The vessels that would not qualify were yachts of length greater than 20m. Power boats up to 40m in length were also omitted as these vessel types are usually scarce for the market where the proposed marinas have been considered.

The incident wave condition selected is shown in Table 7-1 with the motivation as per the comment included.

Table 7-1: Incident waves for proposed marina location

Incident Wave in field		Corresponding wave in model scale		
Hs (m)	Tp (s)	Hs (m)	Tp (s)	Comment
0.94	4	0.28	1.68	As per fetch limited calculated wave in section 3.3.3

Table 7-2: Indicative vessel sizes from previous marina projects (vessels with dimensions highlighted in grey blocks omitted)

Boat Length (m)	Power Boat Draught (m)	Yacht Draught (m)	Boat width / Beam (m)
6	0.9	1.5	2.8
8	0.9	1.5	3.4
10	1.0	1.8	4.0
12	1.0	2.0	4.4
15	1.2	2.5	5.0
20	1.5	2.9	5.7
40	2.3	4.2	10

Table 7-3 represents a summary of allowable wave heights for various orientations and vessel lengths. These were derived from literature including CEM, AS 3962-2001 and UFC 4–152-07N.

Table 7-3: Allowable wave conditions for small craft

Vessel Length (m)	Beam/Quartering Wave Height (m)	Beam/Quartering Wave Period (s)	Head on Wave Height (m)	Head on Wave Period (s)
4 - 10	0.2 0.15 0.1	< 2 2 – 4 > 4	0.2 0.2 0.15	< 2.5 2.5 – 4 > 4
10 - 16	0.25 0.2 0.15	< 2 2 – 4 > 4	0.3 0.3 0.2	< 2.5 2.5 – 4 > 4
20	0.3 0.25 0.13	< 2 2 – 4 > 4	0.3 0.3 0.25	< 2.5 2.5 – 4 > 4

In addition to this table, the following allowances are given by the Red Book (2008) for exceedence target of 1 in 50 years,:

Head seas greater than 2 s: 0.6m

Oblique greater than 2 s: 0.4m

Beam seas greater than 2 s: 0.25m

7.3 Breakwater concept evaluation

For the incident waves as shown in Table 7-1, the corresponding transmitted waves were interpolated from the test data set and scaled back to the prototype scale. These transmitted wave heights are shown in Table 7-4.

Table 7-4: Transmitted wave height at proposed marina location for various pile configurations (prototype)

		Pile Element Shape and Porosity (%)				
		Round 4 %	Round 20 %	Square 10 %	Square 25 %	D Square 5 %
Nr of Piles per 10 m		24	20	24	20	18
1.4m	K_T	40%	66%	60.72%	63%	47%
4 sec	H_T	.376	.62	.573	0.592	0.442

In most of the cases the transmitted wave height exceeded the allowable heights from Table 7-3, although the Red Book (2008) allowances seem to be more lenient. Therefore, depending on the orientation of the moored vessel and its exposure in terms of head, beam and quarter seas from all directions, the circular and diagonal square piles could be considered in this case.

7.4 Discussion

As expected the lower porosity screens would be favoured for achieving acceptable tranquillity conditions. In this case the performance requirements determined that the square and diagonal square pile elements were the least viable to consider for piled row breakwater configurations. However, for lower energy wave environments, the diagonal square options could in the end be a more viable option.

8 Conclusions and Recommendations

8.1 Conclusions

In order to better understand the wave interaction at piled row breakwaters for the purpose of estimating marina basin tranquilities, a scale model was set up to test various configurations. This paper compared three piled element shapes for varying porosity values over a range of input wave parameters. A comparison of the transmission and reflection incurred at these configurations with the predicted performance from literature was also presented. The tests were scaled from possible marina locations and therefore the performance criteria measured could be applied to potential site locations.

It was concluded that most theories were developed around the velocity potential function. In many cases the theories were compared with physical model testing, which prompted the testing method for this thesis. Empirical theories in research papers similar to this thesis, have presented user friendly equations that could easily be applied by designers.

As for testing of model piled row breakwaters, numerical modelling methods for testing of piled screens are not yet fully developed, although steps towards simulating the hydrodynamics at a piled row breakwater have proven that this could be a useful approach in future, especially when combining numerical and physical testing.

Various dependencies were investigated and it was found that for a fixed screen configuration in terms of pile element shape and porosity, the performance is reasonably dependent on wave steepness. This is likely due to the increased velocity for the steeper waves and the resulting losses for higher particle velocities that could cause more turbulence. For a given porosity, circular piles perform the best (have lower transmission coefficients) followed by square piles and then diagonal square. When comparing the material used, diagonal square piles yielded less costly breakwaters due to the expanded cross section gained in elevation.

The physical model that was set up provided a seemingly close simulation of theoretical work. Previous empirical equations also correlated fairly well with test data obtained.

It is suggested that when evaluating the target tranquillity for shallow water protected marinas in practice, the piled row breakwater presents a viable option as alternative to the rubble mound mass breakwater. It would be advisable to consult a wide base of empirical equations and also consider conducting physical model testing for concept design stages of marina projects. Curve fitted equations produced in this thesis can be applied to potential marina sites to evaluate piled row breakwater concepts in addition to available equations and data from literature.

8.2 Recommendations

The piled row breakwater study field has received considerable effort from academics on a theoretical level. For evaluation of potential concepts for use in practice, more data on case studies and performance of similar structures would be required. The broader topic has potential to draw more interest on a research level as the type of application could be favoured in practice by key stakeholders, especially considering environmental impacts on marinas and small craft harbour facilities. It would be prudent to have the right data and theoretical understanding to adopt this as a concept in early project stages in order to generate realistic performance and evaluation criteria or else the proposed concepts will be ill-conceived.

There are several more study areas that fall within the field of piled row breakwaters that should be explored in future research efforts. On the configuration of piled row breakwaters, there are further areas that could be explored for impacts on the wave and breakwater interactions. The efficiency of double wave screens for various spacing and porosities, as an extension of work done previously (for example Thomson, 2000) should be further. When looking closer at what options exist to vary the composition and shape of pile elements, the effect of perforated elements as well as elongated depth in plan (*t* dimension) should be studied further.

In the context of a marina, the optimal design of structures and how they interact with the environment is considered critical. For instance, considering that a piled row breakwater could serve as support to access walkways above or integrated with pontoon elements, it would be beneficial to understand the implications of piled row breakwaters integrated into other marina components. The forces from waves on piles and wave run-up are also crucial inputs to adequately design the piled elements.

For future research and applications of piled row breakwaters, the value of case studies and field data would be useful. Data on the performance of field prototypes and case studies would be highly valuable as these would supplement existing knowledge in this field. The setting up of

field recording at existing and new marina projects could potentially be shared between Clients, practicing engineers and academic or research institutions.

For navigation safety aspects, the combined effects of transmitted and reflected waves in the navigation channel areas are paramount to navigation safety. Safety evaluation in the early stages of the design process could eliminate flawed layouts and streamline the option selection and downstream phases.

Shoreline responses within and outside of marinas created by piled row breakwaters are not well captured in literature, and in the one reference found on this topic, it was found to differ with methods for parallel breakwaters as well as for submerged reefs (e.g. the formation of a salient in the lee of a piled breakwater). This is an area that would require better understanding for the purpose of designing piled row breakwaters in marina applications.

The advancement of numerical modelling of piled row breakwaters should be beneficial in combination with physical testing. This will most likely require more sophisticated measuring equipment in the physical laboratory setup in order to do calibration and validations between the types of testing and also to feed into the refinement of existing theories and empirical equations.

9 References

Allsop, N. W., and Hettiarachchi, S. S. (1988). “Reflections from Coastal Structures,” *Proceedings of the 21st International Coastal Engineering Conference*, American Society of Civil Engineers, Vol 1, pp 782-794.

AS3962-2001. Guidelines for Design of Marinas. Australian Standards (2001).

Atkins, R., Mocke, R, (2009). “ Shoreline Response to an Offshore Wave Screen, Blairgowrie Safe Boat Harbour, Victoria, Australia”

Hughes, S.A. (1993) *Physical models and laboratory techniques in coastal engineering*, World Scientific.

Isaacson, M., Premasiri. S., and Yang, G., (1998), "Wave Interactions with Vertical

Slotted Barrier", Journal of Waterway, Port, Coastal, and Ocean Engineering, ASCE, Vol

124, NO. 3, pp 118-126.

Jebel Ali Free Zone Authority, Civil Engineering Department Marinas & Small Craft Harbour: Regulations & Design Guidelines – Red Book (First Edition – 2007)

Kakuno, S., Liu, P. 1993. “Scattering of Water Waves by Vertical Cylinders”. Journal of Waterway, Port, Coastal, and Ocean Engineering, ASCE, Vol 1993, NO. 119, pp 302-322.

Kim, M., 1993. “Interaction of Waves with N Vertical Circular Cylinders”. Journal of Waterway, Port, Coastal, and Ocean Engineering, ASCE, Vol 1993, NO. 119, pp 671-689.

Li, J., Wang, Z., Liu, S. 2013 “Experimental study of interactions between multi-directional focused wave and vertical circular cylinder, Part I: Wave run-up”, Coastal Engineering Journal, Elsevier, Vol 64, pp 151 – 160

Li, J., Wang, Z., Liu, S. 2013 “Experimental study of interactions between multi-directional focused wave and vertical circular cylinder, Part II: Wave force”, Coastal Engineering Journal, Elsevier,

Mansard, E.P.D. and Funke, E.R. (1980) ‗The measurement of incident waves and reflected spectra using a least square method‘, 17th Int. Conf. of Coastal Engineering, Proc. ICCE‘80, ASCE, pp.154-172, Sydney.

Nilsen, Arne O; Buchanan, Steven J and Hooper, Glenn R. 2000. “Development of a Piled Arch Tug Harbour” *Coasts & Ports 2003 Australasian Conference : Proceedings of the 16th Australasian Coastal and Ocean Engineering Conference, the 9th Australasian Port and Harbour*

Conference and the Annual New Zealand Coastal Society Conference. Barton, A.C.T.: Institution of Engineers, Australia, 2003: [324]-[332].

Papini, M., 2003. “Wave Interaction with a Pile-Supported Breakwater”. University of Hawaii, Civil and Environmental Engineering.

Park, W. S., Kim, B. H., Suh, K. D. and Lee, K. S.,(2000). *SCATTERING OF IRREGULAR WAVES BY VERTICAL CYLINDERS*, Coastal Engineering Journal, Vol. 42, No. 2 (2000) 253 271.

Raudkivi, A. 1996. “Permeable Pile Groins”. Journal of Waterway, Port, Coastal, and Ocean Engineering, ASCE, Vol 1996, NO. 122, pp 267-272.

Reedijk, J. S., 2003. “Shore parallel pile row breakwaters, an example of an effective coastal protection scheme. Delta Marine Consultants, the Netherlands.”

Schlenkhoff, A., Oertel, M., Ahmed, H.2012. “Numerical Solutions of Hydrodynamic Performance of a Permeable Breakwater”, Proceedings of the Eighth International Conference on Coastal and Port Engineering in Developing Countries (PIANC-COPEDEC 2012)

Suh, K, Kim, Y., Ji, C., 2011 “An empirical formula for friction coefficient of a perforated wall with vertical slits”, Coastal Engineering Journal, Elsevier, Vol 58, pp 85 – 93

Suh, K, Ji, C., Kim, Y., , 2011 “Closed-form solutions for wave reflection and transmission by vertical slotted barrier”, Coastal Engineering Journal, Elsevier, Vol 58, pp 1089 – 1096

Thomson, G. 2000. “Wave Transmission though Multi-layered Wave Screens”. Queen’s University, Kingston, Ontario, Canada.

UFC 4-152-07N Design: Small craft berthing facilities (US). USACE

USACE EM 1110-2-1100 (2008) “Coastal Engineering Manual”. United States Army Corps of Engineers

Zhu, D., 2011 “Hydrodynamic characteristics of a single-row pile breakwater”, Coastal Engineering Journal, Elsevier, Vol 58, pp 446 – 451

Appendix A: Photos of laboratory equipment and test runs

Right Side (behind)

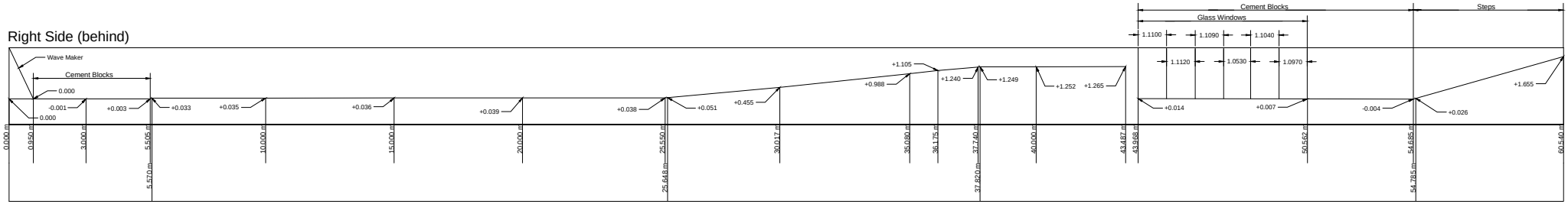

Left Side (front)

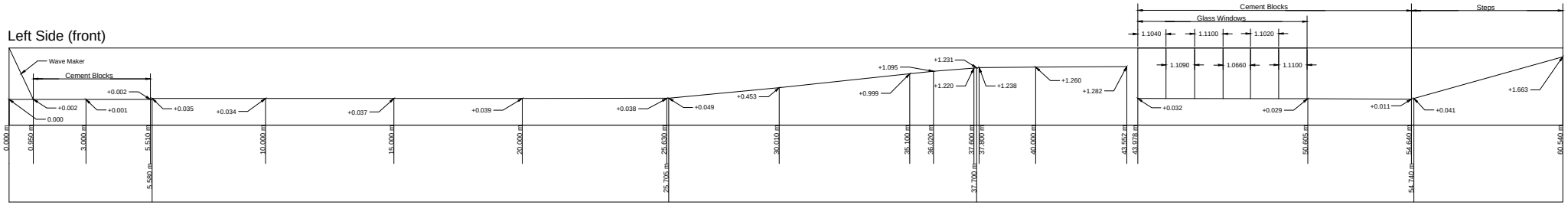

Large Wave Flume: Wave generation and absorption schematics

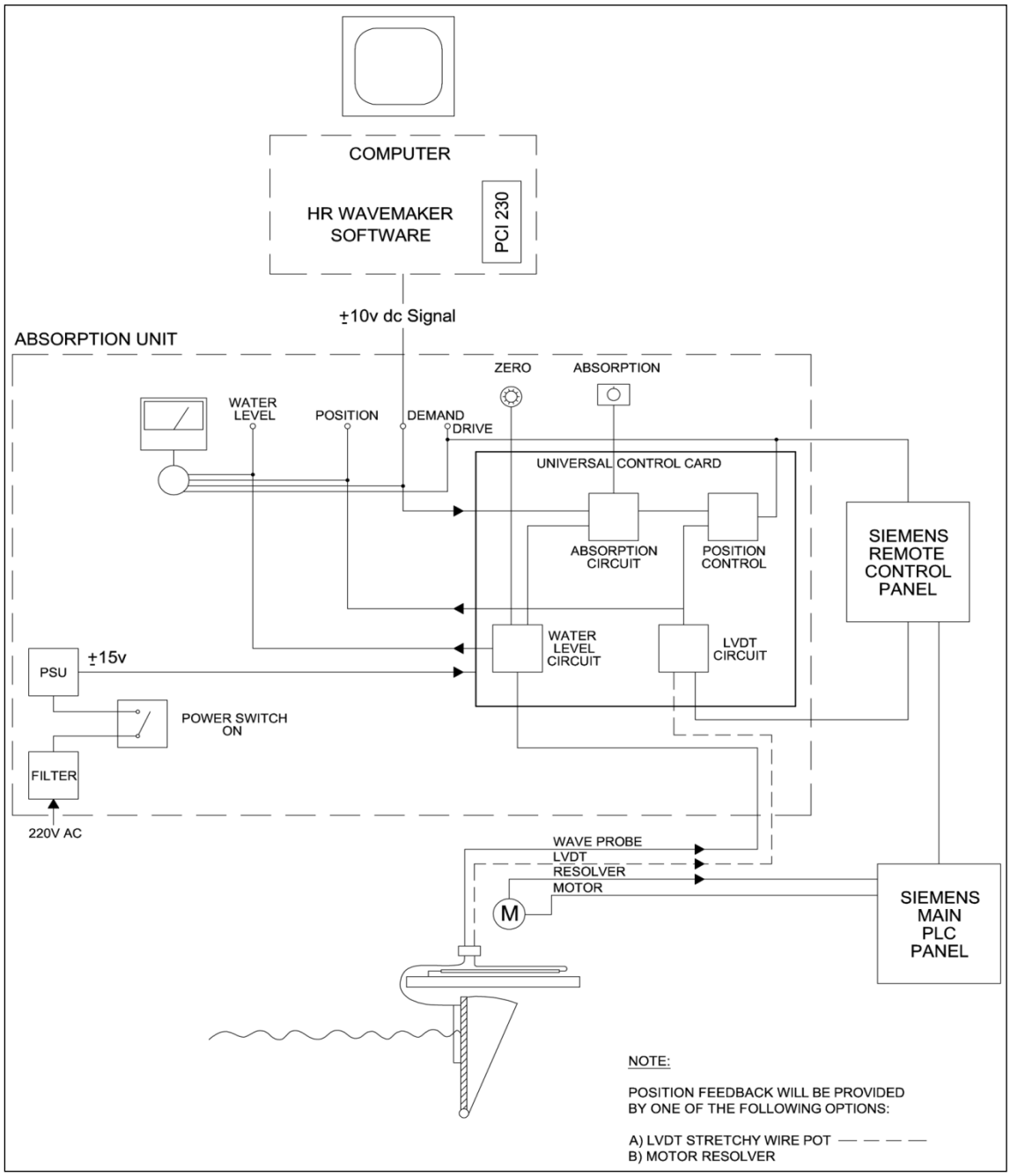

Figure A: Panoramic view of laboratory

Figure B: Surveying the wave flume

Figure C: Circular piles secured by bottom rail

Figure D: Wave probe data receiver box

Figure E: Flume paddles from close by (drive motor and pulley system visible on top)

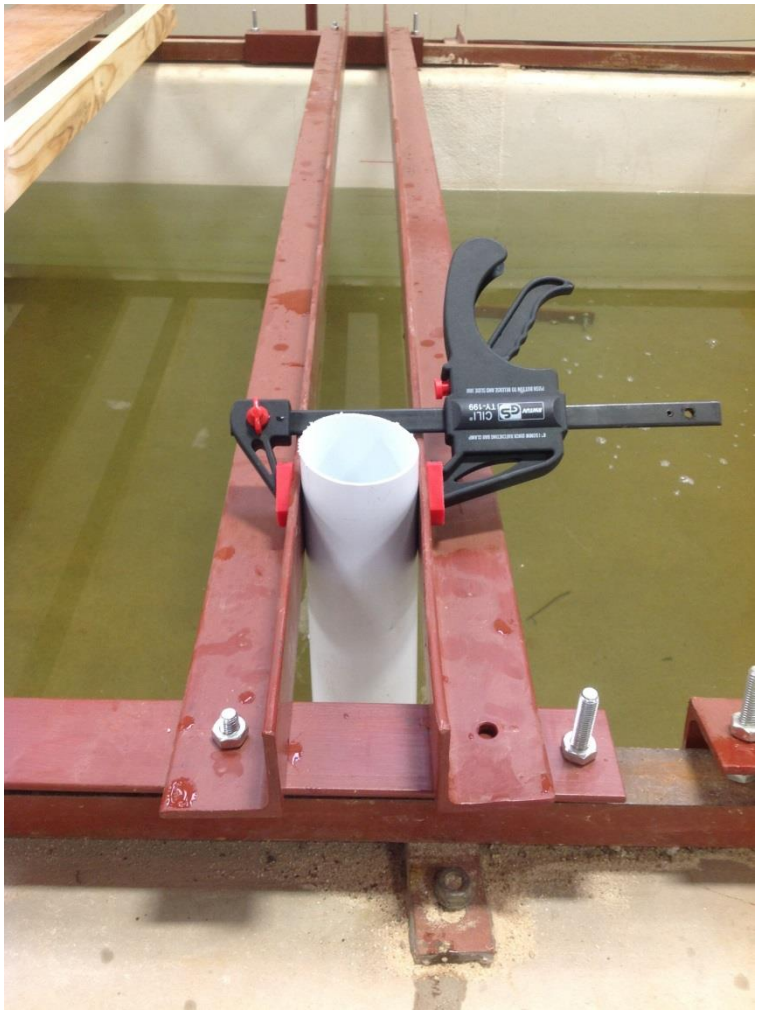

Figure F: Example of simple clamping bracket, showing one test pile already positioned

Figure G: Absorption beach working during a test shown here

Figure H: Mild turbulence for high porosity is visible next to the piled row.

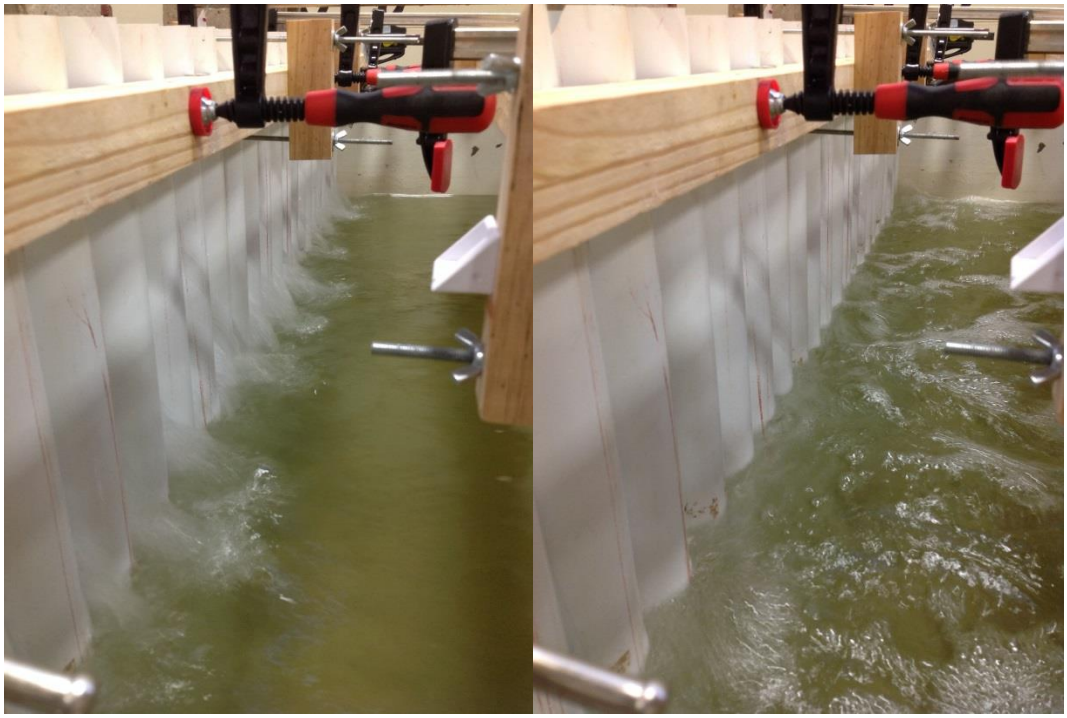

Figure I: Turbulence on leeward side of piled row, during (LH) transmission, shortly after a wave was transmitted (RH).

Figure J: Turbulence around the piled row section for square pile elements shown here.

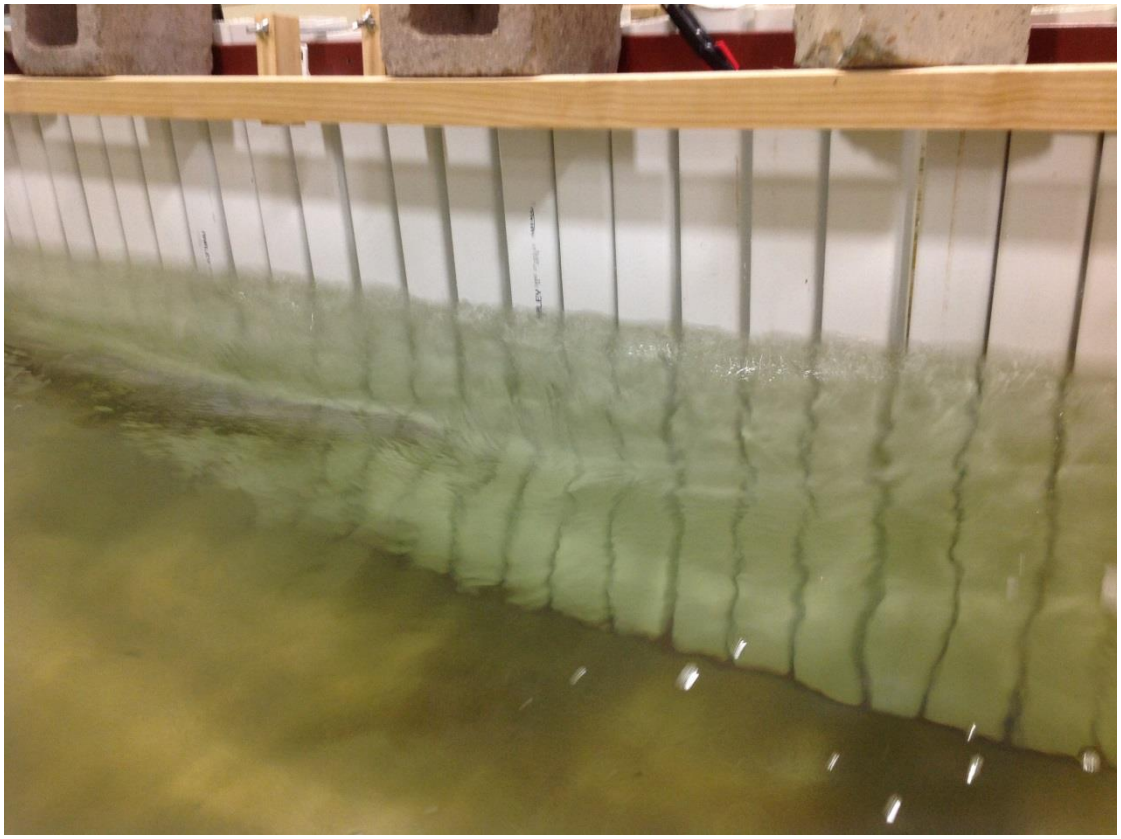

Figure KL: For lower porosity, the square piles performed reasonably well.
\

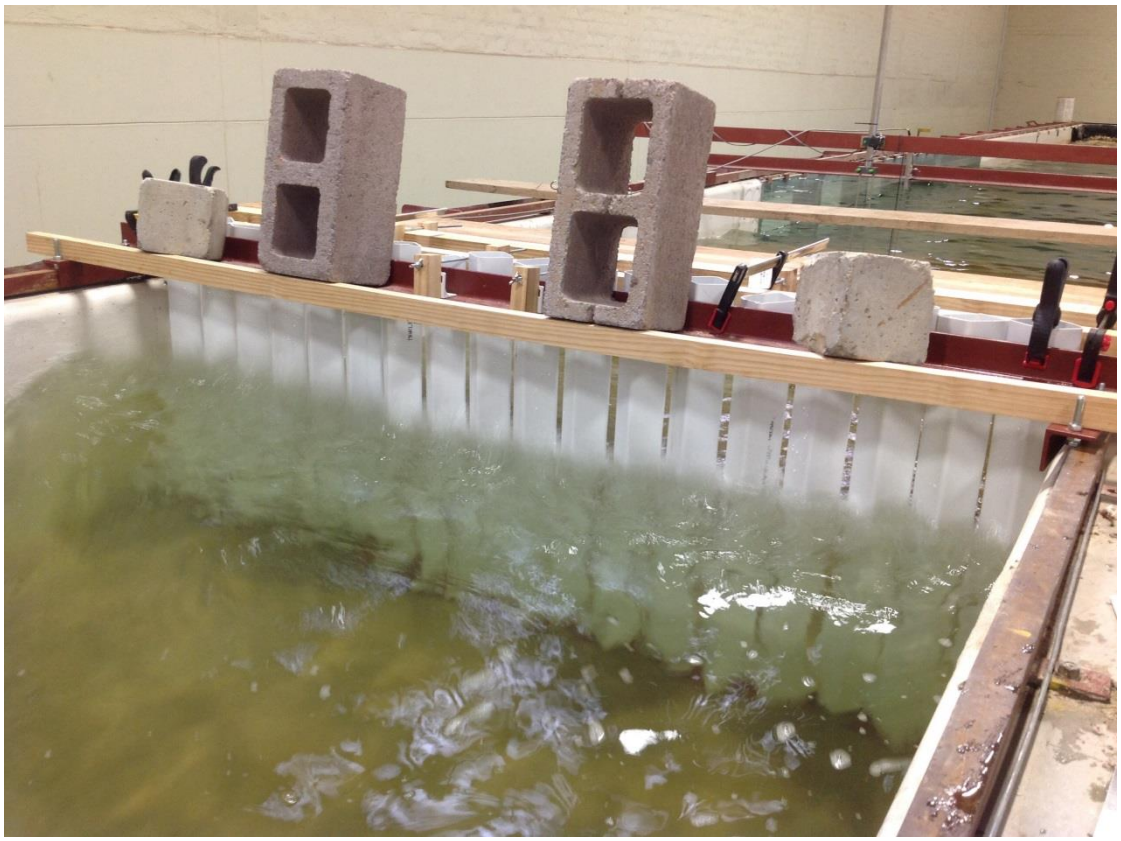

Figure L: Diagonal square section at low porosity

Appendix B: Model setup for testing

WGOUS 12557722 Calculation of distance between probes for the 2D flume: wave reflection Analysis
Calc Sheet by CSIR, customised by WGOUS

Offshore, 3m CD

Prototype Depth	3	m
Model Chainage		m
Distance from Breakwater	3	m
Model Scale	5	:1

0.6

Prototype							
s	fp	m	m	m	m	m	
Tp		L	Lp/10	Lp/6	Lp/3	Lp/5	3Lp/10
3.00	**0.33**	13.1	1.3	2.2	4.4	2.6	3.9
3.75	**0.27**	18.3	1.8	3.1	6.1	3.7	5.5
5.00	**0.20**	26.1	2.6	4.4	8.7	5.2	7.8
6.65	**0.15**	35.6	3.6	5.9	11.9	7.1	10.7
8.00	**0.13**	43.1	4.3	7.2	14.4	8.6	12.9

Prot	Model		
Tr	f	Tp	fp
3	0.33333	1.34164	0.74536
4.0	0.3	1.8	0.6
5.0	0.2	2.2	0.4
6.0	0.2	2.7	0.4
8.0	0.1	3.6	0.3

Model

		s		cm	cm	cm	cm	cm	cm
f		Tp	fp	Lp	Lp/10	Lp/6	Lp/3	Lp/5	3Lp/10
3	0.33	**1.342**	0.745	262.4	26.2	43.7	87.5	52.5	78.7
3.75	0.27	**1.677**	0.596	366.2	36.6	61.0	122.1	73.2	109.9
5	0.20	**2.236**	0.447	522.9	52.3	87.1	174.3	104.6	156.9
6.65	0.15	**2.974**	0.336	712.8	71.3	118.8	237.6	142.6	213.8
8	0.13	**3.578**	0.280	862.9	86.3	143.8	287.6	172.6	258.9
					54.5	**90.9**	**181.8**	**109.1**	**163.6**

<		<			
X12	Lp/6	X13	Lp/3	Lp/5	3Lp/10
26	44	66	87	52	79
37	61	92	122	73	110
52	87	131	174	105	157
71	119	178	238	143	214
86	144	216	288	173	259
	HMIN		LMAX		
	144		**87**		

Model

s	cm	cm	cm	Used	Used
Tp	X_{12}	X_{13}	Y	X_{12}	X_{13}
1.3	26.2	65.6	39.4	26.2	
1.7	36.6	91.6	54.9	36.6	
2.2	52.3	130.7	78.4	52.3	
3.0	71.3	178.2	106.9	71.3	
3.6	86.3	215.7	129.4	86.3	
Average Distance	**54.5**	**136.4**	**81.8**		

Distance Used

* Note	X12 = Lp/10
**	Lp/6 < X13 < Lp/3 and X13 should not equal to Lp/5 and X13 should not equal to 3Lp/10
***	Reference Mansard & Funke
X12	Closer to wave generator from centre probe
X13	Distance to probe closer to structure
Y	Distance from Centre probe to X13 (i.e. X23)

X13 selected **180**

Test 1	Test 2	Test 3	Test 4
180	**180**	**180**	**180**
136	-93	128	101
119	-58	107	70
93	-6	75	23
61	58	37	-34
36	108	7	-79
Lp/6	**Lp/3**	**Lp/5**	**3Lp/10**
black	**black**	**not zero**	not zero

160

Test 1	Test 2	Test 3	Test 4
160	**160**	**160**	**160**
116	-73	108	81
99	-38	87	50
73	14	55	3
41	78	17	-54
16	128	-13	-99
Lp/6	**Lp/3**	**Lp/5**	**3Lp/10**

150

Test 1	Test 2	Test 3	Test 4
150	**150**	**150**	**150**
106	-63	98	71
89	-28	77	40
63	24	45	-7
31	88	7	-64
6	138	-23	-109
Lp/6	**Lp/3**	**Lp/5**	**3Lp/10**

140

Test 1	Test 2	Test 3	Test 4
140	**140**	**140**	**140**
96	-53	88	61
79	-18	67	30
53	34	35	-17
21	98	-3	-74
-4	148	-33	-119
Lp/6	**Lp/3**	**Lp/5**	**3Lp/10**

130

Test 1	Test 2	Test 3	Test 4
130	**130**	**130**	**130**
86	-43	78	51
69	-8	57	20
43	44	25	-27
11	108	-13	-84
-14	158	-43	-129
Lp/6	**Lp/3**	**Lp/5**	**3Lp/10**

120

Test 1	Test 2	Test 3	Test 4	Tp	fp
120	**120**	**120**	**120**		
76	-33	68	41	1.34	0.75
59	2	47	10	1.68	0.60
33	54	15	-37	2.24	0.45
1	118	-23	-94	2.97	0.34
-24	168	-53	-139	3.58	0.28
Lp/6	**Lp/3**	**Lp/5**	**3Lp/10**		

2013-09-23

Model scale factors

	Prototype (site)			Prototype DIAM (mm)	Model DIAM (mm)	Similitude Ratio	Time scale		Model		Reflection analysis limits Probe spacing measurement date			
T	f		Piles	349.99992	70	4.999999	2.236068	T	f			2013-09-18	2013-09-23	
			Depth	3000	600.0001	600.0001								
			Hs	1.4	0.28									
	1	1.000							0.447214	2.236				**SELECTED MODEL f & T**
	2	0.500							0.894427	1.118				**f** **T (sec)**
	3	0.333							1.341641	0.745		0.777	0.929	
	3.6	0.278							1.609969	0.621				
	4	0.250							1.788855	0.559				**0.596** **1.678**
	5	0.200							2.236068	0.447				**0.450** **2.222**
	6	0.167							2.683282	0.373				
	7	0.143							3.130496	0.319				**0.340** **2.941**
	8	0.125							3.577709	0.280				
	9	0.111							4.024923	0.248				
	10	0.100							4.472136	0.224				
	11	0.091							4.91935	0.203				
	12	0.083							5.366564	0.186		0.129		
													0.171	

Figure 1: Large & small wave flume wave generation capacity
Univ. of Stellenbosch, Dept. Civil Engineering
[Large wave flume dim: 2m wide x 2m deep x 60m long ; max **water depth=1.5m**]
[Small flume dim: 1m wide x 1m deep x 40m long; max **water depth=0.8m**]

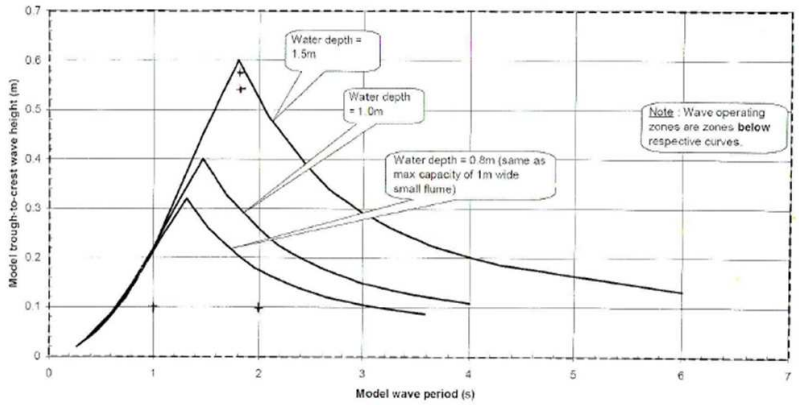

Figure 2-6: Generation capacity curves for the small and large wave flume (Department Civil Engineering)

Appendix C: Test Data gathered

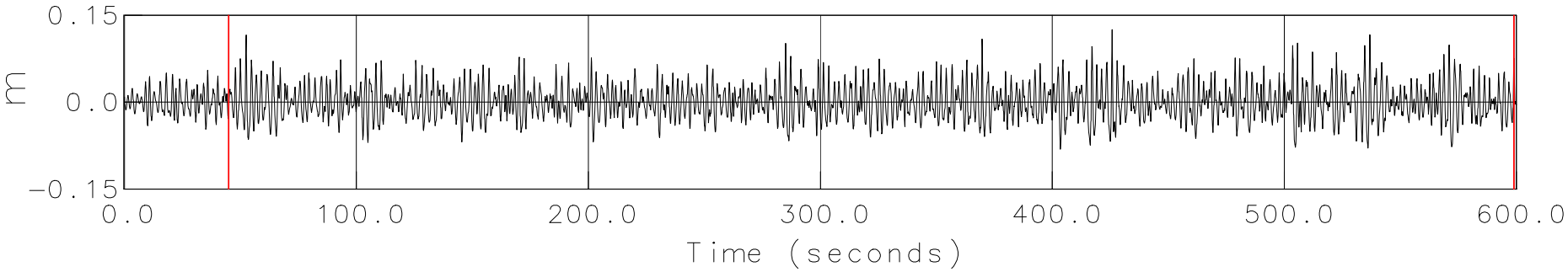

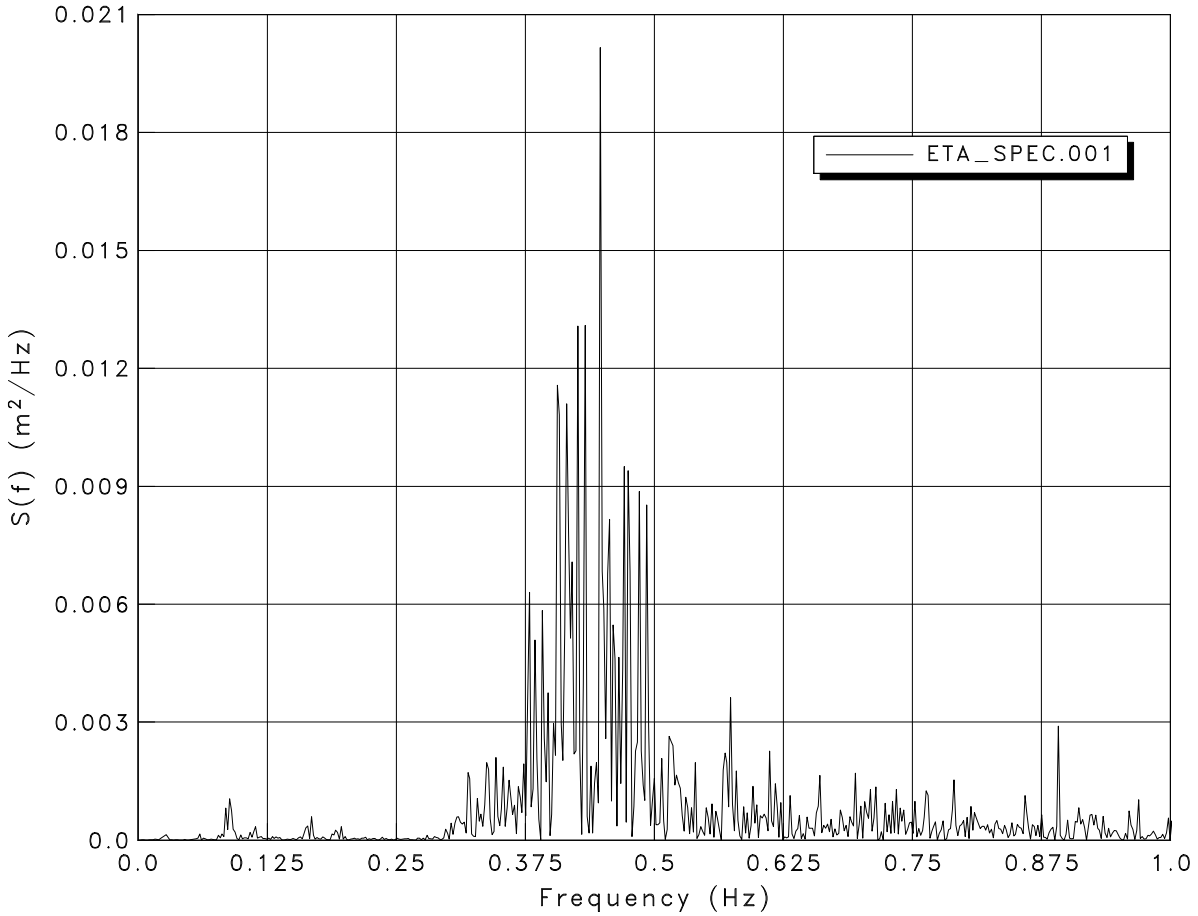

TEST : {DAC_TEST_NUMBER}

Wave Probe: {DAC_SENSOR_NAME}

HM0 = .116 m

H13 = .115 m

HMAX = .196 m

TP = 2.234 s

TPD = 2.234 s

TAV = 1.894 s

GF = .787

DOF = 2.000

WATER LEVEL:1.000

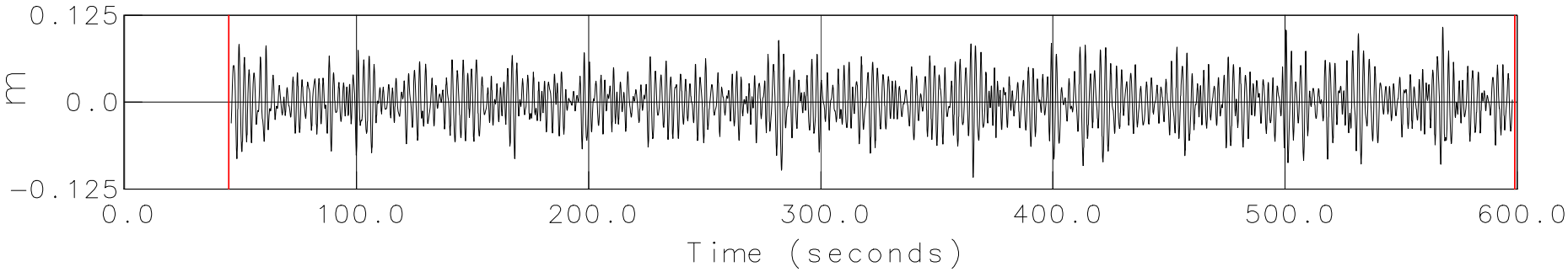

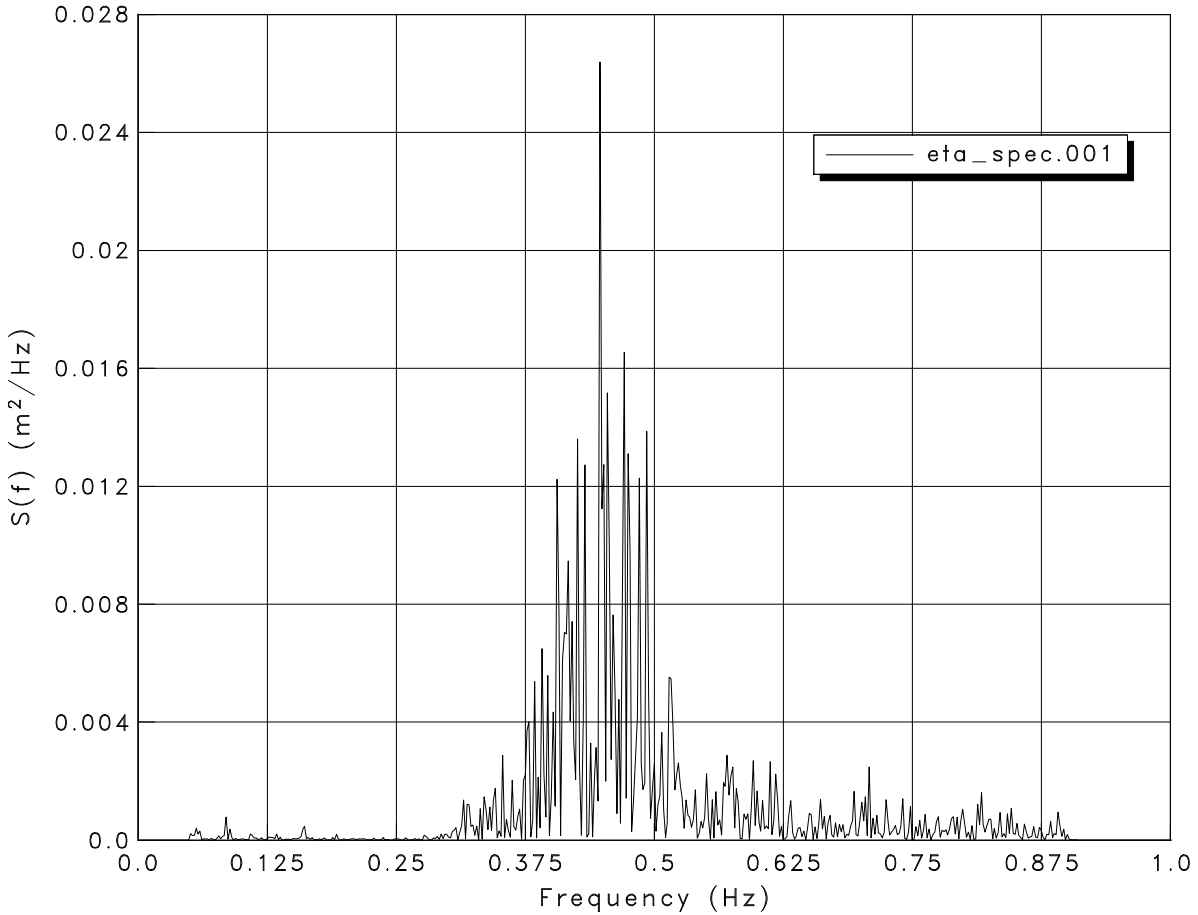

TEST : {DAC_TEST_NUMBER}

Wave Probe: {DAC_SENSOR_NAME}

HM0_I = .125 m

H13_I = .121 m

HMAX_I = .197 m

TP_I = 2.235 s

TPD_I = 2.234 s

TAV_I = 2.025 s

GF = .802

DOF = 2.000

AVG REFL COEF: 18.27

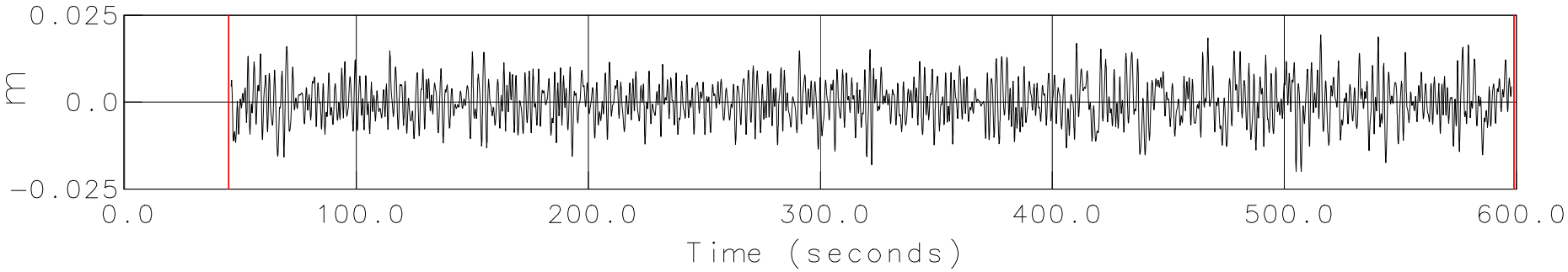

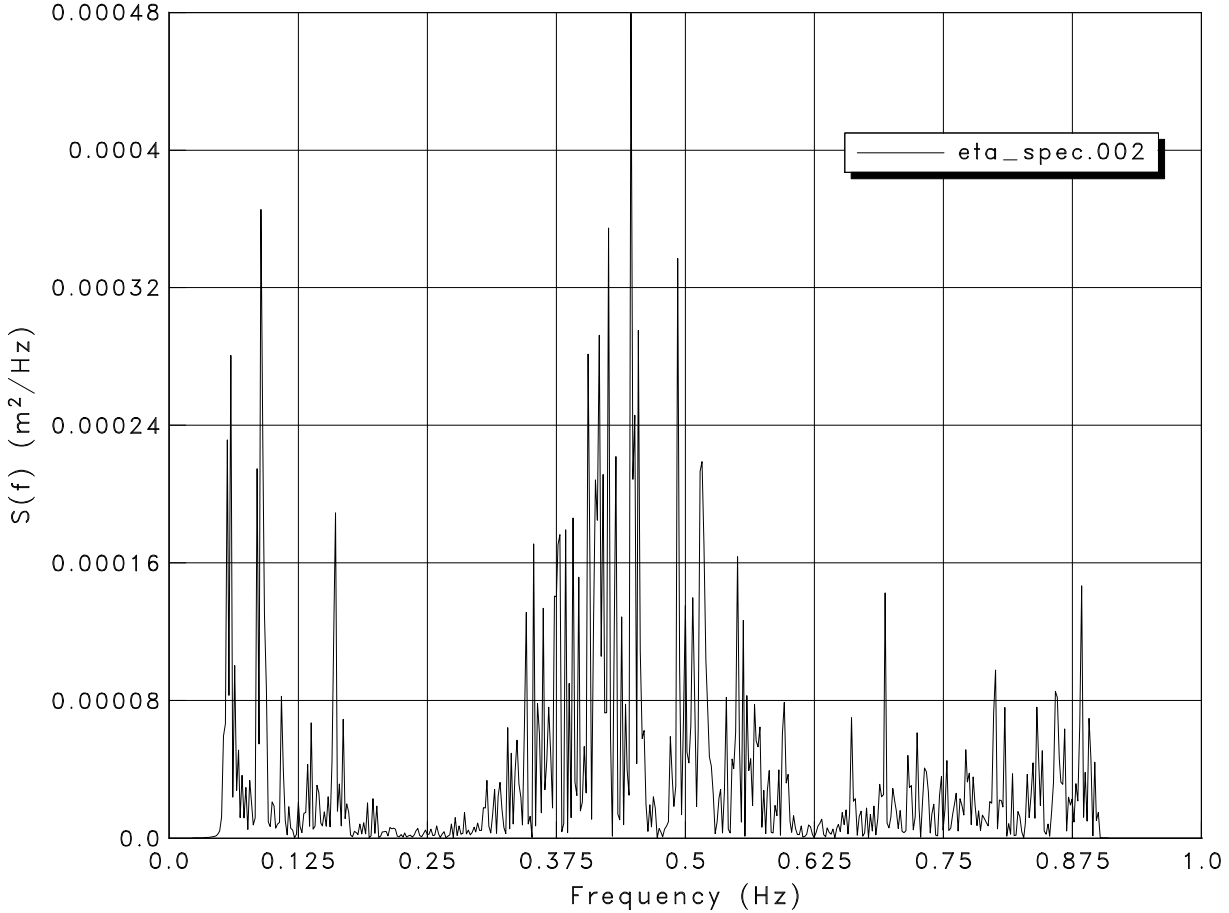

TEST : {DAC_TEST_NUMBER}

Wave Probe: {DAC_SENSOR_NAME}

HM0_R = .023 m

H13_R = .021 m

HMAX_R = .032 m

TP_R = 2.235 s

TPD_R = 2.234 s

TAV_R = 2.043 s

GF = .663

DOF = 2.000

AVG REFL COEF: 18.27

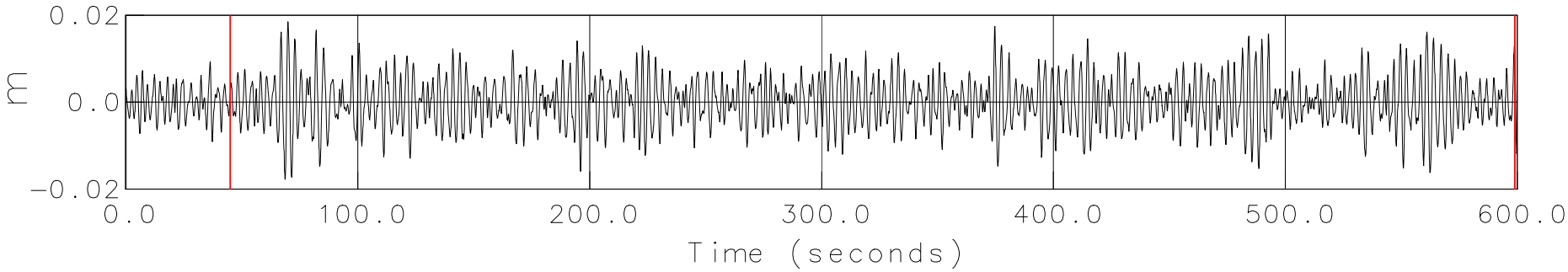

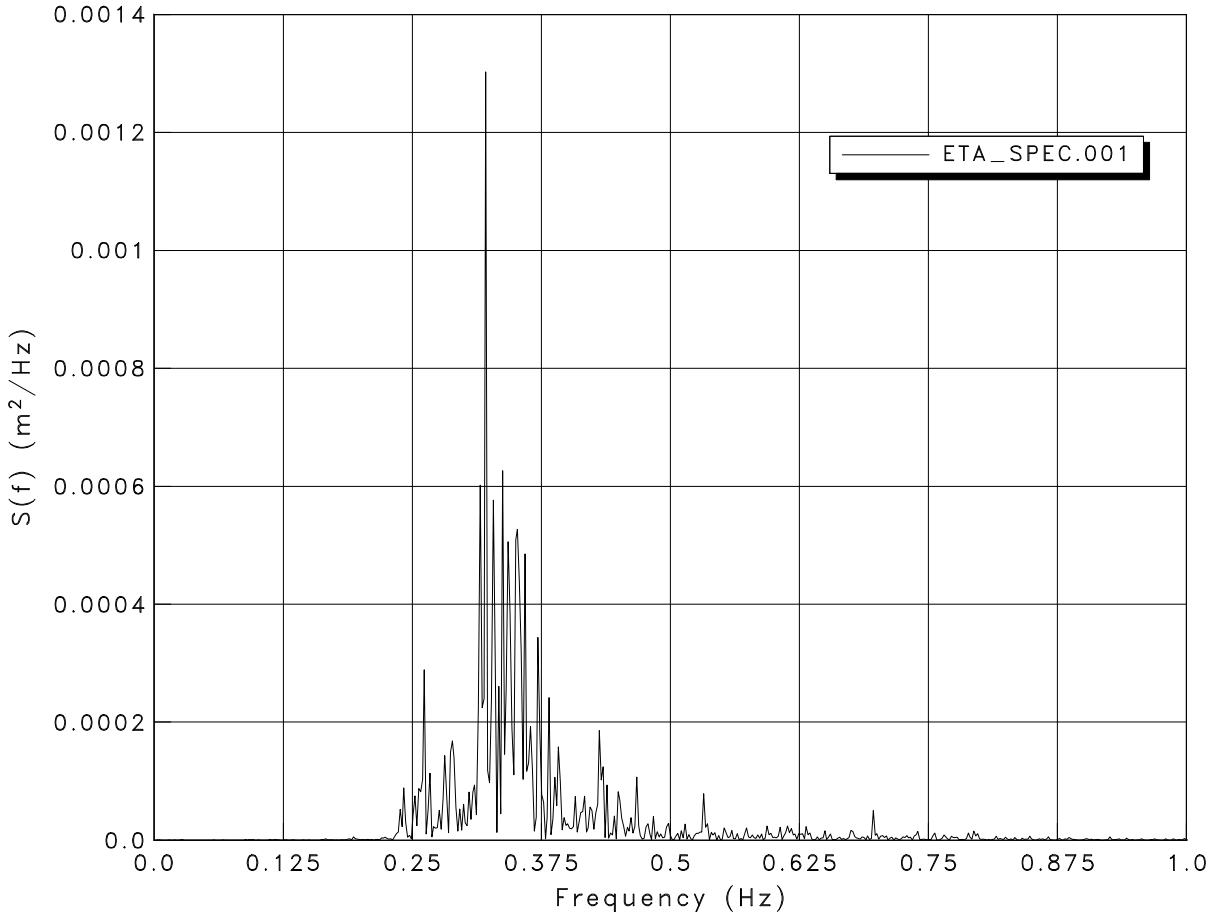

TEST : {DAC_TEST_NUMBER}

Wave Probe: {DAC_SENSOR_NAME}

HM0 = .022 m

H13 = .021 m

HMAX = .036 m

TP = 3.112 s

TPD = 3.113 s

TAV = 2.671 s

GF = .846

DOF = 2.000

WATER LEVEL:1.000

CSIR our future through science

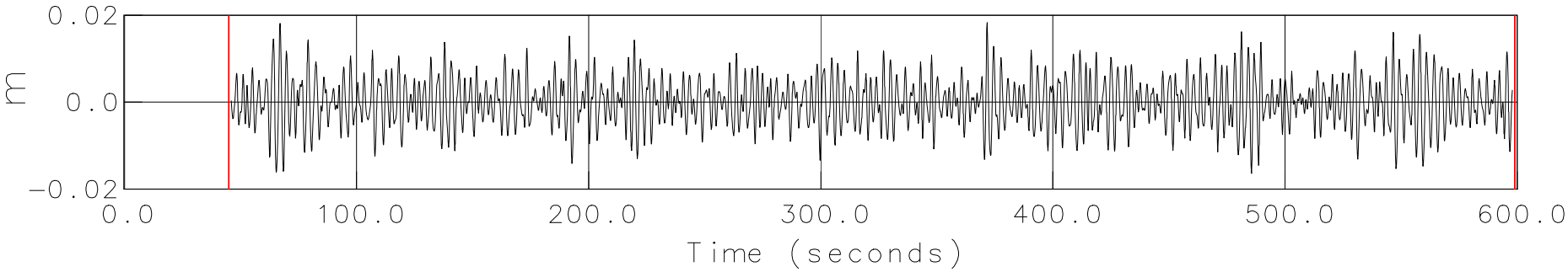

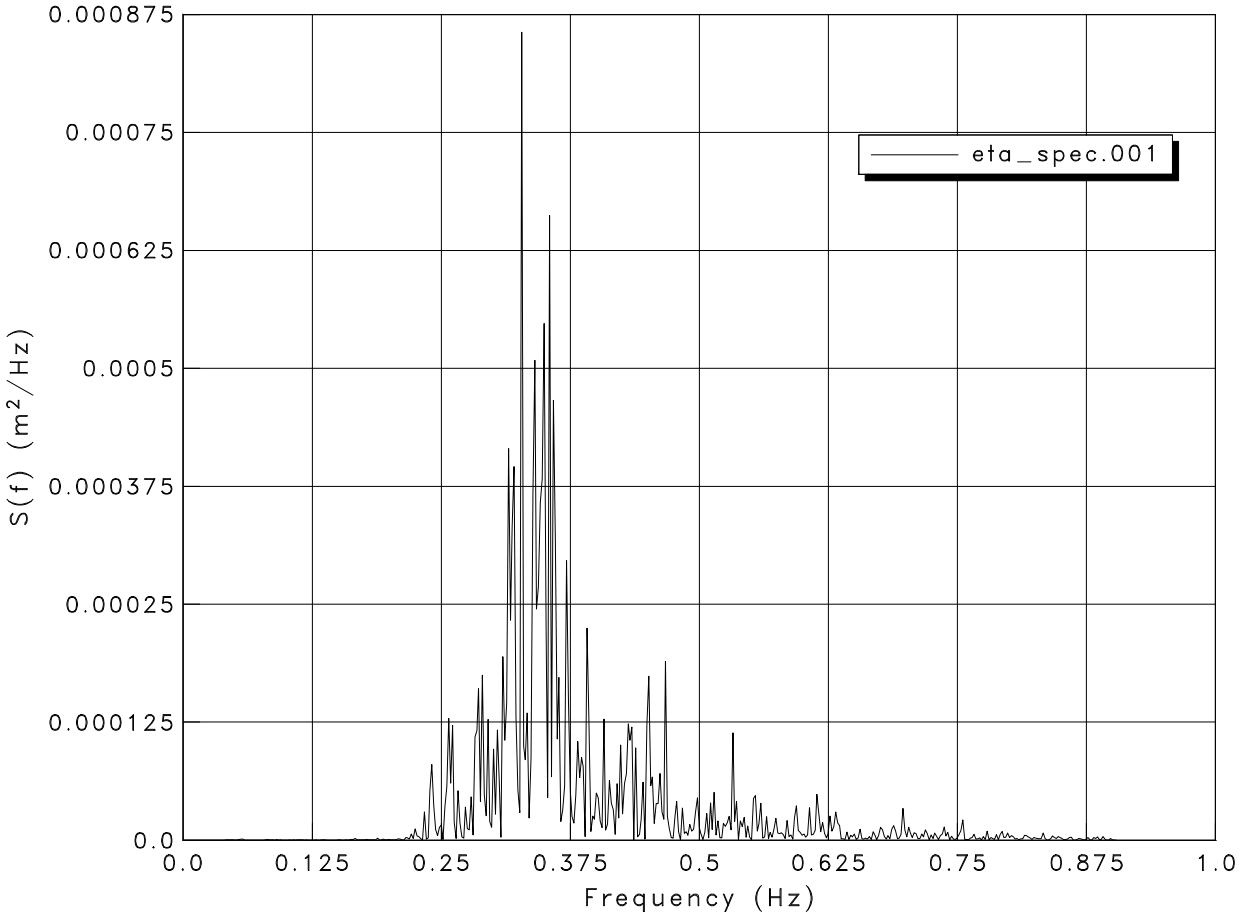

TEST : {DAC_TEST_NUMBER}

Wave Probe: {DAC_SENSOR_NAME}

HM0_I = .021 m

H13_I = .021 m

HMAX_I = .034 m

TP_I = 3.050 s

TPD_I = 3.050 s

TAV_I = 2.547 s

GF = .804

DOF = 2.000

AVG REFL COEF: 27.89

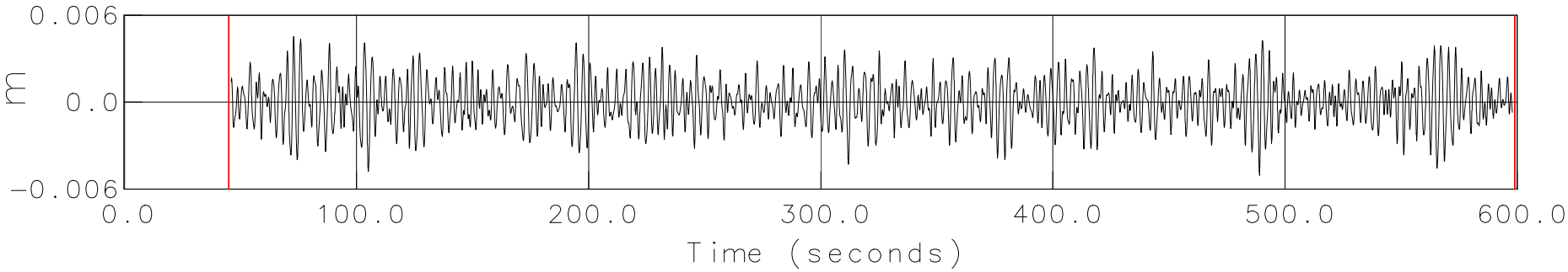

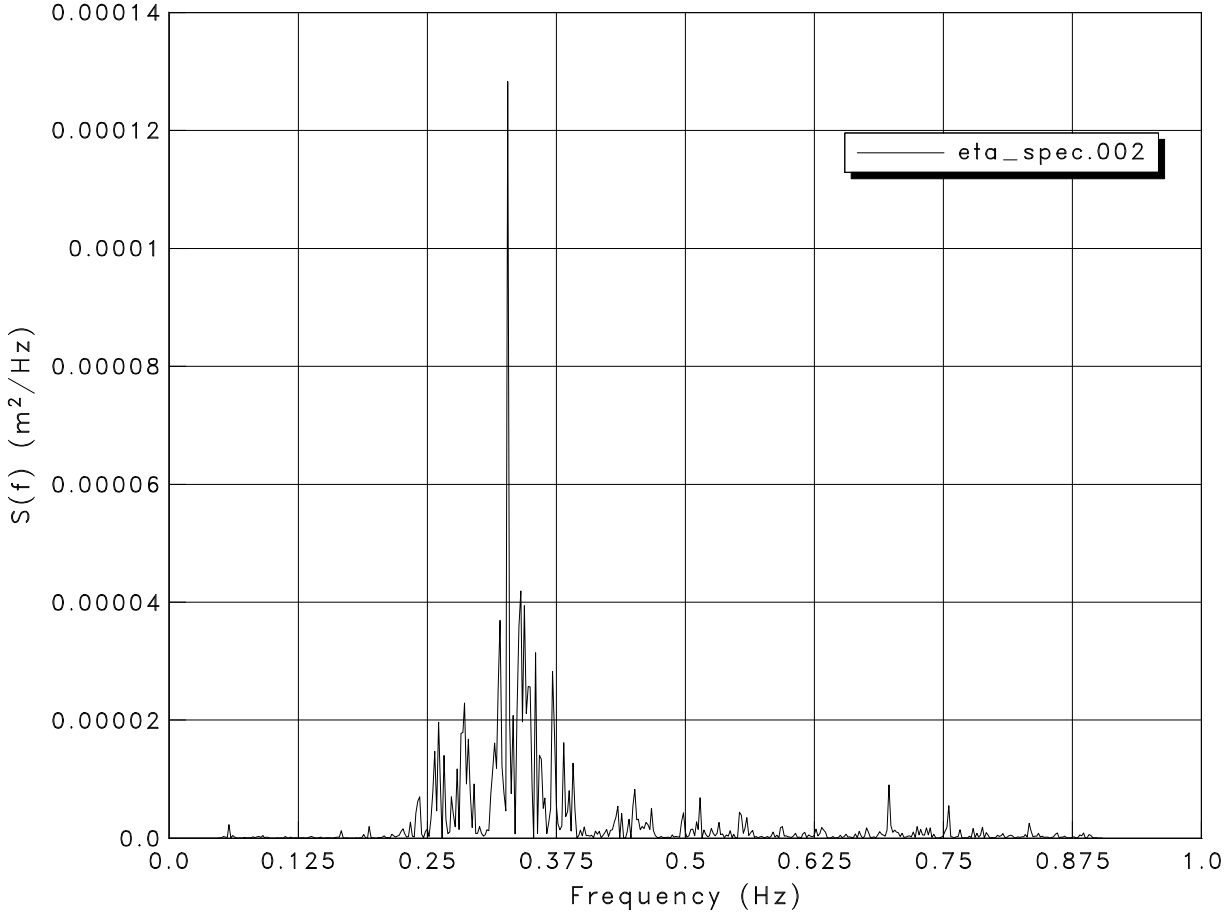

TEST : {DAC_TEST_NUMBER}

Wave Probe: {DAC_SENSOR_NAME}

HM0_R = .006 m

H13_R = .006 m

HMAX_R = .009 m

TP_R = 3.050 s

TPD_R = 3.050 s

TAV_R = 2.612 s

GF = .807

DOF = 2.000

AVG REFL COEF: 27.89

CSIR our future through science

WGOUS 12557722

Test results for piled row breakwater

		mmdd scr# e# H f		porosit	porosity sq							incident						Reflected						Transmitted			
Nr	date	run name	n pile	circ	sq	shape	t	Reg / H	f	d	Hm0 i	H13 i	Hmax i	TP i	TPD i	Refl Coeff	Hm0 r	H13 r	Hmax r	TP r	TPD r	Refl Coeff	Hm0 t	H13 t	Hmax t	TP t
11	01-Oct-13	1001_05 1 14 0-3s_0-6	14	44%	48%	circ	0.080	Spec	0.3	0.596	0.620	0.118	0.115	0.193	1.798	1.744	19.040	0.023	0.021	0.032	1.798	1.798	19.040	0.111	0.108	0.160	1.620
12	01-Oct-13	1001_06 1 14 0-2s_0-6	14	44%	48%	circ	0.080	Spec	0.2	0.596	0.620	0.118	0.115	0.193	1.798	1.744	19.040	0.023	0.021	0.032	1.798	1.798	19.040	0.077	0.075	0.121	1.620
13	01-Oct-13	1001_07 1 14 0-1s_0-6	14	44%	48%	circ	0.080	Spec	0.1	0.596	0.620	0.040	0.039	0.059	1.798	1.798	21.710	0.009	0.008	0.014	1.798	1.798	21.710	0.039	0.038	0.060	1.620
14	01-Oct-13	1001_08 1 14 0-05s_0-6	14	44%	48%	circ	0.080	Spec	0.05	0.596	0.620	0.020	0.020	0.033	1.798	1.798	22.490	0.004	0.004	0.008	1.798	1.798	22.490	0.020	0.019	0.029	1.620
34	08-Oct-13	1008_32 1 24 0-05s_0-4	24	4%	10%	circ	0.080	Spec	0.05	0.45	0.600	0.021	0.021	0.036	2.060	2.169	51.430	0.011	0.011	0.023	2.060	2.060	51.430	0.010	0.010	0.015	2.308
35	08-Oct-13	1008_33 1 24 0-1s_0-45	24	4%	10%	circ	0.080	Spec	0.1	0.45	0.600	0.048	0.047	0.086	2.060	2.060	60.660	0.029	0.029	0.058	2.060	2.060	60.660	0.019	0.018	0.027	2.308
36	08-Oct-13	1008_34 1 24 0-2s_0-45	24	4%	10%	circ	0.080	Spec	0.2	0.45	0.600	0.102	0.099	0.177	2.060	2.060	68.520	0.070	0.068	0.136	2.060	2.060	68.520	0.032	0.030	0.049	2.308
37	08-Oct-13	1008_35 1 24 0-3s_0-45	24	4%	10%	circ	0.080	Spec	0.3	0.45	0.600	0.154	0.150	0.247	2.060	2.060	73.290	0.113	0.109	0.193	2.060	2.060	73.290	0.045	0.042	0.078	2.638
54	08-Oct-13	1008_37 1 24 0-05s_0-3	24	4%	10%	circ	0.080	Spec	0.05	0.34	0.600	0.023	0.022	0.031	3.172	3.025	51.740	0.012	0.012	0.017	2.816	3.052	51.740	0.013	0.013	0.017	3.112
55	08-Oct-13	1008_38 1 24 0-1s_0-34	24	4%	10%	circ	0.080	Spec	0.1	0.34	0.600	0.050	0.049	0.067	3.154	3.161	59.730	0.030	0.030	0.042	30154.000	3.011	59.730	0.023	0.022	0.028	3.166
56	08-Oct-13	1008_39 1 24 0-2s_0-34	24	4%	10%	circ	0.080	Spec	0.2	0.34	0.600	0.107	0.105	0.155	3.154	3.159	69.210	0.074	0.074	0.107	3.154	3.158	69.210	0.038	0.036	0.044	3.166
57	08-Oct-13	1008_40 1 24 0-3s_0-34	24	4%	10%	circ	0.080	Spec	0.3	0.34	0.600	0.158	0.159	0.233	3.154	3.154	74.080	0.117	0.115	0.175	3.154	3.154	74.080	0.049	0.045	0.062	3.148
15	01-Oct-13	1001_08a 1 14 0-4s_0-6	14	44%	48%	circ	0.080	Spec	0.4	0.596	0.620	0.158	0.154	0.221	1.798	1.753	19.180	0.030	0.027	0.041	1.798	1.798	19.180	0.146	0.143	0.197	1.620
16	01-Oct-13	1001_09 1 16 0-3s_0-6	16	36%	40%	circ	0.080	Spec	0.3	0.596	0.620	0.121	0.118	0.200	1.798	1.798	20.020	0.024	0.023	0.040	1.798	1.798	20.020	0.112	0.109	0.169	1.620
17	01-Oct-13	1001_10 1 16 0-2s_0-6	16	36%	40%	circ	0.080	Spec	0.2	0.596	0.620	0.081	0.080	0.135	1.798	1.798	20.890	0.017	0.016	0.024	1.798	1.798	20.890	0.076	0.074	0.107	1.620
18	01-Oct-13	1001_11 1 16 0-1s_0-6	16	36%	40%	circ	0.080	Spec	0.1	0.596	0.620	0.040	0.040	0.066	1.798	1.798	22.980	0.009	0.009	0.015	1.798	1.798	22.980	0.039	0.037	0.058	1.620
19	02-Oct-13	1001_12 1 16 0-05s_0-6	16	36%	40%	circ	0.080	Spec	0.05	0.596	0.615	0.020	0.019	0.033	1.798	1.675	24.840	0.005	0.005	0.008	1.798	1.798	24.840	0.019	0.018	0.030	1.620
29	02-Oct-13	1002_18 1 20 0-05s_0-4	20	20%	25%	circ	0.080	Spec	0.05	0.45	0.615	0.021	0.021	0.035	2.235	2.235	22.970	0.005	0.005	0.008	2.217	2.100	22.970	0.019	0.019	0.031	2.308
30	02-Oct-13	1002_19 1 20 0-1s_0-45	20	20%	25%	circ	0.080	Spec	0.1	0.45	0.615	0.043	0.042	0.071	2.123	2.161	20.510	0.009	0.008	0.013	1.937	2.202	20.510	0.037	0.035	0.058	2.308
31	02-Oct-13	1002_20 1 20 0-2s_0-45	20	20%	25%	circ	0.080	Spec	0.2	0.45	0.615	0.086	0.083	0.147	2.235	2.235	22.240	0.019	0.018	0.037	2.464	2.412	22.240	0.069	0.067	0.104	2.308
32	02-Oct-13	1002_21 1 20 0-3s_0-45	20	20%	25%	circ	0.080	Spec	0.3	0.45	0.615	0.127	0.122	0.219	2.310	2.278	25.480	0.032	0.030	0.063	2.464	2.463	25.480	0.100	0.096	0.150	2.308
33	02-Oct-13	1002_22 1 20 0-4s_0-45	20	20%	25%	circ	0.080	Spec	0.4	0.45	0.615	0.168	0.161	0.267	2.235	2.155	27.510	0.046	0.043	0.084	2.464	2.444	27.510	0.130	0.126	0.208	2.308
49	02-Oct-13	1002_23 1 20 0-05s_0-3	20	20%	25%	circ	0.080	Spec	0.05	0.34	0.615	0.021	0.021	0.034	3.050	3.050	27.890	0.006	0.006	0.009	3.050	3.050	27.890	0.022	0.021	0.036	3.112
50	02-Oct-13	1002_24 1 20 0-1s_0-35	20	20%	25%	circ	0.080	Spec	0.1	0.34	0.615	0.043	0.042	0.066	2.816	2.881	24.880	0.011	0.011	0.018	2.936	2.886	24.880	0.043	0.042	0.065	3.112
51	02-Oct-13	1002_25 1 20 0-2s_0-35	20	20%	25%	circ	0.080	Spec	0.2	0.34	0.615	0.086	0.083	0.129	2.816	2.816	25.480	0.022	0.021	0.037	2.816	2.816	25.480	0.078	0.077	0.113	3.112
52	02-Oct-13	1002_26 1 20 0-3s_0-35	20	20%	25%	circ	0.080	Spec	0.3	0.34	0.615	0.128	0.125	0.189	2.816	2.816	27.920	0.036	0.036	0.065	2.816	2.816	27.920	0.111	0.110	0.159	3.112
53	02-Oct-13	1002_27 1 20 0-4s_0-35	20	20%	25%	circ	0.080	Spec	0.4	0.34	0.615	0.169	0.167	0.255	2.816	2.816	30.330	0.051	0.050	0.095	2.816	2.816	30.330	0.143	0.144	0.208	3.112
20	02-Oct-13	1001_13 1 20 0-3s_0-6	20	20%	25%	circ	0.080	Spec	0.3	0.596	0.615	0.120	0.117	0.202	1.688	1.738	26.340	0.032	0.030	0.057	1.798	1.745	26.340	0.094	0.092	0.138	1.742
21	02-Oct-13	1001_14 1 20 0-2s_0-6	20	20%	25%	circ	0.080	Spec	0.2	0.596	0.615	0.080	0.078	0.127	1.688	1.673	25.790	0.021	0.020	0.034	1.798	1.753	25.790	0.066	0.064	0.097	1.742
22	02-Oct-13	1001_15 1 20 0-1s_0-6	20	20%	25%	circ	0.080	Spec	0.1	0.596	0.615	0.040	0.039	0.066	1.798	1.798	27.420	0.011	0.011	0.016	1.798	1.798	27.420	0.035	0.034	0.052	1.620
23	02-Oct-13	1001_16 1 20 0-05s_0-6	20	20%	25%	circ	0.080	Spec	0.05	0.596	0.615	0.020	0.019	0.032	1.798	1.676	30.440	0.006	0.006	0.009	1.798	1.798	30.440	0.018	0.017	0.027	1.620
39	08-Oct-13	1008_42 1 16 0-05s_0-4	16	36%	40%	circ	0.080	Spec	0.05	0.45	0.600	0.021	0.020	0.034	2.235	2.234	21.960	0.005	0.004	0.007	2.235	2.234	21.960	0.020	0.190	0.031	2.234
40	08-Oct-13	1008_43 1 16 0-1s_0-45	16	36%	40%	circ	0.080	Spec	0.1	0.45	0.600	0.042	0.041	0.069	2.235	2.189	20.120	0.008	0.008	0.013	2.235	2.234	20.120	0.039	0.038	0.063	2.234
41	08-Oct-13	1008_44 1 16 0-2s_0-45	16	36%	40%	circ	0.080	Spec	0.2	0.45	0.600	0.083	0.081	0.135	2.226	2.184	18.630	0.150	0.014	0.022	2.199	2.082	18.630	0.076	0.074	0.125	2.347
42	08-Oct-13	1008_45 1 16 0-3s_0-45	16	36%	40%	circ	0.080	Spec	0.3	0.45	0.600	0.122	0.118	0.196	2.199	2.147	18.340	0.022	0.020	0.031	2.464	3.116	18.340	0.111	0.109	0.184	2.234
43	08-Oct-13	1008_46 1 16 0-4s_0-45	16	36%	40%	circ	0.080	Spec	0.4	0.45	0.600	0.167	0.159	0.247	2.075	2.195	19.080	0.032	0.028	0.048	11.266	11.278	19.080	0.149	0.144	0.238	2.328
59	08-Oct-13	1008_47 1 16 0-05s_0-3	16	36%	40%	circ	0.080	Spec	0.05	0.34	0.600	0.021	0.021	0.033	2.936	2.928	26.450	0.006	0.005	0.008	3.050	3.050	26.450	0.023	0.023	0.038	3.112
60	08-Oct-13	1008_48 1 16 0-1s_0-34	16	36%	40%	circ	0.080	Spec	0.1	0.34	0.600	0.042	0.040	0.062	2.936	2.884	23.750	0.010	0.010	0.016	2.936	2.901	23.750	0.045	0.044	0.070	3.112
61	08-Oct-13	1008_49 1 16 0-2s_0-34	16	36%	40%	circ	0.080	Spec	0.2	0.34	0.600	0.084	0.081	0.129	2.816	2.969	22.630	0.019	0.018	0.028	2.816	2.816	22.630	0.086	0.085	0.133	3.112
62	08-Oct-13	1008_50 1 16 0-3s_0-34	16	36%	40%	circ	0.080	Spec	0.3	0.34	0.600	0.124	0.121	0.190	2.816	2.618	22.370	0.028	0.027	0.040	2.816	2.816	22.370	0.124	0.125	0.197	3.112
63	08-Oct-13	1008_51 1 16 0-4s_0-34	16	36%	40%	circ	0.080	Spec	0.4	0.34	0.600	0.162	0.160	0.242	2.816	2.919	22.950	0.037	0.036	0.058	2.816	2.816	22.950	0.162	0.165	0.252	3.112
24	02-Oct-13	1002_17 1 20 0-4s_0-6	20	20%	25%	circ	0.080	Spec	0.4	0.596	0.615	0.130	0.123	0.201	1.786	1.786	32.000	0.098	0.092	0.158	1.810	1.739	32.000	0.118	0.115	0.181	1.742
25	03-Oct-13	1002_28 1 24 0-05s_0-6	24	4%	10%	circ	0.080	Spec	0.05	0.596	0.615	0.019	0.018	0.030	1.663	1.693	60.040	0.011	0.011	0.019	1.798	1.675	60.040	0.009	0.009	0.015	1.620
26	03-Oct-13	1002_29 1 24 0-1s_0-6	24	4%	10%	circ	0.080	Spec	0.1	0.596	0.615	0.038	0.037	0.059	1.663	1.692	63.420	0.024	0.023	0.040	1.663	1.697	63.420	0.017	0.016	0.026	1.620
27	03-Oct-13	1002_30 1 24 0-2s_0-6	24	4%	10%	circ	0.080	Spec	0.2	0.596	0.615	0.076	0.074	0.117	1.619	1.692	67.220	0.051	0.050	0.083	1.663	1.675	67.220	0.031	0.029	0.049	1.620
28	03-Oct-13	1002_31 1 24 0-3s_0-6	24	4%	10%	circ	0.080	Spec	0.3	0.596	0.600	0.139	0.134	0.218	1.555	1.555	68.280	0.095	0.092	0.155	1.555	1.555	68.280	0.050	0.049	0.089	1.592
69	09-Oct-13	1009_60 1 16 0-05s_0-6	16	36%	40%	sq	0.075	Spec	0.05	0.596	0.590	0.019	0.019	0.031	1.798	1.672	26.690	0.005	0.005	0.010	1.798	1.803	26.690	0.018	0.018	0.028	1.620
70	09-Oct-13	1009_61 1 16 0-1s_0-6	16	36%	40%	sq	0.075	Spec	0.1	0.596	0.590	0.039	0.038	0.063	1.798	1.672	25.470	0.010	0.010	0.017	1.798	1.804	25.470	0.037	0.036	0.056	1.620
71	09-Oct-13	1009_62 1 16 0-2s_0-6	16	36%	40%	sq	0.075	Spec	0.2	0.596	0.590	0.078	0.076	0.126	1.688	1.739	23.620	0.018	0.018	0.029	1.798	1.771	23.620	0.072	0.070	0.115	1.620
72	09-Oct-13	1009_63 1 16 0-3s_0-6	16	36%	40%	sq	0.075	Spec	0.3	0.596	0.590	0.118	0.115	0.190	1.688	1.688	22.670	0.027	0.025	0.041	1.798	1.750	22.670	0.105	0.102	0.145	1.620
73	09-Oct-13	1009_64 1 16 0-4s_0-6	16	36%	40%	sq	0.075	Spec	0.4	0.596	0.590	0.154	0.148	0.215	1.688	1.687	22.670	0.035	0.033	0.053	1.688	1.745	22.670	0.134	0.131	0.208	1.639
45	08-Oct-13	1008_52 1 14 0-1s_0-45	14	44%	48%	circ	0.080	Spec	0.1	0.45	0.600	0.042	0.041	0.069	2.235	2.233	20.450	0.009	0.008	0.013	2.235	2.234	20.450	0.040	0.039	0.065	2.234
74	10-Oct-13	1009_65 1 20 0-05s_0-6	20	20%	25%	sq	0.075	Spec	0.05	0.596	0.590	0.019	0.019	0.031	1.688	1.755	33.160	0.006	0.006	0.010	1.810	1.810	33.160	0.017	0.017	0.026	1.639
75	10-Oct-13	1009_66-1 1 20 0-1s_0-(	20	20%	25%	sq	0.075	Spec	0.1	0.596	0.590	0.040	0.039	0.063	1.688	1.688	31.100	0.012	0.012	0.019	1.810	1.810	31.100	0.034	0.033	0.048	1.639
76	10-Oct-13	1009_67 1 20 0-2s_0-6	20	20%	25%	sq	0.075	Spec	0.2	0.596	0.590	0.079	0.076	0.130	1.688	1.688	29.900	0.023	0.023	0.038	1.688	1.688	29.900	0.064	0.061	0.090	1.639

77	10-Oct-13	1009_68 1 20 0-3s_0-6	20	~~20%~~	25% sq	0.075 Spec	0.3	0.596	0.590	0.118	0.114	0.189	1.688	1.688	30.030	0.035	0.034	0.061	1.688	1.688	30.030	0.091	0.088	0.131	1.639
78	10-Oct-13	1009_69 1 20 0-4s_0-6	20	~~20%~~	25% sq	0.075 Spec	0.4	0.596	0.590	0.159	0.152	0.221	1.758	1.758	31.170	0.050	0.047	0.074	1.822	1.761	31.170	0.118	0.115	0.169	1.759
80	14-Oct-13	1009_70 1 24 0-1s_0-6	24	~~4%~~	10% sq	0.075 Spec	0.1	0.596	0.575	0.043	0.042	0.071	1.638	1.629	55.270	0.024	0.023	0.045	1.638	1.618	55.270	0.021	0.021	0.033	1.639
81	14-Oct-13	1009_71 1 24 0-2s_0-6	24	~~4%~~	10% sq	0.075 Spec	0.2	0.596	0.575	0.086	0.084	0.136	1.648	1.643	58.350	0.050	0.049	0.099	1.600	1.623	58.350	0.038	0.036	0.062	1.649
82	14-Oct-13	1009_72 1 24 0-3s_0-6	24	~~4%~~	10% sq	0.075 Spec	0.3	0.596	0.575	0.129	0.125	0.212	1.648	1.640	60.720	0.078	0.076	0.130	1.555	1.597	60.720	0.052	0.051	0.072	1.649
114	15-Oct-13	1015_103 1 18d 0-05s_(	18	~~28%~~	5% dsq	0.106 Spec	0.05	0.596	0.575	0.019	0.018	0.029	1.769	1.697	27.390	0.005	0.005	0.008	1.816	1.814	27.390	0.016	0.015	0.023	1.770
115	15-Oct-13	1015_104 1 18d 0-1s_0-	18	~~28%~~	5% dsq	0.106 Spec	0.1	0.596	0.575	0.039	0.038	0.058	1.638	1.694	28.030	0.011	0.011	0.019	1.810	1.813	28.030	0.029	0.027	0.040	1.770
116	15-Oct-13	1015_105 1 18d 0-2s_0-	18	~~28%~~	5% dsq	0.106 Spec	0.2	0.596	0.575	0.080	0.077	0.119	1.638	1.694	35.020	0.028	0.028	0.058	1.600	1.708	35.020	0.051	0.049	0.082	1.639
117	15-Oct-13	1015_106 1 18d 0-3s_0-	18	~~28%~~	5% dsq	0.106 Spec	0.3	0.596	0.575	0.121	0.116	0.183	1.769	1.696	40.640	0.049	0.049	0.106	1.769	1.682	40.640	0.071	0.068	0.109	1.649
118	15-Oct-13	1015_107 1 18d 0-4s_0-	18	~~28%~~	5% dsq	0.106 Spec	0.4	0.596	0.575	0.159	0.151	0.218	1.769	1.700	44.510	0.071	0.069	0.112	1.769	1.769	44.510	0.088	0.085	0.124	1.770
84	09-Oct-13	1009_73 1 16 0-05s_0-4	16	~~36%~~	40% sq	0.075 Spec	0.05	0.45	0.590	0.021	0.021	0.035	2.235	2.188	23.660	0.005	0.005	0.008	2.235	2.233	23.660	0.020	0.019	0.033	2.234
85	09-Oct-13	1009_74 1 16 0-1s_0-45	16	~~36%~~	40% sq	0.075 Spec	0.1	0.45	0.590	0.042	0.041	0.070	2.235	2.234	21.740	0.009	0.009	0.014	2.235	2.235	21.740	0.040	0.038	0.065	2.234
86	09-Oct-13	1009_75 1 16 0-2s_0-45	16	~~36%~~	40% sq	0.075 Spec	0.2	0.45	0.590	0.084	0.081	0.137	2.235	2.234	20.240	0.017	0.016	0.024	2.235	2.157	20.240	0.077	0.075	0.123	2.234
87	09-Oct-13	1009_76 1 16 0-3s_0-45	16	~~36%~~	40% sq	0.075 Spec	0.3	0.45	0.590	0.126	0.122	0.181	2.156	2.242	19.690	0.025	0.022	0.037	2.688	2.688	19.690	0.110	0.106	0.171	2.318
88	09-Oct-13	1009_77 1 16 0-4s_0-45	16	~~36%~~	40% sq	0.075 Spec	0.4	0.45	0.590	0.165	0.158	0.251	2.199	2.168	20.220	0.033	0.030	0.057	3.718	3.718	20.220	0.145	0.142	0.234	2.451
89	10-Oct-13	1009_78 1 20 0-05s_0-4	20	~~20%~~	25% sq	0.075 Spec	0.05	0.45	0.590	0.020	0.020	0.036	2.235	2.140	27.690	0.006	0.005	0.009	2.029	2.147	27.690	0.018	0.018	0.031	2.347
90	14-Oct-13	1009_79 1 20 0-1s_0-45	20	~~20%~~	25% sq	0.075 Spec	0.1	0.45	0.575	0.041	0.039	0.069	2.165	2.212	25.790	0.011	0.010	0.018	2.029	2.122	25.790	0.035	0.034	0.057	2.347
91	14-Oct-13	1009_80 1 20 0-2s_0-45	20	~~20%~~	25% sq	0.075 Spec	0.2	0.45	0.575	0.081	0.078	0.132	2.199	2.166	25.660	0.021	0.020	0.039	2.199	2.249	25.660	0.066	0.064	0.104	2.347
92	14-Oct-13	1009_81 1 20 0-3s_0-45	20	~~20%~~	25% sq	0.075 Spec	0.3	0.45	0.575	0.121	0.116	0.186	2.199	2.198	27.340	0.033	0.031	0.061	2.464	2.459	27.340	0.095	0.092	0.158	2.451
93	14-Oct-13	1009_82 1 20 0-4s_0-45	20	~~20%~~	25% sq	0.075 Spec	0.4	0.45	0.575	0.162	0.155	0.235	2.165	2.165	29.590	0.048	0.044	0.081	20453.000	2.926	29.590	0.124	0.119	0.206	2.347
95	14-Oct-13	1009_84 1 24 0-1s_0-45	24	~~4%~~	10% sq	0.075 Spec	0.1	0.45	0.575	0.045	0.044	0.075	2.060	2.231	51.520	0.023	0.022	0.046	2.165	2.235	51.520	0.024	0.022	0.039	2.462
96	14-Oct-13	1009_85 1 24 0-2s_0-45	24	~~4%~~	10% sq	0.075 Spec	0.2	0.45	0.575	0.093	0.091	0.159	2.464	2.464	56.470	0.053	0.050	0.099	2.464	2.290	56.470	0.041	0.040	0.073	2.462
100	09-Oct-13	1009_89 1 16 0-1s_0-34	16	~~36%~~	40% sq	0.075 Spec	0.1	0.34	0.590	0.042	0.040	0.062	2.816	2.959	25.270	0.011	0.010	0.017	2.816	2.873	25.270	0.045	0.044	0.064	2.916
101	09-Oct-13	1009_90 1 16 0-2s_0-34	16	~~36%~~	40% sq	0.075 Spec	0.2	0.34	0.590	0.084	0.081	0.127	3.154	2.963	24.320	0.020	0.020	0.029	2.816	2.837	24.320	0.086	0.085	0.124	2.916
102	09-Oct-13	1009_91 1 16 0-3s_0-34	16	~~36%~~	40% sq	0.075 Spec	0.3	0.34	0.590	0.127	0.125	0.188	2.936	2.901	23.970	0.030	0.030	0.044	2.816	2.873	23.970	0.128	0.128	0.197	3.112
105	14-Oct-13	1009_94 1 20 0-1s_0-34	20	~~20%~~	25% sq	0.075 Spec	0.1	0.34	0.575	0.042	0.041	0.061	2.936	2.983	28.620	0.012	0.012	0.016	2.860	2.859	28.620	0.042	0.041	0.058	2.916
106	14-Oct-13	1009_95 1 20 0-2s_0-34	20	~~20%~~	25% sq	0.075 Spec	0.2	0.34	0.575	0.086	0.084	0.123	2.890	2.890	29.150	0.025	0.024	0.038	2.890	2.890	29.150	0.079	0.077	0.110	2.885
107	14-Oct-13	1009_96 1 20 0-3s_0-34	20	~~20%~~ ,	sq	0.075 Spec	0.3	0.34	0.575	0.125	0.124	0.186	3.154	3.158	31.170	0.039	0.039	0.070	2.860	2.949	31.170	0.110	0.109	0.148	2.916
110	14-Oct-13	1009_99 1 24 0-1s_0-34	24	~~4%~~	10% sq	0.075 Spec	0.1	0.34	0.575	0.048	0.046	0.067	3.172	3.030	50.980	0.024	0.024	0.035	2.890	3.005	50.980	0.030	0.029	0.040	2.885
111	14-Oct-13	1009_100 1 24 0-2s_0-3	24	~~4%~~	10% sq	0.075 Spec	0.2	0.34	0.575	0.102	0.099	0.161	2.890	2.998	57.460	0.059	0.057	0.092	2.890	2.983	57.460	0.053	0.052	0.073	2.871
112	14-Oct-13	1009_101 1 24 0-3s_0-3	24	~~4%~~	10% sq	0.075 Spec	0.3	0.34	0.575	0.154	0.154	0.220	2.890	3.016	61.820	0.095	0.092	0.142	2.890	3.006	61.820	0.072	0.070	0.095	2.885
129	15-Oct-13	1015_118 1 14d 0-1s_0-	14	~~44%~~	48% dsq	0.106 Spec	0.1	0.596	0.575	0.038	0.037	0.057	1.769	1.733	24.470	0.009	0.009	0.015	1.816	1.814	24.470	0.037	0.035	0.050	1.770
130	15-Oct-13	1015_119 1 14d 0-3s_0-	14	~~44%~~	48% dsq	0.106 Spec	0.3	0.596	0.575	0.115	0.112	0.164	1.769	1.695	19.270	0.022	0.021	0.038	1.816	1.768	19.270	0.101	0.096	0.140	1.770
141	16-Oct-13	1016_130 2-1 15 0-05s_	15	40%	~~44%~~ circ	0.080 Spec	0.05	0.596	0.570	0.018	0.018	0.027	1.769	1.667	23.210	0.004	0.004	0.008	1.816	1.820	23.210	0.017	0.016	0.023	1.770
142	16-Oct-13	1016_131 2-1 15 0-1s_0	15	40%	~~44%~~ circ	0.080 Spec	0.1	0.596	0.570	0.038	0.037	0.063	1.699	1.698	20.170	0.008	0.007	0.014	1.699	1.748	20.170	0.034	0.033	0.047	1.625
143	16-Oct-13	1016_132 2-1 15 0-2s_0	15	40%	~~44%~~ circ	0.080 Spec	0.2	0.596	0.570	0.076	0.073	0.115	1.600	1.673	17.220	0.013	0.012	0.020	1.810	1.811	17.220	0.066	0.063	0.090	1.639
120	15-Oct-13	1015_109 1 18d 0-1s_0-	18	~~28%~~	5% dsq	0.106 Spec	0.1	0.45	0.575	0.041	0.040	0.066	2.199	2.197	29.120	0.012	0.011	0.023	2.464	2.415	29.120	0.030	0.029	0.048	2.347
121	15-Oct-13	1015_110 1 18d 0-2s_0-	18	~~28%~~	5% dsq	0.106 Spec	0.2	0.45	0.575	0.084	0.082	0.133	2.199	2.198	37.260	0.031	0.031	0.057	2.464	2.462	37.260	0.053	0.051	0.085	2.462
122	15-Oct-13	1015_111 1 18d 0-3s_0-	18	~~28%~~	5% dsq	0.106 Spec	0.3	0.45	0.575	0.128	0.124	0.195	2.464	2.290	43.160	0.055	0.053	0.093	2.464	2.307	43.160	0.075	0.071	0.114	2.462
125	15-Oct-13	1015_114 1 18d 0-1s_0-	18	~~28%~~	5% dsq	0.106 Spec	0.1	0.34	0.575	0.043	0.042	0.065	3.154	3.044	33.210	0.014	0.014	0.023	2.860	2.848	33.210	0.037	0.036	0.051	2.916
126	15-Oct-13	1015_115 1 18d 0-2s_0-	18	~~28%~~	5% dsq	0.106 Spec	0.2	0.34	0.575	0.092	0.090	0.138	2.890	3.015	40.670	0.038	0.038	0.065	2.890	2.890	40.670	0.067	0.064	0.086	2.885
127	15-Oct-13	1015_116 1 18d 0-3s_0-	18	~~28%~~	5% dsq	0.106 Spec	0.3	0.34	0.575	0.137	0.135	0.208	3.154	3.008	45.780	0.063	0.064	0.116	2.890	2.996	45.780	0.090	0.890	0.121	2.916
144	16-Oct-13	1016_133 2-1 15 0-3s_0	15	40%	~~44%~~ circ	0.080 Spec	0.3	0.596	0.570	0.114	0.110	0.156	1.769	1.694	17.120	0.019	0.018	0.032	1.810	1.778	17.120	0.098	0.094	0.132	1.639
145	16-Oct-13	1016_134 2-1 15 0-4s_0	15	40%	~~44%~~ circ	0.080 Spec	0.4	0.596	0.570	0.145	0.141	0.219	1.609	1.684	17.540	0.025	0.023	0.040	1.693	2.298	17.540	0.119	0.116	0.179	1.574
131	15-Oct-13	1015_120 1 14d 0-1s_0-	14	~~44%~~	48% dsq	0.106 Spec	0.1	0.45	0.575	0.041	0.040	0.068	2.349	2.166	22.140	0.009	0.009	0.013	2.029	2.029	22.140	0.039	0.037	0.065	2.347
132	15-Oct-13	1015_121 1 14d 0-3s_0-	14	~~44%~~	48% dsq	0.106 Spec	0.3	0.45	0.575	0.122	0.116	0.190	2.199	2.167	19.770	0.024	0.022	0.042	11.745	3.556	19.770	0.105	0.102	0.149	2.347
133	15-Oct-13	1015_122 1 14d 0-1s_0-	14	~~44%~~	48% dsq	0.106 Spec	0.1	0.34	0.575	0.042	0.040	0.061	3.154	2.981	25.180	0.010	0.010	0.017	2.860	2.899	25.180	0.044	0.043	0.062	2.916
134	15-Oct-13	1015_123 1 14d 0-3s_0-	14	~~44%~~	48% dsq	0.106 Spec	0.3	0.34	0.575	0.124	0.122	0.190	3.154	3.042	24.540	0.030	0.030	0.053	2.860	2.899	24.540	0.122	0.118	0.168	2.916
46	08-Oct-13	1008_53 1 14 0-2s_0-45	14	44%	~~48%~~ circ	0.080 Spec	0.2	0.45	0.600	0.084	0.081	0.135	2.235	2.150	18.900	0.016	0.015	0.024	2.235	2.235	18.900	0.078	0.076	0.127	2.234
47	08-Oct-13	1008_54 1 14 0-3s_0-45	14	44%	~~48%~~ circ	0.080 Spec	0.3	0.45	0.600	0.125	0.121	0.197	2.235	2.234	18.270	0.023	0.021	0.032	2.235	2.234	18.270	0.116	0.115	0.196	2.234
65	08-Oct-13	1008_56 1 14 0-1s_0-34	14	44%	~~48%~~ circ	0.080 Spec	0.1	0.34	0.600	0.042	0.040	0.063	2.816	2.863	23.400	0.010	0.009	0.016	2.952	2.891	23.400	0.045	0.044	0.064	2.916
66	08-Oct-13	1008_57 1 14 0-2s_0-34	14	44%	~~48%~~ circ	0.080 Spec	0.2	0.34	0.600	0.084	0.082	0.129	2.936	2.966	22.120	0.019	0.018	0.029	2.816	2.816	22.120	0.088	0.087	0.138	3.112
67	08-Oct-13	1008_58 1 14 0-25s_0-3	14	44%	~~48%~~ circ	0.080 Spec	0.25	0.34	0.600	0.106	0.103	0.162	2.936	2.883	21.880	0.023	0.022	0.034	2.816	2.871	21.880	0.110	0.111	0.172	3.112